ENVIRONMENT FORCE ESTIMATION WITH STOCHASTIC NOISE AND CONTROL FOR ROBOTICS

A Thesis submitted to the

Delhi Technological University

For the award of the Doctor of Philosophy

in

Electrical Engineering

by

NEELU NAGPAL

(2K14/PhD/EE/08)

Under the supervision of

Prof. Bharat Bhushan and Prof. Vijyant Agarwal

DEPARTMENT OF ELECTRICAL ENGINEERING

DELHI TECHNOLOGICAL UNIVERSITY

DELHI-110042, INDIA

JUNE 2019

Certificate

This is to certify that the thesis entitled "**Environment Force Estimation with Stochastic Noise and Control for Robotics**" submitted for the award of the Doctor of Philosophy is original to the best of our knowledge. The work was carried out by **Ms. Neelu Nagpal** under our guidance and has not been submitted in parts or full to this or any other University for award of any degree or diploma. All the assistance and help received during the course of study has been duly acknowledged.

Supervisors

Prof. Bharat Bhushan
Department of Electrical Engg.
Delhi Technological University
Delhi-110042

Prof. Vijyant Agarwal
Division of MPAE
Netaji Subhas University of Technology
Delhi-110078

Acknowledgement

Writing this thesis has been fascinating and extremely rewarding. First of all, I am thankful to God, who has blessed me strength and support throughout my life and always provides me with a path to acquire knowledge and learning.

It gives me immense pleasure to express my gratitude to my supervisors Prof. Bharat Bhushan and Prof. Vijyant Agarwal, for all the readymade help, guidance, valuable suggestions, explanation, advice and above all, their support for carrying out this work. Throughout my thesis-writing period, they were immense helpful.

I would also like to thank Prof. Harish Parasarthy, NSUT, Delhi, Prof. Akshay Kumar Rathore, Concordia University, Canada and the reviewers of our papers for their valuable suggestions and comments which motivated me to look into areas which we never thought of venturing into.

Sincere thanks to Delhi Technological University, Netaji Subhas University of Technology and Maharaja Agrasen Institue of Technology authorities for providing me necessary facilities for the smooth completion of my work. I would like to give special thanks to Prof. Parmod Kumar, Dr. Devanjali Relan, and Mr. U. K. Jha for their help and moral support during my study. I am indebted to my husband Mr. Harish Nagpal, daughter Yashika for their tremendous support and patience throughout my study period. I would like to express my deepest regards and gratitude to my parents for their unmitigated love.

Finally, I especially extend appreciation to my son, Hardik Nagpal for his faith, encouragement, understanding, and unfailing support. To him, I dedicate this thesis.

Neelu Nagpal

Abstract

The proposed work entitled "Environment Force Estimation with Stochastic Noise and Control for Robotics" focuses on estimation of state vector and controller's parameters and control of a robot in the presence of noise. Also, environment force is estimated when robot has interaction with randomly structured environment. In the present work, two typical issues are investigated for the robotic system. The first one deals with the noise present in the system. Noise is wiped out from the output measurement by utilizing state-observer which in turn, feeds the estimated state to a controller in spite of noisy state. Thus, any further randomness is restricted and focus of the work is to design, implement and test the optimal state-observer-based controller. It aims for trajectory control of the state of an n-link robot to track the desired trajectory in the presence of stochastic noise. The novel feature of the present control algorithm is based on $It\hat{o}'s$ stochastic calculus. It is used for the minimization of the conditional expectation of the instantaneous tracking error energy differential with respect to the feedback matrix. This instantaneous minimization results in an adaptive action of the controller. At the same time, it also maintains the energy constraints in the feedback coefficients to avoid actuator saturation. This enables to validate the real-time implementation of state-observer-based controller by an experimental set up of "Phantom Omni Bundle" robot manipulator. Furthermore, the sensitivity analysis of controller gain variation and parameter variation on the error process is performed, and the robustness of the system is assured by the bounded errors.

Another important and relevant issue is that when noise appears in the form of environmental torque and randomness becomes a part of the closed-loop system and makes the dynamics of the nonlinear system 'stochastic'. Utilizing the sample data of noisy measurement of joint position, the 'likelihood function' of tracking error is computed. Minimization of this function estimates the unknown controller gain parameters. The trajectory of stochastic environment force is also computed

from the estimates of controller gain parameters. Subsequently, the performance of estimation is determined using convergence analysis and imposing lower bound on the variance of estimation errors.

In the present study, both issues are addressed for a nonlinear dynamical system in a stochastic scenario. Controllers are designed based on estimation without using any velocity sensor or force sensor.

Contents

List of Figures

List of Tables

Acronyms

CTC	Computed Torque Control
CRLB	Cramer Lower Bound
DOF	Degree of Freedom
DOB	Disturbance Observer
EKF	Extended Kalman Filter
KF	Kalman Filter
FLC	Fuzzy Logic Control
i.i.d.	Independently and Identically Distributed
LSE	Least Square Estimation
MF	Membership Function
MLE	Maximum Likelihood Estimation
ODE	Ordinary ordinary differential equation
PDF	Probability Distribution Function
PD	Proportional-Derivative
RMS	Root Mean Square
SDE	Stochastic Differential Equation
SNR	Signal to Noise Ratio
WGN	White Gaussian Noise

Notation

$\mathbb{R}$	Real space of dimension n
q	Joint position vector
$\dot{q}$	Joint velocity vector
$\ddot{q}$	Joint acceleration vector
q_m/q_s	' Master/Slave joint position vector
$\dot{q_m}/\dot{q_s}$	Master/Slave joint velocity vector
$\ddot{q_m}/\ddot{q_s}$	Master/Slave joint acceleration vector
$\lvert . \rvert$	Absolute value of a scalar function
$\lVert . \rVert$	Euclidean or any other consistent norm of a vector or matrix
$(.)^T$	Transpose of matrix
$tr[\ A\ ]$	Trace of matrix; $tr[A\ A^T] = \lVert A \rVert^2$
$diag(\ .\ .\ .\ )$	Diagonal elements of a square matrix
λ	Eigen value of matrix
$(\ \hat{.}\ )$	Estimated variable
$\mathbb{E}[\ .\ ]$	Expectation operator
$\mathbb{E}[\ .\ \lvert\ .\ ]$	Conditional expectation
∂	Partial derivative operator
$N(\mu, \sigma)$	Gaussian distribution, mean value μ and covariance σ
I	Identity matrix
I	Lagrange Multiplier
0	Zero, zero vector or zero matrix
k	Discrete time index
N	Number of iterations
ν	System noise
ω	Measurement noise
dB/dt	Brownian motion
$A \otimes B$	Kronecker product of matrices A and B

Chapter 1

Introduction

The study of nonlinear dynamics with application to robotics in real-time have many challenges and needs continuous investigation. In this paradigm, every new advancement is either an improvement or an improvisation of the existing one.
The subject of research investigated in this thesis is related to tracking control problems of the robotic system in the presence of uncertainty. Uncertainty is present in almost all the systems in measurements, process, etc., and to safeguard the system from these noises is an expensive venture. However, if it is not taken care of, adverse effects on the performance restrict the applications of a robot. Beside uncertainty, some vital issues associated with the control of robotic systems are discussed, propelling the present research to move in the direction to control the stochastic robots.

1.1 Background and existing challenges

In time-varying tracking control, the state variables viz. joint position and velocity should follow the desired trajectory and require controller gains to be adjusted accordingly. Further, the parameters of robot functioning in time-varying states require a controller to monitor the system variables and behave on a continuous basis. This requires dynamic controller instead of a static controller that may even become unstable under dynamic conditions which were not predicted a priori.
Thus, there is a need to develop an on-line controller, capable of providing a correction signal to cope up with the nonlinear and time-varying dynamics of robot and effective to guide the system to meet the given set of requirements.

State feedback controllers are designed to provide the necessary control signal to

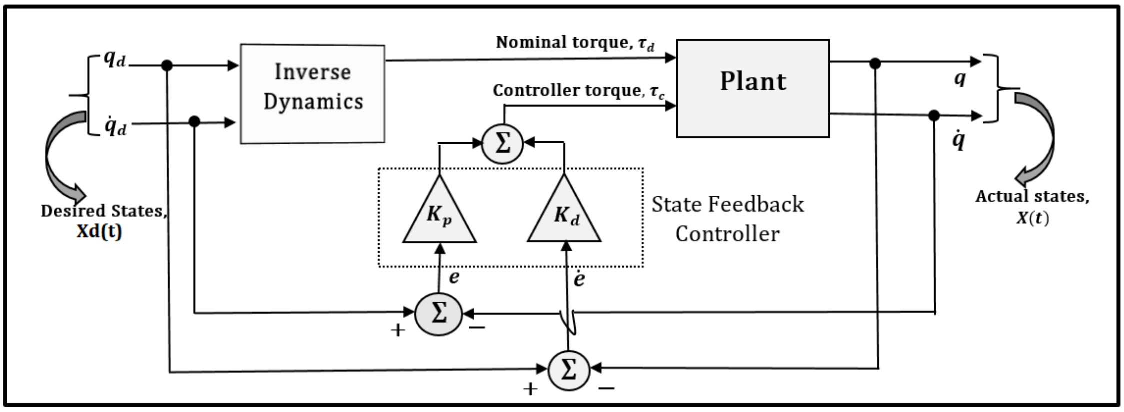

Figure 1.1: Structure of Model Based Control Approach

the actuators so that required torque is developed for the robot to reach from current state to the desired state. Inverse dynamics helps in computing the nominal torque required to provide the desired motion for which controllers are model-based. The basic structure of a model-based controller is shown in Fig. 1.1 where it is assumed that "complete model" is being used while designing the model of controller. But in practice, most of the parameters used in forming the equations of dynamic are imprecisely known. Feedback control action is required to reject the effect of this discrepancy upon the controlled variables to bring the actual states back to their desired values. This need to measure actual states so that measurements are compared with the desired values and the resulting error is fed into the controller so that it can generate the appropriate control signal. Indeed, the control system has to behave correctly even when it is connected to a physical system with true parameter values away from nominal.
Thus, a requirement of robust control design arises which has good tolerance to modeling error. For this to be achieved, the controller needs to know the values of the actual states.

Usually, an optical encoder is fixed at a motor drive of each joint to measure the angular position of it. Velocity sensors are avoided to be used for velocity measurements because it increases the cost, weight, and complexity to a system. An approach to get velocity signal is taking derivative of the position signal which is again contributing noise in the dynamics of the system. This high-frequency signal not only potentially degrade the tracking performance of the system but also, result in wear problems due to undesirable alterations in the control signal. Consequently, an uncertainty results in the relation of state variables and the measured outputs termed as measurement noise.

Noise act as exogenous inputs to the physical system and adversely affect the performance of the system. These are accounted by imperfect mathematical model; driven of dynamic models by unknown disturbances that can't be modeled; partial and inaccurate state variables; creeping of randomness in the closed-loop dynamics of a nonlinear process due to environment force, etc. Deterministic modeling cannot provide sufficient means to analysis and control of the robotic system.

A need arises to formulate the problem of the presence of noise in the dynamics into a proper stochastic framework for controller design to tackle it. Also, an emphasis should be considered to ensure accurate state feedback requirement to avoid noisy states or output which may mislead the controller for doing its corrective action and ultimately lead the system to instability at the worst.

The control signal which is fed to actuators of various joints causes the state manipulation of the robot. Saturation of actuators, which ia a critical limiting factor is decisive of the maximum level of a control signal.

It needs an appropriate constraint control design to consider both the magnitude and rate of change of control signal.

Stability is a fundamental attribute of a well-designed system to retain its state regardless of perturbations of the initial conditions and parameters of the system caused by regular and random disturbances. It is a concept which must never be confused with its so-called definitions, whether mathematical or empirical. Instead, emphasis should be made on the basis of the very existence of stability. However, for a variant class of system, the notion of stability can be presented differently and thus, interpretation of stability concepts can be done in various manners.

Thus task is to define and satisfy the prerequisite condition of stability before implementing the proposed control strategy to a system.

In designing the controller, some assumptions are involved to enable simpler and feasible computations and simulations. However, during implementations on hardware, such assumptions may jeopardize the performance of a system and need to review. While implementing the developed controller on hardware, one has to consider the range of inputs that it can bear safely without hampering its performance, i.e. customize the features of a controller in accordance to the real system in hand. For example, going by the specification, the maximum force and maximum angular movement that can be applied to any joint may be 1 N and $-\pi/2$ to $\pi/2$ radians respectively. The reference trajectory and control scheme should be designed taking care of these specifications. Further, during hardware implementation, a problem may arise due to lack of synchronization of sampling time of processor and sampling time of interfaced set-up. Most of the suppliers provide only end solutions for an exact problem. They generally not disclose the calculations and logic behind the control solutions.

Thus, many challenges are encountered in implementing the new controller on the hardware due to limited information available for the device. A need arises to design a realizable controller which can be tested on a real platform along with the care that the desired trajectory should respect the specifications set for that particular system.

Mostly, an environmental force has been modeled as a spring-damper system and its variants for designing the controller. However, in several applications, it is unrealistic to represent an environment model as a fixed one. Further, when robot interacts with the unstructured environment, its dynamic alter as the external force not only physical perturb the system but also, introduces uncertainty in the measurement of states. It is desirable that a robot should follow the command trajectory.

So, seeking the solution of tracking problem while the interaction of the robot with a random nature of the environment is an open research topic.

Many potential applications strive for the need to know the environment interaction force. To overwhelm these issues, a suggestion is offered to estimate the contact force between the robot and the environment.

It is evident that estimation has a vital role in a stochastic control system. Whether it is parameter estimation or state estimation to the true value, the problem lies in a careful choice of appropriate estimation method and ensuring the performance of the estimation. This helps in ensuring the performance of remaining procedure rely upon how well the estimated values are closer to true value that has been replaced by the latter one for designing controller or calculation point of view. Hence it is imperative to monitor the quality of the estimation. Moreover, the accuracy of estimation is reliant on how well the modeling of a dynamic system and statistical modeling of randomness is done.

This section has discussed the challenges encountered in the motion control that strive for the solutions of stochastic control problems.

1.2 Motivation

Nonlinear dynamics is the basic characterization feature of the robot. It needs to compensate the existing nonlinearity by transforming the dynamics by suitable linearization techniques enable to design a simple and efficient linear control. Practically it is not possible to have a perfect model and sensor for measurements of the real system. Both modeling and measurements suffer from errors, and these challenges motivate to inject robustness in the control design that ensures to serve effectively even in the presence of uncertainties. The work has motivated the stochastic modeling of a robotic system that can accommodate process and measurement noise and environment noise of the system that can help in analyzing and designing a suitable estimation based controller with the practical approach. Further, the inspiration for this research emerges from the requirements of reliable state or parameter estimation strategies capable for giving consistent and exact evaluations of inaccessible states or parameters of the system for effective control that relies only on the availability of accurate information. Thus, the primary motivation of the research work is to frame stochastic control problem from a theoretical and computational perspective and to utilize the tools of optimal control theory to developed a general framework to accommodate the physical constraints. Further, considering the unified approach of estimation and control, the motivation of work lies to perform a new prominent analysis to find the ultimate boundedness of both the observer and controller tracking errors.

Experimental research through observations, analysis, comparison, and conclusion provides an idea of a better opinion after facing problems in hardware implementation.

This is a motivation to implement the theoretical concepts on a practical framework where several issues during implementation like discretization, synchronization, computational complexity, etc. get exposed. In another case, the presence of randomness in the dynamics of the robot due to interaction with random environment motivates to find estimates of controller parameters and structure of environmental noise. Estimation can exploit the available noisy sample records of measurements of robot position. The estimates should be approved for their accuracy, consistency and unbiased, etc. by some methods.

1.3 Problem Statement

To meet the challenges and existing gaps in the control of robotics, the following research problem is stated:

Devise a realizable state feedback control law for an uncertain, nonlinear and dynamical robotic system such that the time varying trajectory is achieved despite states being inaccessible or being corrupted by noise. Then, design a practicably implementable controller which not only compensate the modelling error but also ensures the robustness by bounding the error signals such that the system is asymptotically stable. Also, when the robot interacts with the environment, it must track the commanded trajectory in the presence of environmental noise, without compromise the performance as before. This would finally help in developing an efficient estimation to determine the stochastic environment force.

1.4 Objectives

Based on the defined motives for the research, the following objectives are set up:

- Development of a state-space stochastic model of a nonlinear time-varying system that accommodates the noise in the state equation and output equation.

- Design of suitable recursive state observer capable of providing noiseless state feedback information to the controller without using velocity sensors.
- Development of an optimal observer-based controller to satisfy the requirements to:
  (i) result in establishing asymptotic bounds for the estimation and tracking error;
  (ii) have structure practically suitable to implement on a developed model;
  (iii) impose the constraint on a control signal for safe operation;
  (iv) have adaptive tuning of controller gain to cope up with nonlinear dynamics, error-prone output measurements and time-varying reference trajectory.
- Validation of the proposed control solutions by performing real-time experiments on available Phantom Omni Bundle robot in the lab.
- Examination of sensitivity analysis and ensuring robustness concerning possible disturbances and uncertainty in the values of the system variables.
- Development of the model of a master-slave robotic system when the slave interacts with the stochastic environment.
- Design of controller for slave robot utilizing the batch measurement of noisy slave position and subsequently, computation of environmental force from the estimates of controller gain parameters.
- Study of different methods to ensure the goodness of estimations.

1.5 Methodology of the research work

The flow of the research consists of investigating the techniques for the tracking control of a robotic system when noise is present. Following solutions are proposed to meet the control problem of a nonlinear, uncertain, time-varying and stochastic dynamics of the system:

Solution I– State-observer based control is proposed where estimation and control

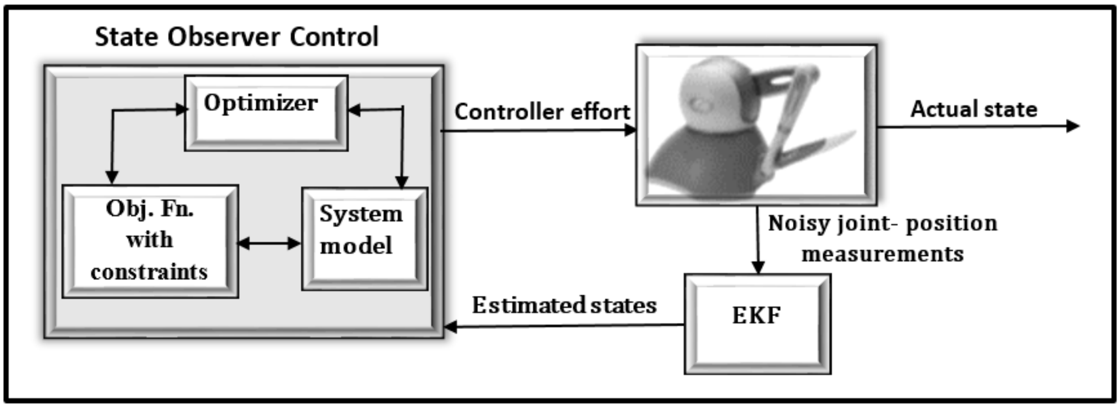

Figure 1.2: Structure of Proposed State-observer-based Control Approach

of states is unified in real-time (refer Fig.1.2).

The methodology employed to meet this solution is presented as:

- **Stochastic modelling of nonlinear dynamical system**

  It exemplifies the stochastic form using Ito's calculus for the development of the stochastic model of the nonlinear system. It describes the joint dynamics of state and observer, taking into consideration (a) desired state, (b) observer error feedback, and (c) process noise and measurement noise, using a vector stochastic differential equation (SDE).

- **Estimation of the states-No need of velocity sensor**

  The estimation process is encouraged for the knowledge of required states to cope up with noisy partial measurement by sensors for the monitoring and control purpose. In this present work, an observer has been used as an alternative to a velocity sensor, which not only reduces the complexity and weight of the system but also provides an economical solution. Extended Kalman filter (EKF) is used as state observer which considers only position signal in order to estimate states of the system, thereby removing any dependency on measurements of entire states.

- **Real-time unified approach of estimation and control with constraints**

  After the design of state observer that has an adaptive capability to compensate for measurement errors, the results of state estimation are integrated into the structure of robust control design to mitigate the effects of uncertainty and disturbances. The proposed controller has the following features:

(i) On-line implementation

The novel feature of the control algorithm is that it is based on It$\hat{o}'$s stochastic calculus for the minimization of the conditional expectation of the instantaneous tracking error energy differential with respect to the feedback matrix subject to energy constraints. The control action is decided on-line at each discrete-time step on the basis of the instantaneous error, imposing bounds on (a) input control effort and (b) output tracking error. The proposed control scheme in this research is substantiated with real-time experiments on a robot.

(ii) Constraint block structure

The controller has a feature of constraint in the structure which is chosen according to the model of the system. This is done by including the constraint in the objective function.

(iii) Energy constraint

The stringent controller action is assured by imposing the constraint on controller error energy for shaping the transient behavior of a system in addition to limiting controller gain input to a motor drive, thereby avoiding saturation/damage.

- **Hardware-implementation and verification**

  The theoretical concept of designing observer-based control with energy constraint in the present work is supported by experimental results carried on a robotic system available in the laboratory. These real-time experiments provide great momentum for theoretical research in nonlinear control systems to tackle the problem of stochastic noise.

- **Sensitivity analysis and ensuring robustness**

  Sensitivity analysis of the proposed control system is investigated to examine the effects of the fluctuations in (a) robot parameters and (b)controller gain, on the combined estimation and tracking error energies. These calculations justify the strength of the proposed work of state observer based controller design under the effect of uncertainty. Quantitative analysis for the robustness measure of proposed control design is done with the use of (a) appropriate signals and (b) system norms, which measures the magnitudes of the involved signals, thereby indicating the possibility of attaining asymptotic stability. Further, the robustness is ensured by converging the errors under parametric variations and controller gain variation, thereby indicating the possibility of attaining asymptotic stability.

Solution II– Maximum likelihood estimation of controller gain parameters and environment noise for master-slave robotic system (refer Fig.1.3).
The methodology employed in this regard is presented as:

- **Stochastic closed-loop dynamics of master-slave robotic system**
  Mostly, an environmental force has been modeled as a spring-damper system and its variants, but in the present work, it is regarded as an external disturbance or environmental noise. The environmental perturbations via stochastic processes are approximated by assuming it as white Gaussian noise. The model of a master-slave robotic system is developed in which slave has to follow master trajectory while having interaction with a vibrating wall. The closed-loop stochastic dynamics considering a master, slave, controller, and environment force is presented which is further utilized for controller design in constrained motion.

- **Estimation of controller gain parameters and stochastic environment force**
  In the proposed approach, stochastic environment force is introduced into the dynamics of the slave robot that added formidable complexity into robotic systems dynamics. It requires reconfiguring the available PD controller gain parameters (K) of the master-slave robotic system by exploiting estimation methods. Hence, maximum likelihood estimation(MLE) is used to estimate the controller gain parameters by maximizing the conditional probability density function (pdf) (or minimizing the negative likelihood

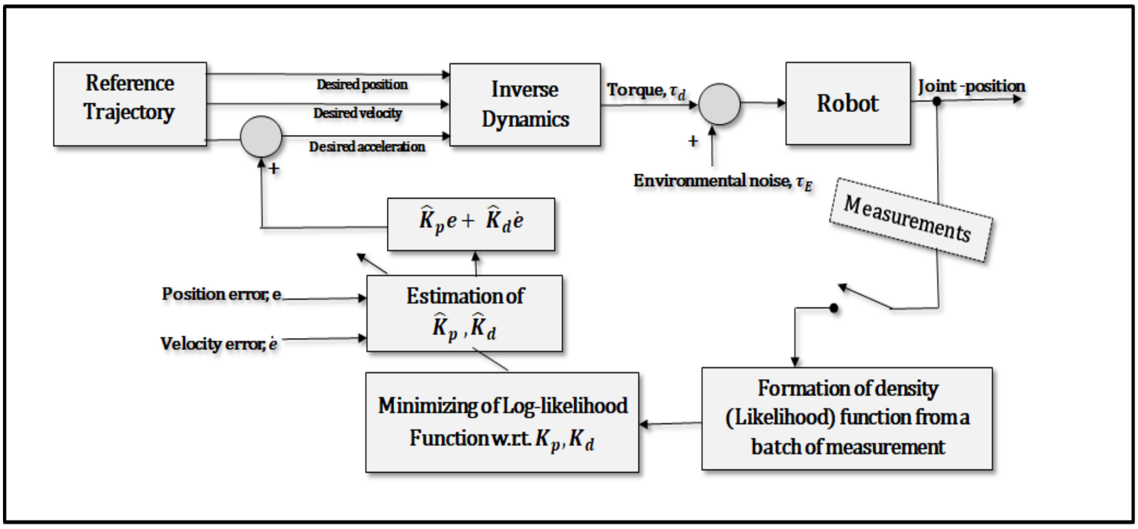

Figure 1.3: Structure of Proposed MLE Based Control Approach

function) w.r.t.'K'. The estimates are further utilized to estimates of sample trajectory of the environmental noise process.

- **Accuracy of estimation**

  The performance of parameter estimation has been explored through formulation of analytical expression of convergence and CRLB. The success of algorithm is exemplified through convergence analysis that provides low noise to signal ratio for the parameter estimates as number of samples(N) increases. Computation of CRLB of parameter estimation has been carried out to show that the estimates are consistent.

1.6 Outline of the thesis

After an introductory chapter, this thesis is organized in the following manner:
Chapter 1 (this chapter) introduces the research problem, proposed solutions and lists the contributions in the thesis.
Chapter 2 presents an overview of the related literature and the background topics to support the concepts developed in the thesis.
Chapter 3 provides an expression for the state observer based controller developed for the time-varying trajectory tracking control of nonlinear dynamical system in the presence of stochastic noise.

Chapter 4 The proposed control algorithm works in real-time which is tested on an experimental set-up of laboratory robot. The implementation of the state observer based controller is done by infering the available mathematical model and literature related to the robot.

Chapter 5 presents the sensitivity analysis of the system under the influence of parameteric uncertainty and controller gain fluctuations. Furthermore, the robustness of system is ensured by imposing bounds on the error energy of developed observer and controller.

Chapter 6 This chapter has discussed the trajectory control problem of master-slave robotic system and contributed in the MLE the controller gain parameters for a slave robot interacting with stochastic environment. It is followed by the derivation of the structure of environment noise from the estimates. Further, performance analysis of estimation is carried out using different methods.

Chapter 7 Finally in the chapter, a summary of this study is presented and some conclusions are drawn and projects future plan of action for further research.

This is followed in succession by references.

1.7 Conclusion

This chapter summarizes some of the correlated issues regarding the control of a robotic system. These crucial issues have motivated the research to pursue in exploring some of the control tactics of the motion control so that various applications can exploit tracking control capability of the system with excellent performance. Also, motivations and objectives of research have been brought out. In this chapter, stochastic control problems of the robot have been defined. This thesis comprises contributions to the methodology on state estimation and controller gain parameters estimation of the stochastic models.

Chapter 2

Literature Survey

2.1 Introduction

Chapter 1 has defined the problem and objectives of the present research work. A brief literature survey on the defined problem is carried out on the following issues.

(i) Control of a nonlinear and uncertain system

(ii) Stochastic dynamical systems and modeling

(iii) Estimation of state vector and parameters

(iv) State observer based control

(v) Stability of the nonlinear and uncertain system

(vi) Control of robot interacting with an environment

The survey helps to identify the methods to be considered for modeling and identification of the systems which are uncertain and of practical interest. This provides valuable insights into the issues related to the nonlinear, and stochastic system followed by attempts to make in the direction of tracking control of robotic systems. Furthermore, the need, concepts, and principles of the parameter and state estimation are also discussed. Also, this chapter serves a concept of robust control to preserve stability in the presence of uncertainty and noise in the system.

2.2 Control of nonlinear and uncertain system

Tracking control [1] requires the following predefined time-varying trajectory, $X_d(t)$ by a system state, $X(t)$ such that it meets optimally one or more of the specified performance indices, i.e. accuracy, dynamic response, sensitivity to disturbance, etc. The objective of the tracking problem is fulfilled by finding a suitable control law for the input $(u^*(t, X_d(t), X(t)))$ such that as t tends to infinity, $X(t) \to X_d(t)$. Mathematically, $\lim_{t\to\infty} \|X(t)-X_d(t)\| = 0$. This implies that under a steady-state condition, the tracking error asymptotically tends to zero. When the size of input is bounded as $\|u(t)\| \leq u_{max}$,$\forall t \geq 0$, tracking control formulation is treated as a constraint problem and the solution requires a design of an optimal controller which has constrained control signal. The constraint optimal problem has been solved by Lagrange multiplier and dynamic programming [2]. Lagrange multipliers are additional variables which when introduced in the constrained problem, transform it into an unconstrained minimization problem. Quite often, tracking control problems employs performance index to minimize the energy of the system under the given constraints [3], [4], [5].

Presence of nonlinearities in robot has inspired many solutions, and in general, the controller of a robotic system is designed either considering it as (i) nonlinear model (ii) linearized model. The methods proposed for transforming the nonlinear model of the robot into a linear model are:(a) linear approximation at a small region around an operating point, and (b) Feedback linearization [6]-[7]. In the situation of a system moving away from the operating point particularly for real uncertain system, where accurate tracking is required, it is found that performance of the control system in method (a) degrade [8].

The aim of the method (b) attempts to linearize and decouple the nonlinearities from the dynamics in such a manner that the system can be regarded as linear for the purposes of control design. This can be compensated merely using nonlinear dynamics with a nonlinear control signal, i.e., by adding Coriolis and centrifugal terms as well as gravity terms to the control input which is represented by $N(q, \dot{q})$ in Fig.2.2. Due to this nonlinear state feedback(shown as an inner loop), a linear and decoupled state model (double integrator) is obtained. The outer feedback

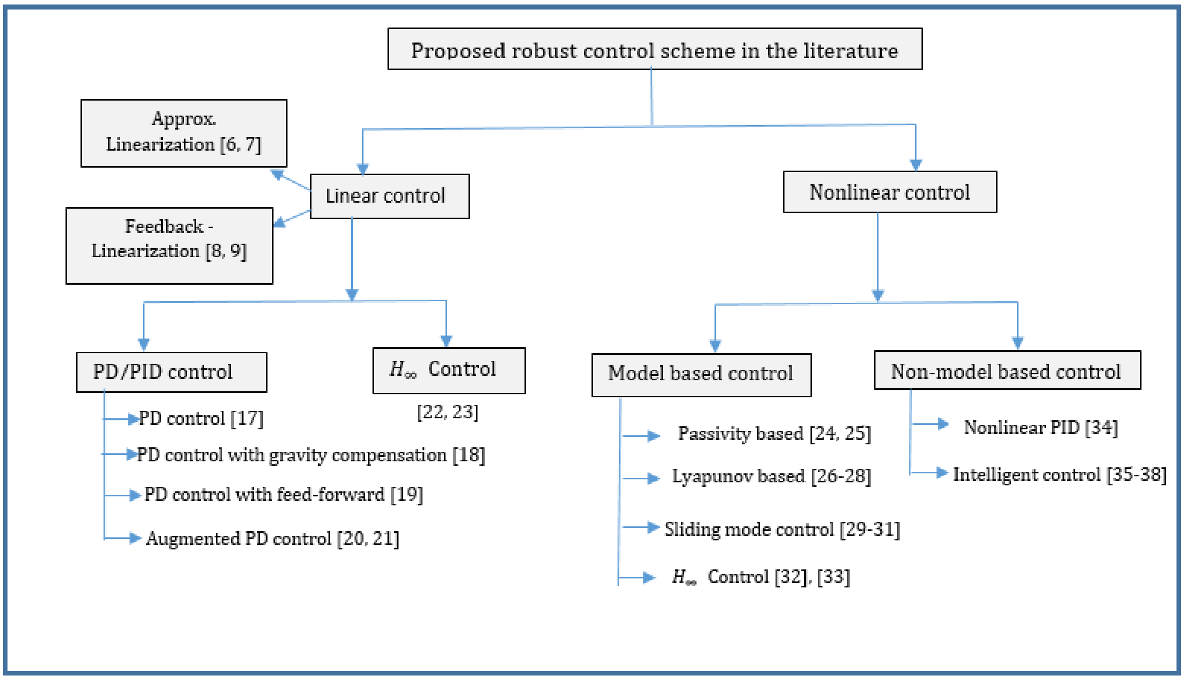

Figure 2.1: Available Robust Control Solution Proposed in Literature.

loop performs in the similar manner as it stabilizes the linear system. The control using feedback linearization used in a robot is known as Inverse dynamics control or computed torque control (CTC). This is based on state feedback and requires that all the terms in the manipulator dynamic model $M(q), N(q, \dot{q})$ must be known and can be computed in real-time. In order that the actual states, $X(t)$ to track a desired trajectory, $X_d(t)$, control signal is defined as: $u^* = \ddot{q} + K_p e + K_d \dot{e}$.

Further, for the linearized system, an appropriate controller can be synthesized with the same procedure as applied for linear system [7]. This technique requires the knowledge of model parameters; bears the burden of additional computation and has the limitation in the case of discontinuous nonlinear system [9]. Since feedback linearization relies on the exact cancellation of nonlinearities and performs effectively with a well known rigid robot. Robust control provides the solution to overcome the drawback of uncertainties present in the system and guarantees a level of performance with the help of fixed controller [10]. The issue of nonlinearity with or without uncertainty has been studied using hybrid approaches of inverse dynamics by combining it with Lyapunov function based control [11], nonlinear H- infinity control, neural network, variable structure control [12], and

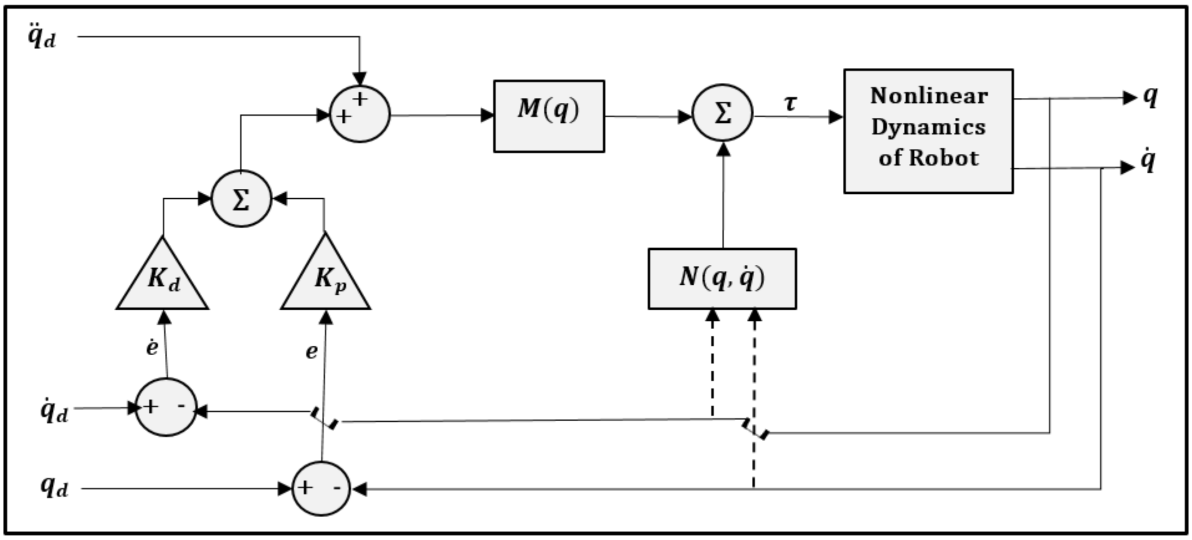

Figure 2.2: Feedback Linearization Control.

linear parameter-varying (LPV) control [13].

Although, adaptive control is also suited against uncertainty but is used only in case of the system with linearly parameterizable uncertainties [14]. Nevertheless, robust controllers are designed assuming that uncertainties are unknown but bounded. A robust control in contrast to adaptive control obeys the static control strategy, adaptive controller works according to variations in system parameters. Moreover, most practical systems do exhibit time-varying response and behave differently at different times. This is mainly due to system nonlinearities, failure or drift of parameters, the presence of external disturbance, and environmental changes. Subsequently, a different approach in the form of Robust control and optimal control emerged, which developed fixed controllers with a novice form of tolerating a limited range of variations in plant parameters to deal with dynamic uncertainty. A detailed survey has summarized the different approaches to handle the nonlinear tracking control of the robot [15],[16] and shown in Fig. 2.1. Robustness is injected in the form of linear control using many versions of PD control[17]-[31] and H-∞ control [22],[23] for nonlinear dynamics. Further, robust nonlinear control is classified as model-based [24]-[32] and non-model based using various approaches [34]-[37].

Robot manipulator can be interpreted as independent chains of double integrators for which proportional-derivative (PID) controllers have an instinct tendency to stabilize it and solve the regulation problem [17]. These controllers act as virtual spring-damper system suppress the oscillations as the Lagrange model of robot enjoy the property of passivity. However, these controllers are based on a linear approximation of nonlinear dynamics at a small region around an operating point and face problems as discussed above. Further, applying integral control to the system like a robot which has limited operating range, i.e., bounded in movement suffers the problem of Integral windup. Since it is the measured value which remains the same due to an operating limit but causes the summarized error to grow by the presence of integral component [38].

The robot with high gear-transmission mechanisms can be modeled as linear and decoupled rigid-body, and PD controllers are well suited for tracking control. Dominating the practice of control for a long time, PID controllers can't assure satisfactory performances in tracking control problems in the presence of uncertainties in model dynamics, and external disturbance as either accuracy or stability has to compromise with gain adjustment [39] especially at the time of discrete implementation [40]. In this regard, the work of Jingqing [41] not only elegantly present the limitations of PID but also given the solution in the form of nonlinear control by introducing error-based control law.

The perturbations may be in its physical parameters due to variations, aging or changes in the operating conditions and termed as parametric perturbations within the system. However, the presence of these perturbations and uncertainty in the system are considered to be within known bounds along with known dynamical properties in most of the reported work of controller design [37], [42]. Even for a controller with fixed structure but having adjustable parameters is responsible for parametric variation problem and should be checked for closed-loop stability of the system. This issue has been resolved by interpreting the robust control problem as an optimal control problem, where the uncertainties are manifest in the cost function and expressed that the solution to the optimal control problem is indeed a resolution of the issue of robustness in the system [43], [44]. Further, min-max LQR control has been considered as a robust extension of optimal control and applied to a nonlinear uncertain MIMO system. The robustness is incorporated by imposing an integral quadratic constraint that represents uncertainty in the cost function [45]. The nonlinear optimal method in tracking control has been devised using a formulation of (a) Hamilton Jacobi Bellman (HJB) [46], [47] and (b) Pontryagins Maximum Principle [48]. The solution of approach (a) involves nonlinear partial differential equation which is globally optimal but simple only for the low dimensional system. Approach (b) is based on the calculus of variations. The challenge of the nonlinearity and uncertainty has been taken care of the use of a sliding mode controller; however, the application gets restricted to only such cases, where chattering in the control signal is acceptable [49]. Further, in adaptive control [51] and sliding mode control, the performance of a system is not predicted quantitatively for a given robustness level. This limit the practical applications of these controllers where it is prior to knowing the worst case motion accuracy in an uncertain scenario.

The problem of uncertain nonlinear dynamic systems has been be tackled with the selection of suitable control design method according to the type of uncertainty [50]. Further, uncertainty has been considered as unknown nonlinear function and they referred adaptive control for the system having known nonlinearity but has constant parameter; sliding mode control for upper bounded uncertainty by inequality and learning control for periodic uncertainty with known period and much more strongly influenced by the type of uncertainty associated with the system model.

Although multifarious robust control approaches have been reported to tackle the nonlinear and uncertain systems, they have been developed from different prospects, but the mentioned control approaches have a fundamental requirement of exact feedback information to controller, i.e., accurate measurement of the states. Failing to fulfill this requirement, a controller misleads for its corrective action and ultimately drives the system towards instability.

2.3 Stochastic dynamical systems and modeling

In the presence of random noise in the measurement, the measurand vector has distributed values rather the deterministic state function. Further, the dynamic of states are modulated with process noise. Noise is used for modeling the uncertainties in the system dynamics [52]. Noise, a stochastic process has been described as unknown inputs to represent a model of the system in the form of stochastic differential equation(SDE). Generally, real applications have considered white Gaussian noise (WGN) in the formulation of SDE [53]. It is quite reasonable to consider randomness in the system to have Gaussian distribution according to the Central Limit theorem which states that a large sum of small independent random variables converges to the Gaussian law [54]. In this work, process and measurement noise and environment force have been assumed to follow the structure of Gaussian statistics. The whiteness of the environmental noise is based on the fact that usually the environmental kicks appear randomly and independent of each other similar to a molecule that kicks a pollen particle in a fluid leading to the pollen particle executing Brownian motion [55], [56]. The WGN source, $dW(t)$ is a statistical noise with a known normal pdf having flat power spectral density i.e. it contains equal power within any frequency band with a fixed width. The Brownian motion has each increment independent of each other in the sense of magnitude and direction and thus, results white noise, $\omega(t)$ i.e. $\frac{dB_t}{dt} = \omega(t)$ having covariance $Q\delta t$ where, Q is a diffusion matrix of Brownian motion and $\delta t = T_{k+1} - T_k$ [57].

Exploiting the benefits of enriched stability concepts of the deterministic modelling, it can be extended for stochastic systems. Although it is considered that the model incorporates all the information of the system, still some random effects remain unaccounted. These can be usually represented by white noise as it is entirely random without temporal correlation and infers that it gives a decent model with these impacts. The stochastic model includes model uncertainty (white noise) as a driving force in differential equations assuming the additive effect of noise in the deterministic model. Model uncertainties may be due to imprecise known or slowly varying parameters, approximate/unmodelled dynamics and can be included in a model by lumping a noise term [57], [58], [59].

Suppose a model is represented as: $\frac{dy}{dt} = \psi(X, \theta, t)$. After the introduction of noise in the system dynamics, it becomes $\frac{dy}{dt} = \psi(X, \theta, t) + N(t)$, where, N(t) represents noise. So, the stochastic model of a system incorporated both random and non- random forces and represented as SDE. Presence of random forcing function gives the solution of SDE, a random process. Further, for Gaussian noise, the formulation of $It\hat{o}$ SDE is

$$dX(t) = A(X(t), t)dt + \sigma_\nu(X(t), t)d\omega(t) \tag{2.1}$$

As in the general $It\hat{o}$ differential, $A(X(t), t)dt$ is the drift term, and $\sigma_\nu(X(t), t)d\omega(t)$ is the martingale term which has an unbounded and discontinous white noise process. We often call $\sigma_\nu(X(t), t)$ as volatility. A solution is an adapted process that satisfies above equation in the sense that

$$X(T) - X(0) = \int_0^T A(X(t), t)dt + \int_0^T \sigma_\nu(X(t), t)d\omega(t) \tag{2.2}$$

where, term, $\int_0^T A(X(t), t)dt$ is Riemann integral and term, $\int_0^T \sigma_\nu(X(t), t)d\omega(t)$ is known as an $It\hat{o}$ integral. Thus, model of continuous time stochastic systems is given by $It\hat{o}$ SDE doesn't evaluated like ODE. Rather, solution of $It\hat{o}$ SDE results Markov activities in which future value rely on the past only through the present.

The framework of $It\hat{o}'s$ is preferred over Stratonovitch for stochastic model due to the simplicity of $It\hat{o}'s$ to compute expectations, the existence of stability theory for $It\hat{o}'s$ integral, and application of many stochastic theorems including nonlinear filtering to this form [60]. However, a Stratonovich SDE can be transformed into an equivalent $It\hat{o}'s$ equation using simple formulas [61].

Consider two $It\hat{o}'s$ processes α_1 and α_2 $\forall(0, T)$ presented in integral form as:

$$d\alpha_1(t) = x_1(t)dt + y_1(t)d\omega(t)$$
$$d\alpha_2(t) = x_2(t)dt + y_2(t)d\omega(t)$$

$$\text{Then, } d(\alpha_1(t)\alpha_2(t)) = \alpha_1(t)d\alpha_2(t) + \alpha_2(t)d\alpha_1(t) + d\alpha_1(t)d\alpha_2(t)$$

The product $d\alpha_1(t)d\alpha_2(t)$ can be computed by employing $It\hat{o}$ rules:

$$dt.dt = 0,$$
$$dt.dB(t) = 0,$$
$$dB(t).dB(t) = dt.$$

In the proposed work, $It\hat{o}'s$ stochastic modeling has been used for a nonlinear dynamical system under the influence of stochastic noise. This stochastic model is further used for an optimal controller design using state observer approach in chapter 3. Then, control law has been formulated using $It\hat{o}'s$ calculus for getting the error dynamics of the system.

2.4 Estimation of state vector and parameters

A dynamical system is described by a mathematical model that involves a set of differential equations comprise of dependent and/or independent variables termed as states and involve constants known as parameters. The states can be measured directly using sensors etc., but parameters are not. The process to approximate the values of any quantity is termed as estimation and can be done for state or parameter for both purposes.

Estimation can be done in two ways. Off-line estimation, also known as static estimation, which is carried out using batch processing approach with observed data. In On-line estimation, the present estimate is acquired utilizing the information accessible so far could be refreshed when another bit of information is received.

State estimation

States of the system refer to a set of variables of interest that describe it completely. State of a robot, i.e., position, velocity, and orientation describe the motion of a robot at any time instant. The observation of system state lacks perfection due to some limitations like cost, technical feasibility, low quality, thus, introduces the problem in obtaining desired control features [62]. The velocity signal after derivating the position signal contains noise. Thus, to overcome the problem of unmeasured state or noisy state an estimator/observer to reconstruct the state from the available information has been suggested so that state observer based control can be implemented. The work of [63], [65] has demonstrated classification and applications of observers. Some of the popular approaches for estimating the states of a nonlinear system are given as:

- Extended Kalman filter(EKF): Extension of linear Kalman Filter [63], [64]
- Unscented Kalman Filter (UKF): Mix of Monte-Carlo with Kalman Filter [66].
- Recursive prediction error (RPE): Based on the sensitivity equation [67]
- Moving horizon Estimation [68].
- Particle Filter: For nonlinear and non-Gaussian Dynamic [69]
- High Gain Observers: PI observer uses integrated estimation error for robust estimation, Model-free observer: [70]
- Neural network observer: Model-free observer [71]
- Siding mode observer: Model-free observer [72], [73]

The comparative study of various real-time estimation methods of velocity signal from the observations of position is summarized in [73]. The issue of using model-based observer arises in the condition of poor knowledge of the plant which may be overcome using by High-gain observers and sliding mode observers. Although being model-free but suitable for a particular class of plants due to discontinuous behavior [74]. Further, an adaptive state estimation for partially known nonlinear dynamics has been proposed using neural networks which involves a prediction step and an update step, similar to the EKF [75].

The procedure of EKF approximates the nonlinear dynamics around the previous estimated state whereas, UKF uses the exact nonlinear dynamics and instead apply an approximate transformation law for the belief mean and covariance. EKF requires less information of the system in the controller design for the uncertain systems [76]. Generally, the selection of estimation method depends upon the particular application. Kalman filter is preferred as the best estimator in case of a unimodal distribution parametrized by its mean and covariance. It has the moderate computational burden as compared to other sampling approaches like particle filter [77], UKF, etc.

Convergence of observer is the primary concern while designing an observer for the nonlinear system. The issues involved in the design of the observers for the nonlinear system along with the possible solutions have been discussed in [78]-[79]. In this present study, EKF is the algorithm of choice for state estimation.

Extended Kalman Filter (EKF)

The commonly used filter for an unconstrained linear system that has normally distributed state and measurement noise is Kalman filter. It is a recursive optimal state estimator. The recursive in the sense that allows it to be practically implemented that it reprocess the latest measurement in spite of keeping all data in storage. EKF is a nonlinear version of the Kalman filter, and unlike this, it is a suboptimal estimator where propagation of state vector and the covariance matrix is done differently due to nonlinearity present in the system. The Kalman Filter periodically predict the state variables based on the system equations and subsequently correcting them by considering the sensor measurements. In a nonlinear system, state equation and measurement equations are a nonlinear function of state variables, so it is required to linearize the process and measurement equation at the current mean estimate and compute the Jacobian matrix. During the estimation process, the EKF algorithm linearizes the nonlinear transformation and calculates Jacobian matrices. The various steps in the process of the EKF algorithm are shown in Fig. 2.3.

Extended Kalman filter provides the solution of state estimation from a noisy measurement of a nonlinear system in the recursive process, i.e. prediction of states followed by a correction step. The prediction step projected the current state estimation and error covariance ahead over time and known as a prior estimate, $\widehat{X}(k)$. The correction step of the process incorporates the latest measurement into a priori estimate in order to correct the projected estimate and get the a-posteriori estimate $\widehat{X}(k+1)$ as shown in Fig. 2.4.

Parameter estimation

It is aimed to estimate the values of parameters dependent upon noisy observations. The maximum likelihood method is used to estimate the unknown parameter, $\boldsymbol{K}$ that maximizes the Log-likelihood function, or that minimizes the negative log-likelihood function [80]. The problem of parameter estimation lies

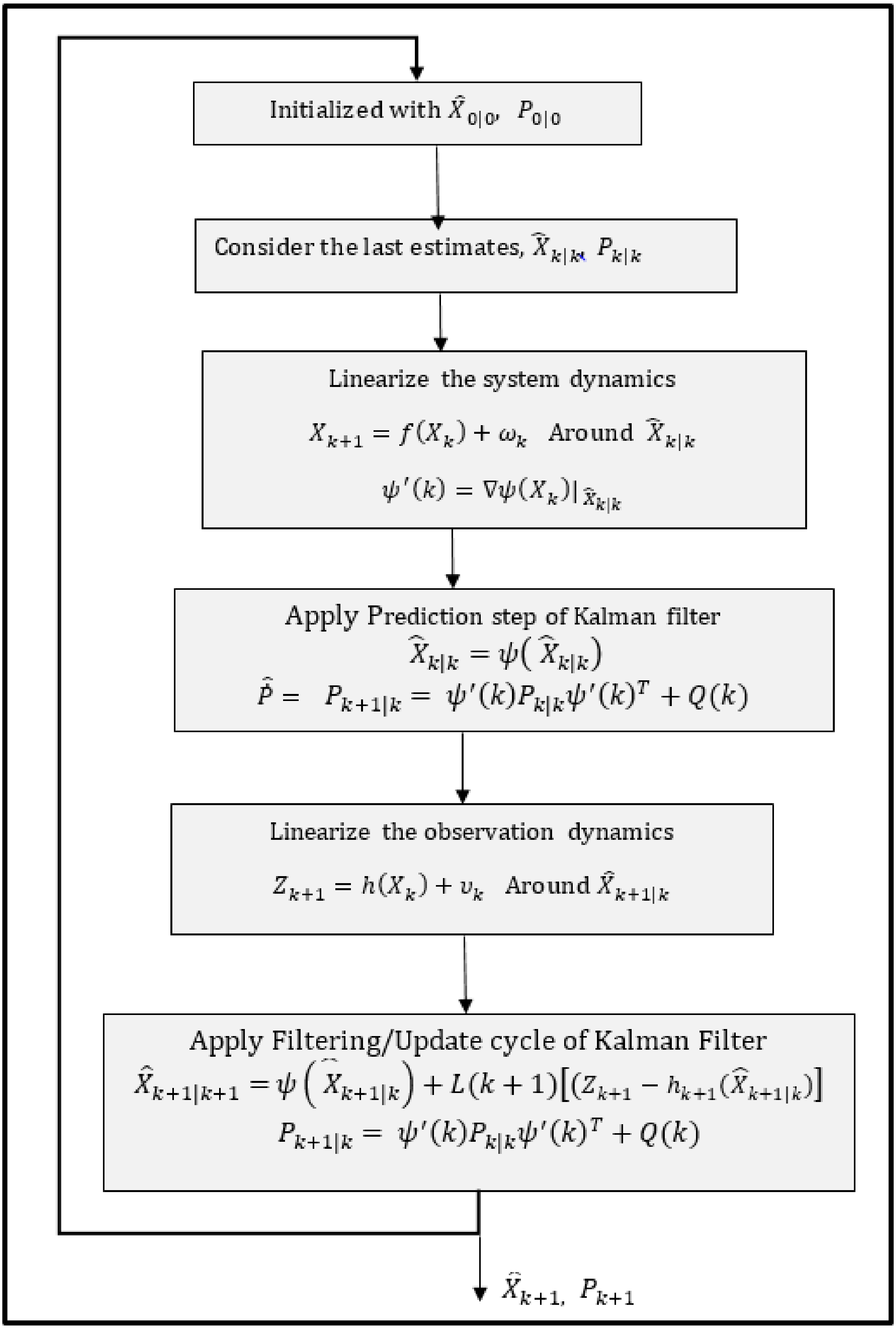

Figure 2.3: Algorithm of Extended Kalman Filter

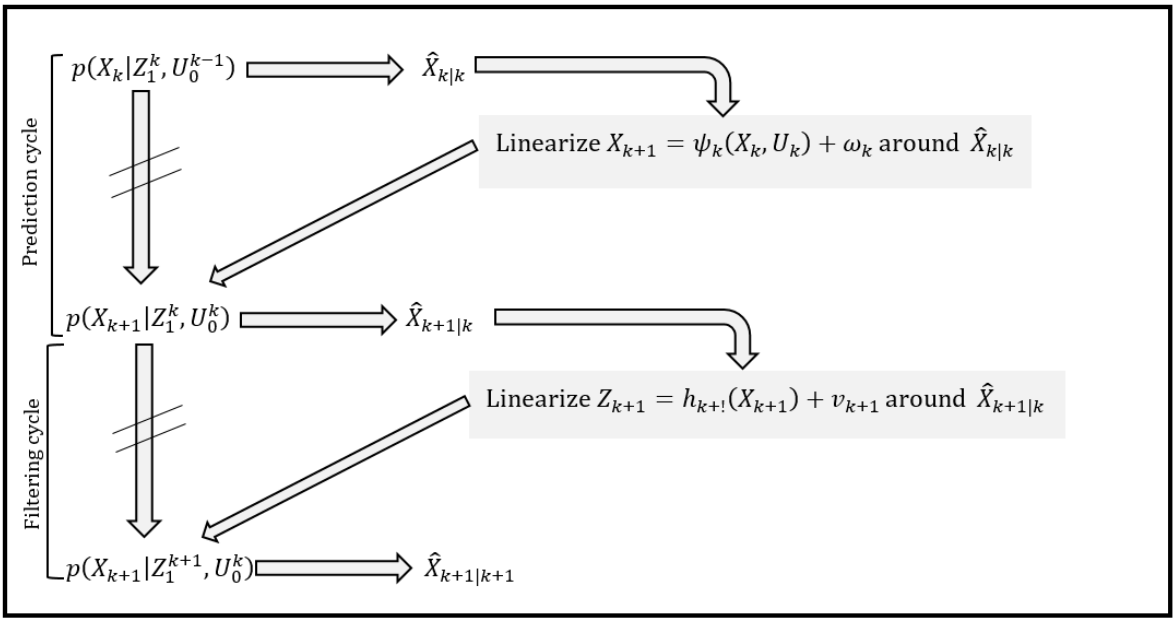

Figure 2.4: Concept of Extended Kalman Filter Dynamics

in predicting the values of parameter embodied in the noisy observations, $\boldsymbol{X[n]}$ which can be described by the probability distribution function (pdf). This pdf has dependence on unknown parameter, $\boldsymbol{K}$ i.e. parameterized by $\boldsymbol{K}$ as its value affect the distribution of observed data so, $\boldsymbol{K}$ can be inferred from the $\boldsymbol{X[n]}$. This can be shown as $\boldsymbol{p(X[n]|K)}$.

Maximum Likelihood Estimation (MLE)

A technique used to estimate an unknown quantity of interest from a sample of measurement such that the estimate maximizes the probability density function or equivalently likelihood function, $\boldsymbol{\mathcal{L}}$ formed from that measurements. This refers to that value of parameter responsible for producing the observed data most likely to have been observed [81]. Suppose, the data belong to a probability distribution, $\boldsymbol{p([X[n]|K)}$ with an unknown parameter, $\boldsymbol{K}$, the MLE of $\boldsymbol{K}$ is that maximizes the probability of observing the data most probable. Suppose, we have a sample of measurements $[\boldsymbol{q_1, q_2, ...q_k}]^{\boldsymbol{T}}$ of a system that depends upon an unkown parameter $\boldsymbol{K}$. These measurements are considered to be independently and identically distributed (i.i.d.). The aim is to find a MLE of $\boldsymbol{K}$ from these measurements. We need to maximize the augment of the likelihood function w.r.t.

$\boldsymbol{K}$ which is presented as $\boldsymbol{\mathcal{L}|K[q_1, q_2, ..., q_k]}$ that is equivalent to maximize the joint pdf i.e. $\boldsymbol{f[q_1|K, q_2|K, ...q_k|K]} = \sum_{k=1}^{N} \boldsymbol{f(X_k|K)}$. It would be more convenient to take argmax of log-likelihood function i.e.

$$\arg\max_{\boldsymbol{K}} \; \boldsymbol{log\mathcal{L}[K|q_1, q_2, ..., q_k]}$$

Thus, MLE of $\widehat{\boldsymbol{K}}$ is that value of $\boldsymbol{K}$ for which $\boldsymbol{\mathcal{L}[K|q_1, q_2, ..., q_k]}$ attains a maximum.

After estimation of parameter, the requirement is to check the goodness of the estmation of the unknown parameter. Some of the essential properties evaluate the quality of an estimator as described below:

Unbiasness: The difference between the expected value of the estimate and the true parameter value is called bias and estimation without bias is termed as unbias estimation. It is well known that in statistical inference, random samples are drawn from the population that provides an inference of that population. An estimator computes an unknown quantity from the sample which retains the information of that unknown quantity in the population. An estimator provides a mean to estimate a parameter value of population using sample data. This property satisfied for an estimate of a given parameter when the expected value of estimator is equal to the parameter being estimated. In other words, sample mean should be equal to unknown parameter for an estimator to be unbiased i.e. $\mathbb{E}(\widehat{\boldsymbol{K}}) - \bar{\boldsymbol{K}} = \boldsymbol{0}$, where, $\boldsymbol{K}$ is true value and $\mathbb{E}(\widehat{\boldsymbol{K}})$ is expected estimated value that is equal to mean value $\bar{\boldsymbol{K}}$.

Efficiency: The efficiency of estimator is measured by its variance. Estimator with minimum variance is said to be more efficient. The variance of an estimator is given as $\boldsymbol{Var(\hat{K})} = \mathbb{E}(\widehat{\boldsymbol{K}} - \bar{\boldsymbol{K}})$ which is an indicator that estimated value is more concentrated around the true value $\boldsymbol{K}$. An estimator with lowest variance is more efficient among two different unbiased estimators used to estimate same parameter.

Consistency: The unbiased estimator $\widehat{\boldsymbol{K}}$ of a parameter $\boldsymbol{K}$ is said to be consistent estimator if $\boldsymbol{var(\widehat{K})} = \boldsymbol{0}$ as $\boldsymbol{n} \to \infty$.

Unbiasness: The difference between the expected value of the estimate and the true parameter value is called bias and estimation without bias is termed as unbias estimation. It is well known that in statistical inference, random samples are drawn from the population that provides an inference of that population. An estimator computes an unknown quantity from the sample which retains the information of that unknown quantity in the population. An estimator provides a mean to estimate a parameter value of population using sample data. This property satisfied for an estimate of a given parameter when the expected value of estimator is equal to the parameter being estimated. In other words, sample mean should be equal to unknown parameter for an estimator to be unbiased i.e. $\mathbb{E}(\widehat{\boldsymbol{K}}) - \bar{\boldsymbol{K}} = \mathbf{0}$, where, $\boldsymbol{K}$ is true value and $\mathbb{E}(\widehat{\boldsymbol{K}})$ is expected estimated value that is equal to mean value $\bar{\boldsymbol{K}}$.

Accuracy: The degree of accuracy of estimation depends upon the dependency of pdf on unknown parameter [82]. This is shown in Fig. 2.5 where (i) indicates low influence of pdf on parameter as compared strong influence of pdf on parameter as shown in (ii). With fixed $\boldsymbol{X}$, pdf is equivalent to likelihood function, $\boldsymbol{\mathcal{L}(.)}$ and the accuracy of estimates is measured by the sharpness of the function. Sharpness of curve is measured in term of curvature. The curvature is negative of the second derivative of the likelihood function i.e. average curvature of average over random vector, X is given as

$$\boldsymbol{J}(\boldsymbol{X}|\boldsymbol{K}) = \mathbb{E}\left[\left(\frac{\boldsymbol{\partial^2 \ln p(X|K)}}{\boldsymbol{\partial K^T \partial K}}\right)\right]$$

This expression is known as the Fisher information matrix (FIM). Sharp curvature in (ii) indicates, concentrated pdf and thus, an indication of accurate estimation as compared to (i) of Fig. 2.5.

The related uncertainty of estimation is measured by its covariance w.r.t. the pdf of measurement noise. This can be done using Cramer-Rao Lower Bound (CRLB) which states that under certain regularity conditions, the inverse of the FIM is a lower bound on the true covariance of the estimator i.e. This states that the covariance of any estimator of $\widehat{K}$ is greater than the inverse of the FIM. Although [83] has suggested a method to evaluate the covariance of the MLE unlike the method of FIM. In spite of unmodelled dynamics, this approach has shown asymptotic accuracy of estimation but lacks consistency. Suppose, $\boldsymbol{K}$ denotes a deterministic variable that influences the outcome of a random variable, $\boldsymbol{X}$. Then, the representation of pdf for $\boldsymbol{X}$ depending on $\boldsymbol{K}$ is $\boldsymbol{p(X|K)}$.

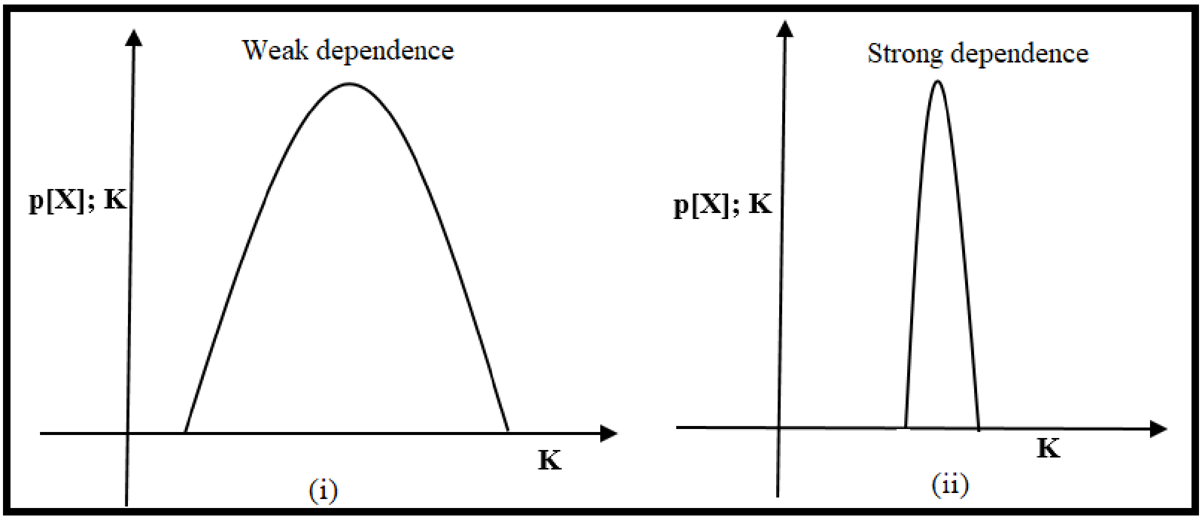

Figure 2.5: Indication of Dependence of pdf on K

Further, the unbiased estimate of $\boldsymbol{K}$ based on measurement, $\boldsymbol{Z}$ is $\widehat{\boldsymbol{K}}$ where, $\boldsymbol{Z}$ is drawn from $\boldsymbol{p}(\boldsymbol{X}|\boldsymbol{Z})$: $\boldsymbol{Z} \leftarrow \boldsymbol{p}(\boldsymbol{X}|\boldsymbol{K})$. Then, according to CRLB, the covariance of any unbiased estimate, $\widehat{\boldsymbol{K}}$ (which is based on $\boldsymbol{Z}$) of $\boldsymbol{K}$, is bounded by the FIM, $\boldsymbol{J}(\boldsymbol{X}|\boldsymbol{K})$ i.e. $\boldsymbol{cov}(\widehat{\boldsymbol{K}}|\boldsymbol{Z}) = \mathbb{E}[(\widehat{\boldsymbol{K}} - \boldsymbol{K})(\widehat{\boldsymbol{K}} - \boldsymbol{K})^{\boldsymbol{T}}] \geq \boldsymbol{J}^{-1}(\boldsymbol{X}|\boldsymbol{K})$
'Unbiased' refers $\mathbb{E}[(\widehat{\boldsymbol{K}} - \boldsymbol{K})] = \boldsymbol{0}$ and expression, $\boldsymbol{cov}(\widehat{\boldsymbol{K}}|\boldsymbol{Z} - \boldsymbol{J}^{-1}(\boldsymbol{X}|\boldsymbol{K}) \geq \boldsymbol{0}$ i.e. positive semidefinite, refers to 'bounded' estimation .
The expression for FIM is presented as:

$$\boldsymbol{J}(\boldsymbol{K}) = -\mathbb{E}\left(\frac{\boldsymbol{\delta^2} \log}{\boldsymbol{\delta K \delta K^T}} \boldsymbol{p}(\boldsymbol{X}(.)|\boldsymbol{K})\right)$$

A detailed account of parameter estimations has been given for the models that are linear in the parameter vectors [84]. Instead of a finite linear model in block form, implementation of the MLE on the non-linear time series generator of the robot dynamics is accomplished in the present work. Though the dynamical system is nonlinear in the states, its differential equation is linear in the parameters. The discussion of parameter estimation in diffusion process is illustrated in [85] and problem-related to this article is a particular case of these methods. The maximum likelihood estimation technique combined with CRLB for efficient estimation of parameters is shown in [56], [86] [87], [88], [90] with reference to linear and non-linear stochastic systems. Various examples of MLE of parameters applied to problems has been explained in the form of $X(t) = S(t;\theta) + W(t); t \,\epsilon\, [0;T]$ and also to dynamic linear state model of form $X(t) = A(t;\theta)X(t) + W(t)$ but [89] does not focus on non-linear differential equations of the form $X(t) = A(x(t); t; \theta) + W(t)$ which is relevant to problem mentioned in the proposed work. The disadvantage of MLE is that it frequently requires an assumption about the structure of data. In this thesis, an investigation of both methods of estimations as mentioned earlier is carried out. Two separate research problems are framed by considering state estimation and parameter estimation from the noisy observations and known input. First, the state estimation of n-link robot manipulator is done through EKF for the implementation of state observer based tracking control and the second problem is to estimate the controller gain parameters via MLE for trajectory control of a master-slave robotic system.

2.5 State-observer-based control

A comprehensive survey of robust controllers is presented in section 2.1, contributed to the tracking control of the robot. All claimed their best to fit in the scenario of nonlinearlity and uncertainty in the system. However, a question arises, "Is the feed to a controller is a clean signal"? This evokes the need to look at the problems faced in the cases of noisy sensors, unavailability of the velocity signal, etc. State observer based control has become an alternate approach [100],[101] and used where the realization of carrying out measurements is technically challenging and economically not viable. In the present study, the primary objective is recursive optimal redesign by combining the procedure of state estimation and robust control into a unified stabilizing controller.
An algorithm used to reconstruct the unobservable states from the output measurements of the system. For estimation of state, it requires the information of dynamics of plant and measurement, statistics of process and measurement noise and initial conditions.
It is considered as a dynamical system which takes process input(u) and output(y) as its input. The rate of change of estimate, $\dot{X}$ consists of two-term: (i) $A\widehat{X} + L(Y - \widehat{Y})$ with estimated state $\widehat{X}$ replaced with actual state X. (ii) $L(Y - \widehat{Y})$; where L denotes observer-gain that decides the weight and distribution of error 'e' among states. The error, $e = (Y - \widehat{Y})$, i.e. difference of measured

output Y and estimated output, $\widehat{Y} = C\widehat{X}$, also known as predicted output by the observer. It has the advantage that the error feedback to a controller is based on the observer output rather than the actual state incorporating noise. In state observer based control, the dynamics of the controller is generated by the observer. The state of the present dynamical system is defined by position and velocity at any given time. Velocity signal is achieved either by direct measurement or by differentiating the measured position signal, which may add cost, weight, and noise [102]. This degrades the performance of the system [103]. In this present work, the authors have, therefore, estimated the states using Extended Kalman Filter (EKF). Here, position estimates $(\widehat{q})$ and velocity estimates $(\widehat{\dot{q}})$ are used to implement computed torque control (CTC) for the tracking control of n-link robotic manipulator.

Developing the observer-based controller for a nonlinear system is not an easy task due to the absence of the separation principle, and usually, the design of an observer is coupled with the design of controller [104]. Although the convergence of observer is the main concern while designing an observer for the nonlinear system, still the stability of the closed-loop system is threatened due to phenomena of finite escape time [105]. A robust linear filter has been proposed a state-space model with real time-varying norm-bounded parameter uncertainty and nonlinear disturbances meeting the boundedness condition [106].

Feedback control using filtered tracking error has been proposed based on quadratic Lyapunov energy function [107]. Despite selecting a quadratic Lyapunov function, a highly nonlinear logarithm function has been suggested for the tracking control of n-link robot manipulator [108]. The control law ensures bounded asymmetric Lyapunov function for the state to be bounded. This approach prevents the state from reaching a boundary where the Lyapunov function becomes infinite and ensures bounded tracking errors. However, there would be a small probability of state tracking error escaping away from the boundary in the presence of noise. The proposed algorithm takes into account stochastic disturbances in the state evolution as well as in the measurement process. Here, minimization of the mean square tracking error is based on observer state estimates of noisy state measurements since exact state measurements are

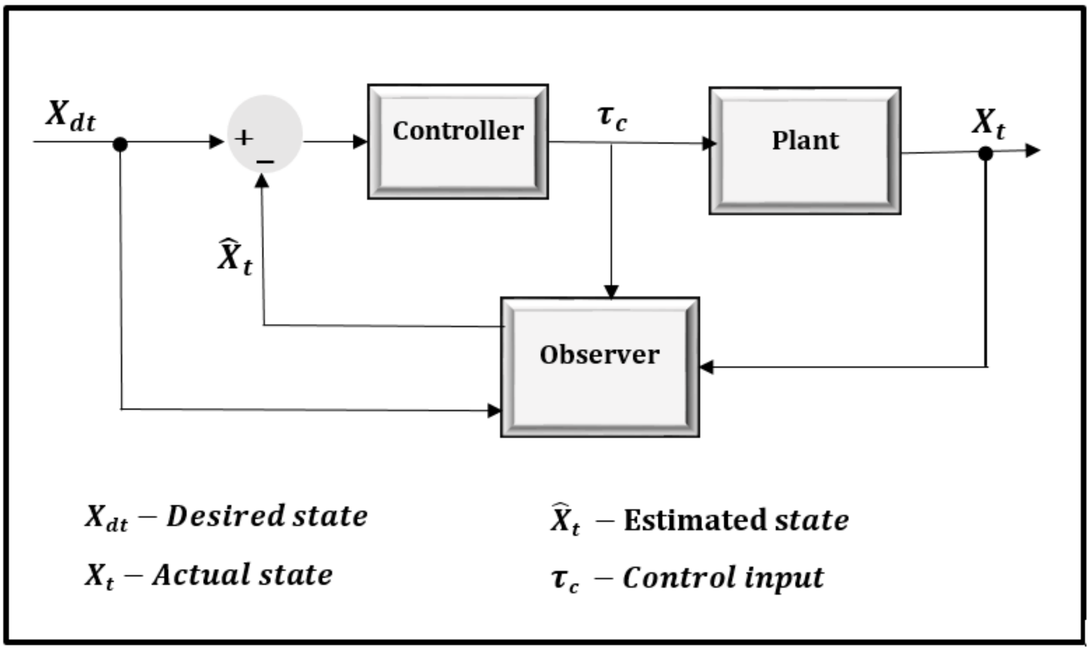

Figure 2.6: Block Diagram of State-observer-based Control

not feasible in general. In the present work, minimization of instantaneous conditional mean square tracking error energy is considered instead of Lyapunov criterion for control design. The results of He et al.[108] guarantee that the trajectory tracking error remains bounded for a deterministic problem while the results of the proposed algorithm guarantee that the mean square error is minimized for a stochastic problem. Both nonlinearity and external disturbance have been accommodated as a total disturbance in the nonlinear state-space model and employed PI observer to observe the state [109]. Further, by using linear control technique, output error has been converged to zero.

In the absence of measurement noise, recent research has been reported on the methods of robust control, adaptive control, nonlinear-PID control, H-∞ control, sliding mode control, DOB control etc., to meet the issues of stable tracking control [110], [111], [112], [113], [114], [115], [116], [117]. However, in the physical system, noise is an inherent part of measurand and need to be considered while designing the controller [118], [119],[120], [121]. Artificial intelligent techniques are used to develop the controllers using input-output data of the process when a model is not available, or uncertainties are present in the system [122], [123], [124]. He and Dong have developed a fuzzy-neural-network-based control strategy so that the tracking error and impedance error remain bounded [123]. They have shown that a quadratic Lyapunov function of the tracking error, auxiliary state, and the neural weight vector has a negative rate of increase, thereby, guarantees asymptotic stability. When stochastic disturbances are present in the robot state model as well as in the output measurement model, it would be interesting to study the response of a feedback controller. The approach of He et al. [123] can be adopted; however, the rate of change of Lyapunov function may use $Ito's$ formulae for stochastic calculations. Further, the result show bounded tracking error, but in the presence of noise, there could be sparsely located random spikes in this error. In the proposed work, the controller takes into account the stochastic disturbances which would smoothen out these spikes, and this may improve the results. An adaptive fuzzy neural network learner of state constraints of a robot has been discussed [124]. The learner requires lesser data for learning about the uncertainties and also, it learns about the robot-environment interaction. The effects of state constraints, i.e. inequality constraints on tracking error are learned, and control law has been designed to ensure stability in accordance with a Lyapunov function. In this proposed work, the authors have developed state model in the form of stochastic differential equation (SDE). It may be modified by considering such inequality constraints when an error is smaller or greater than a threshold value. Chen et al. [125],[126] have studied the uncertainties present in the system using a modified bounded Lyapunov function known as Nussbaum function. They have also developed an adaptive control of a multivariable system for asymptotic stability by adjusting a single control parameter ensuring bounded tracking error [127]. However, such methods do not explicitly intend to relieve the prones of measurement noise [128]. In the latest research, the problem of measurement uncertainty has been solved by developing Risk-sensitive optimal control algorithms [129].

The alternative way to compensate for noise is the implementation of disturbance observer-based(DOB) control which provides feed-forward control [130], [131] to cancel out the uncertainty.

However, the limitation of DOB control is the requirement of sensors to measure the disturbance that is a difficult task in practice. The presence of noise in the system dynamics has been embodied in the stochastic model in the framework of Stratonovich SDE [132]. Subsequently, for tracking control, Lyapunov machinery has been designed to process the state feedback law to assure tendency of mean square tracking error to an arbitrarily small neighborhood of zero. In the proposed approach, the modeling of a stochastic system is done in the framework of It$\hat{o}'s$ that provides effective modeling as well as helps to frame a control law such that system can work adaptively and can be implemented on the real device. These features including assurance of robustness in case of variation in system variables have not found in the work of Ming et al. [132].

Design of Observer-based controller for a nonlinear system has a significant problem of stability due to the absence of separation principle which works only for a linear system. The main problem in observer-based control for a nonlinear system is that stability can't be assured even if the nature of observer is asymptotic convergent and providing estimated states in place of actual states. This is because the separation principle does not work for a nonlinear system where the computation of controller gain and observer gain can be done independently. In the proposed work, the controller design, $\widetilde{K}_t$ that is a function of observed states has taken into account the estimation error, e_t.

2.6 Robot interacting with randomly structured environment

There exists a wide spectrum of controllers to tackle the potential problems related to master-slave robotic systems [133], [134]. The problems of parameter uncertainty, time delay, disturbance, loss of information, transparency, etc. are the subject of present research and researchers have suggested various control techniques to tackle some of these problems. Model prediction adaptive controller [135], Robust μ -Synthesis controllers [136], [137], Intelligent controllers [138], [139], [140], Nonlinear and Composite Adaptive controller [117], [141] have been used to control such dynamical systems. Further, the Environment, Operator and Task (EOT) adaptive controllers have been considered highlighting the importance of online information for the control [142]. However, many times, online information is not available due to various limitations and the researchers have to cope with the uncertainty.

The interaction of environment cause to alter the dynamics of the robot and requires a controller for trajectory tracking. The design of controllers becomes significant when constrained motion occurs, i.e. the manipulator interacts with its environment. Although impedance control [123], [143] and admittance control [144], [145] have been proposed while interacting robot with the environment but these controllers need to know the environment forces. To avoid force sensors, either disturbance observer or force observer are recommended. However, in many cases, determination of impedance or admittance models may be cumbersome in case of a complex environment. Further, iterative learning control (ILC) scheme has been employed for a robot to adapt unknown environment [146]. This requires human learning skills which may be inconvenient as it demands repetitive operation of a device. In the aforementioned schemes and in most of the other cases, environmental force has been modelled as a spring-damper system and its variants [142], [147], [148], [149],[150], [151]. Another approach is to regard it as an external disturbance [100], and disturbance observer has been suggested to estimate the environment forces. Cui et al. [152] has considered a random vibration environment and proposed backstepping control for tracking control in the presence of stochastic environment without estimating it. Environment has been considered as dynamic uncertainty and estimate it using moving horizon estimation [153]. The dynamic environment's effect is more realistically modeled with states of the robot and obstacle as random variables [129], [132]. Emphasizing on the importance of knowing the uncertainty in the system to monitor controller performance and estimator design, [154] has estimated the noise covariance matrices. In the present study, the MLE method has served the purpose of both controlling the system in the presence of noise as well as given the idea of the structure of the sample noise trajectory.

Advance surgery requires knowing the contact forces between the slave robot and the environment (which may be tissues) for better coordination and realizable operation [155]. Dynamics of tissues may be helpful for successful surgery as it improves the control during telemanipulation in addition to simulation development for training and conduction of automatic diagnosis. The problem arises in allocating force sensors to a robot because of size, precision, disposable, complexity due to connections, isolation of tissues and requirement of heavy current and temperature for the procedure of surgery cuts and sterilization of sensors[156]. Thus, the perception of an environment through the sensor is not recommended. Further, in the scenario of the interaction of a robot with an uncertain environment, the function of a controller is to generate an actuating signal which in turn counterbalance the adverse effects of uncertainty. The determination of the actuating signal will be easy if uncertainties are measurable which in general not feasible, so it leads to a significant problem of estimation of the environment. The designing of controllers seeks the evaluation of environmental force as all robots ultimately perceive the world through limited and improper sensors. Estimation of unknown parameters using output noisy measurement data has been used in literature. Least square (LS) method works on minimizing the cost function of squares of residual error [157], and it has been proposed to estimate the time constants of a second order LTI system from discrete output measurements [158] that is essentially a maximum likelihood method with the assumption of measurement noises as i.i.d. Gaussian. Then based on the second order partial derivatives of the measurement error energy w.r.t the parameters, an iterative scheme is proposed to obtain a Newtonian iterative algorithm for parameter estimation. The method will, however, require modification if the system is nonlinear as it is in robotics problems. One way to use that approach for nonlinear systems is to expand the nonlinear terms in the dynamical system as a power series in the state variables and then apply perturbation theory to obtain an approximate solution to the system regarding the parameters. After that, the measurement in error energy can be minimized by the Newton-iteration algorithm. EKF has been used to estimate $\dot{\boldsymbol{q}}$, variation in physical parameter, and the environment force with noisy state measurements [100]. EKF is suboptimal technique as it does not give the minimum mean square state estimate error(MMSE). Although Kushner filter can provide an optimal MMSE, it is not implementable as it is an infinite dimensional filter.

Least square (LS) method to a linear system is applied in the work of Pan et al. [44] whereas, in the present study, it is applied to a nonlinear system followed by linearization. Both LS and ML methods result optimal estimates provided that the disturbance is assumed to be WGN. Multi-variable systems parameters estimation and control are discussed for moving average noise [120]. This is a linear system, and both control inputs and noise are present. The moving average disturbance has been transformed into an autoregressive disturbance and then, the LS algorithm is proposed to identify the system parameters and further, results are compared with the study of Liu et al. [159]. This technique can be adapted to a nonlinear system after some modification. Designing of a controller by considering the measured data as a joint pdf in combination with the estimation and convergence analysis of noise is not available to the best of our knowledge in the literature. Furthermore, no work has been reported on MLE of the Proportional-Derivative controller's coefficients of a robot, nor does exist any computation of CRLB of the component vector comparing the matrix elements of the controller's gain parameters. The proposed work is a novel application of MLE of nonlinear dynamics of a master-slave robotics system. Moreover, the evaluation of the CRLB from approximate statistics of the robot angular position and angular velocity perturbations is obtained from the correlation theory of Gauss-Markov process [80]. In the proposed approach, stochastic environment force is introduced into the dynamics of the slave robot that added formidable complexity into robotic systems dynamics. In this work, MLE has been proposed for estimation of controller gain parameters and then to back substitute these controller estimates into the dynamics and thereby estimate the sample trajectory of the environmental noise process. Finally, an approximate expression is derived for the CRLB on the parameter-estimation-error -covariance matrix. This lower bound sets a limit to the accuracy to estimate a parameter that influences a probability density.

2.7 Stability of nonlinear and uncertain system

Stability of the control system is a primary requirement and must be ensured before implementation of a controller to a system. The approach of Lyapunov is usually applied for ensuring the stability of both linear and nonlinear system [6], [8]. This approach requires the formation of a suitable scalar function known as Lyapunov function and its derivative. Consider a scalar function, $V(x)$ which is continuously differentiable and satisfy the following conditions along the system trajectories i.e. $V(0) = 0$; $V(x) > 0$ and $\dot{V}(x) \leq 0$. The system is stable. Formation of Lyapunov function for each specific problem particularly for a nonlinear system is a challenging task, and upon the availability of this, stability can be analyzed concerning perturbations and time variations. Stability of deterministic nonlinear system using directly or indirectly Lyapunov machinery is widely exploited in literature [160], [161], and further extended to address the stability of stochastic nonlinear control system [149], [162], [163]. Further, various concept and tools are associated with analyzing the stable behavior of the system. A concept such as convergence of error signals are also one of the technique to judge the stable behavior of the system without explicitly solving the dynamic equations, and presents corresponding definitions of stability [6]. For the problem of tracking control, the concept of stability is usually based upon convergence in the mean square criterion.

Investigation of stability has been pursued by various methods for the nominal system that assures the system is not going to explode in some sense. Here, the unperturbed system means a nominal system but if the nominal system is suffered from uncertainty, robustness has to be satisfied that demand stability margin in some form. This assures that system maintains stable behavior even in the presence of uncertainty of an expected range in the nominal system [164]. Robustness refers to an attribute of the dynamic system to tolerate variations in the parts of the system without exceeding pre-defined tolerance bounds in the vicinity of some nominal dynamic behavior [165]. In case of prior knowledge of bounds on noise, techniques of robust control have been worked out [44], [166], [167]. However, in the case of unbounded noise with fast fluctuations, [55] has suggested applying the ensemble average rate of decrease of Lyapunov error energy function rather than a rate of decrease in the Lyapunov function.

Change in any parameter of the closed-loop system may result in a change in the coefficients of closed-loop dynamics concerning characteristics polynomial or state space description. The change in system behavior corresponding to variations in the parameter can be reflected in the state transition matrix, Eigenvalues, state variables, transfer function or step response, stability radius and some index of performance [168]. There may not be direct relation between the changes in the parameters and corresponding changes in the coefficients of the closed-loop system. In spite of that, it is required to check that allowable parameter changes without causing an inadmissible change in the dynamic system behavior. Sensitivity analysis is done to see the effect of parameter variation on the system behavior. Generally, uncertainty is considered to be unknown perturbations and stochastic noise with bounds or norms of their magnitude [169]. For interpretation of stability of the system with unknown uncertainty lies in a prescribed set, mathematical tools like norms are used for the perturbation and error analysis along with boundness of the signals.

The size of signals is measured with the help of norm function by considering them as the elements of a vector space. Different norms are used to express different forms of signals. signals are the function of time so, L_p norm (for $p \in [1; \infty]$)is used. For example, peak magnitude is expressed by $\infty-$ norm, the square root of energy by $2-$ norm and action of a signal is denoted by $1-$ norm.

The square root of the energy of the continuous-time signal, $e(t)$ can be represented as L_2 norm. Where, $e(t)$ is a vector signal.

$$\|e\|_2 = \left[\int_{-\infty}^{\infty} e^T(t)e(t)dt\right]^{1/2}$$

Similarly, peak amplitude of $e(t)$ evaluated over all signal components and all time is given by L_∞.

$$\|e\|_\infty = \sup_t \max_i |e_i(t)| = \sup_t \|e\|_\infty$$

Two types of matrix norm for matrices $X = (e_{ij}) \ \epsilon \ \mathbb{C}^{n,m}$ are defined as follows:

Frobenius norm: $\|X\|_F = (\sum_{i=1}^{n} \sum_{i=1}^{j} |e_{ij}|^2)^{1/2}$

Spectral norm (or 2-norm): $\|X\|_2 = (\rho(X * X))^{1/2} = \sigma_{max}(X)$
where ρ denotes the spectral radius and σ_{max} is the largest singular value.
The concept of uniform asymptotic stability is usually applied for robotics. When it is desired robot to move at a point, the interset is to converge at that point rather than stay nearby to it [170]. Exponential stability refers to uniform asymptotic stability and significant in showing the robustness of the system under perturbations. Gronwall-Bellman lemma approach has been applied for the exponential stability of nonlinear system [171]. The real systems are prone to uncertainty, and practical stability is significant which requires a solution of the system lies around the equilibrium point and thus, guarantee acceptable behavior of the system even in the presence of perturbations.
In recent years, quite many research studies related to the stability analysis of stochastic nonlinear dynamic system have been presented. The asymptotic stability of linear dynamical systems has been assured using a nonlinear controller in which the system and input matrices, as well as the input, are uncertain [172]. Despite what the uncertainties are, ultimately bounded solutions will guaranteed every solution to enter a neighborhood of the zero states infinite time and thereafter start within that neighborhood. Furthermore, the norm of output tracking error will asymptotically converge to a tunable residual set whose level of magnitude depends on a design parameter of an averaging filter as $t \to \infty$ [173].
Aside from control engineering, closed-loop stability is barely an objective, but the optimum solution regarding the energy seems more focused on industrial applications. The genetic-based algorithm has been proposed to minimize the power consumption of a physical system without the stability analysis [5].
Design of robust controller considering system nonlinearity and uncertainty prefers stability to be satisfied in the context of a stabilization region known as the domain of attraction [174] instead investigating stability in a sufficiently small vicinity of the equilibrium point. Robust stability means stability in the presence of any allowable uncertainty or nonlinearity. [175] has analyzed the robustness of nonlinear system which is linearized through state feedback using linear matrix

inequalities for a single input and single output system. Contrast to their work, robustness is ensured in the present work using numerical techniques for an indirect method of Lyapunov for MIMO system on the same concept of Corless et al. [176] that has explored robust stability of uncertain nonlinear systems using quadratic Lyapunov functions. A new stability criterion is derived for the stochastic nonlinear system by using the Lyapunov functional approach. Based on this, the design procedure of observer-based controller is presented, which ensures asymptotic stability in the mean square of the closed-loop system [177].

In this thesis, sensitivity analysis is carried out to check the error-dynamics by varying controller gain values and parameter values.

2.8 Conclusion

In this chapter, the literature survey has been carried out on the defined problem and associated area. The survey urges the research towards investigating such reports and unearth the facts and major of them are as follows:

The challenge of tracking control includes the stochastic behavior of a system that may be due to modeling and measurement error, and robustness of the system is not fully guaranteed. Access to measurements is a prerequisite in the controller design as it helps in to detect faults, monitor performance, or exercise control. The situation, where it is expensive or even impossible to have measurements, estimation is produced instead. An overview of recent developments in the estimation methods of recursive state and batch discrete-time have been presented. Observer-based control provides a solution for output feedback control problem in a situation where it is not possible to imply all states directly for feedback. This serves as the motivation to seek a general framework for the design of observer-based control for robotic manipulators. Apart from the exhaustive survey, the study has included the critical points when a robot has interaction with the environment.

Chapter 3

State-Observer-Based Controller for Stochastic Dynamical System

3.1 Introduction

This chapter deals with a generalized linear feedback matrix controller designed for the state of a nonlinear dynamical system to track the desired trajectory in the presence of stochastic noise. The proposed control algorithm takes into account the stochastic disturbances in state evolution as well as in the measurement process. Here, minimization of the mean square tracking error is based on estimated states of noisy state measurements. Fig. 3.1 shows that the error signals (e and $\dot{e}$) to the controller in the present study depends on the estimated state, $\widehat{\boldsymbol{X_t}}$ from the state observer instead of actual state, $\boldsymbol{X_t}$. Extended Kalman filter (EKF) is used as state observer which using the noisy position signal, $\boldsymbol{q_t}$, provides estimated state, $\widehat{\boldsymbol{X_t}}$. The novel feature of this control algorithm design is based on It$\hat{o}'$s stochastic calculus for the minimization of an objective function. The objective function is defined as the conditional expectation of the instantaneous tracking error energy differential with respect to the controller gain feedback matrix subject to energy constraints. The proposed control algorithm enables the adaptive features for achieving tracking of a system.

The problem is formulated in a general stochastic differential equation (SDE) format considering a specific structure of the controller being described by a quadratic constraint on the PD controller coefficients.

In section 3.2, the state dynamics of the system is formed from a set of coupled stochastic differential equation(SDE) of the plant. In section 3.3, measurement model with white Gaussian noise for the robot state is derived by another SDE related to state observer. Extended Kalman Filter is set up with an appropriate observer gain matrix, $\boldsymbol{L_t}$. In section 3.4, the dynamics of state and observer is computed for the state tracking error($\boldsymbol{k_t}$) covariance matrix and observer state error($\boldsymbol{e_t}$) covariance matrix using the Itô′s differential rule for Brownian motion. The conditional expectation of differential of tracking error-covariance (error-energy) given the previously estimated state has been derived. The trace of this tracking error-energy is minimized with respect to the feedback controller coefficients, $\boldsymbol{K_t}$ under the energy constraints on the $\boldsymbol{K_t}$.

The work presented has exploited the stochastic theory to model the plant, an objective function is framed which is minimized using optimal constraint control, implemented a linearized feedback control effort using inverse dynamics approach.

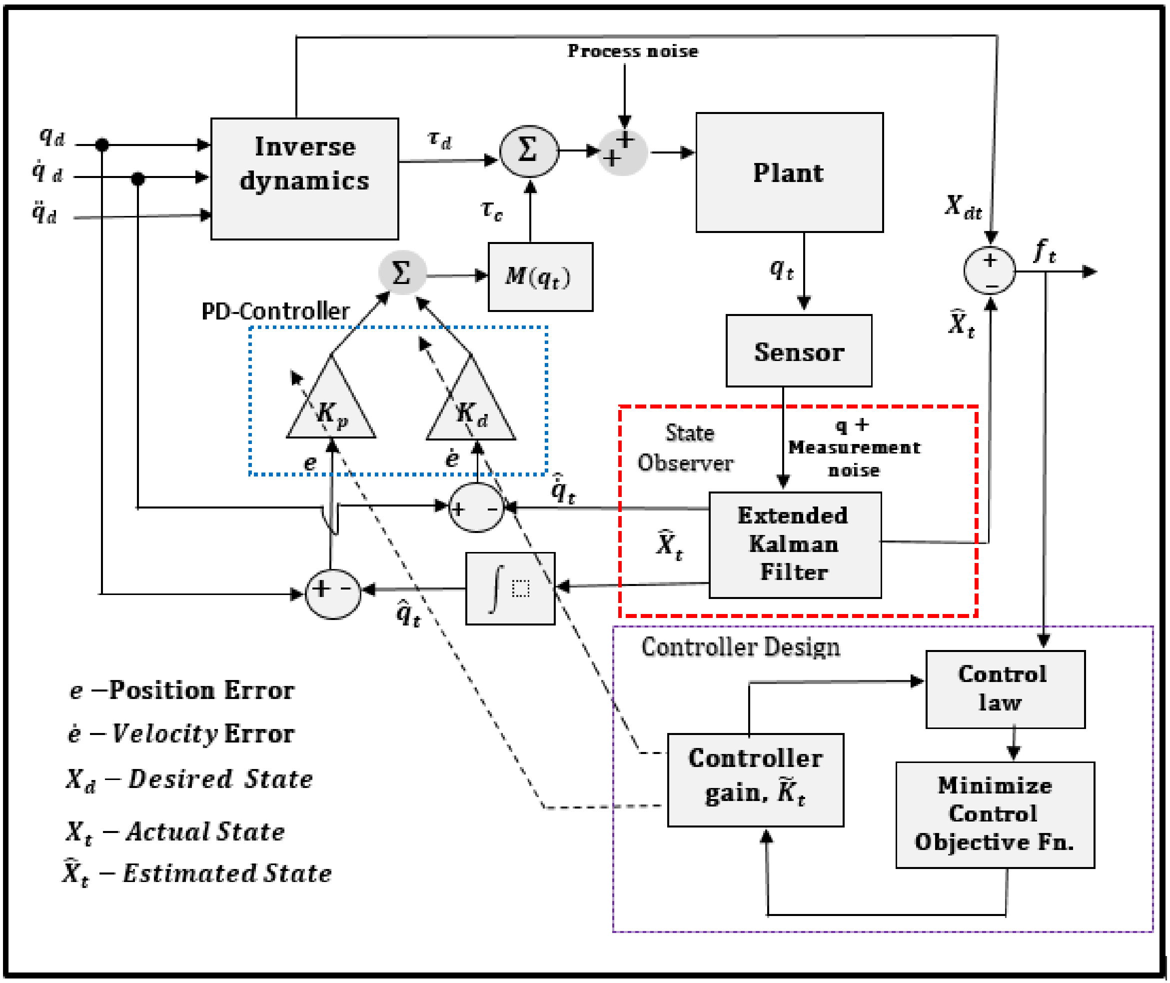

Figure 3.1: Block Diagram of State-Observer- Based Controller Design.

The control system has adaptively incorporated simultaneous estimation process of states and control of the plant. Further, the robustness of the system is ensured by the bounded error signals of the closed-loop system.

3.2 Stochastic model of dynamical system

A stochastic model is an extension of the deterministic model (expressed as ordinary differential equations) perturbed by random noise. The stochastic model for a nonlinear continuous-time system driven by a torque having white Gaussian noise component is represented using the $It\hat{o}'s$ stochastic differential equation in this section.

Consider a system in the framework of Euler-Lagrange model with position and velocity vector as $\boldsymbol{q_t}$ and $\dot{\boldsymbol{q}}_t$ respectively. The representation of state dynamic equations without feedback is given as:

$$\left.\begin{aligned}
&\boldsymbol{dq_t = \dot{q}_t dt,}\\
&\boldsymbol{d\dot{q}_t = F(t, q_t, \dot{q}_t)dt + G(q_t)dB_t}\\
&\text{So in matrix form:}\\
&\boldsymbol{d}\begin{bmatrix}\boldsymbol{q}_t\\ \dot{\boldsymbol{q}}_t\end{bmatrix} = \begin{bmatrix}\dot{\boldsymbol{q}}_t\\ \boldsymbol{F(t, q_t, \dot{q}_t)}\end{bmatrix}\boldsymbol{dt} + \begin{bmatrix}\boldsymbol{0}\\ \boldsymbol{G(q_t)}\end{bmatrix}\boldsymbol{dB_t}
\end{aligned}\right\} \tag{3.1}$$

Where, $F(t, q_t, \dot{q}_t) = -M(q_t)^{-1}N(q_t, \dot{q}_t) + M(q_t)^{-1}\tau(t)$, $G(q_t) = \sigma_\omega M(q_t)^{-1}$ and $\tau(t)$ are the non-random components of the torque while dB_t is the noise component of the state.

Remark 1. The equation (3.1) can be derived by applying the Euler-Lagrange dynamic formulation: $L(q, \dot{q}, t) = \frac{1}{2}\dot{q}^T M(q)\dot{q} - V(q) + \tau(t)^T q$ and then adding noise to the system of differential equation. Here, $L(q)$ denotes Lagrange function, $V(q)$ is the gravitational potential energy. $M(q_t)$ is a positive-definite symmetric matrix which is the function of position and $N(q_t, \dot{q}_t)$ is a function of both position and velocity respectively.

The execution of the control process is illustrated with the help of the block diagram shown in Fig. 3.1. It is required that the system state trajectory, $\boldsymbol{X_t}$

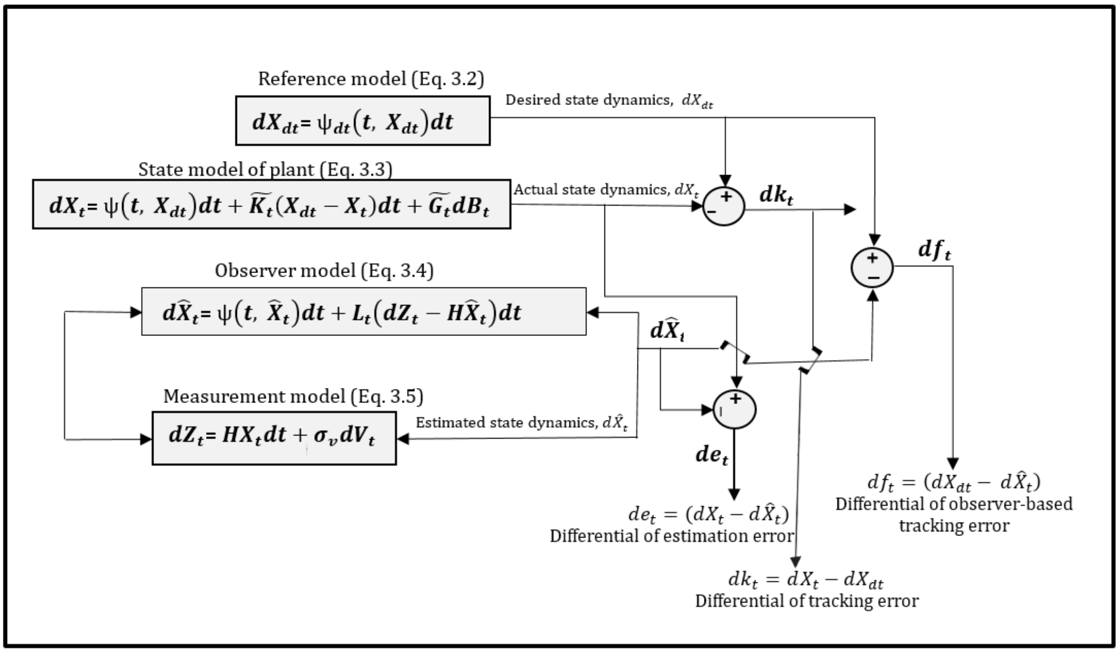

Figure 3.2: Dynamics of Errors Involved in Sytem

should follow the desired state trajectory i.e. $\boldsymbol{X_{dt}}$. The non-random desired state follows the same dynamic as the original state SDE except that neither process noise nor feedback is present in this deterministic dynamics. The situation in which the desired state dynamics is the same as the noiselesss state dynamics can be represented as:

$$\boldsymbol{dX_{dt} = \psi(t, X_{dt})dt} \tag{3.2}$$

The closed loop system state, $\boldsymbol{X_t}$ combines joint angular position and velocity and is given by $\boldsymbol{X_t} = \begin{bmatrix} \boldsymbol{q}_t \\ \dot{\boldsymbol{q}}_t \end{bmatrix}$.

The state observer estimates the states denoted by the vector $\widehat{\boldsymbol{X_t}}$ and is defined as, $\widehat{\boldsymbol{X_t}} = \begin{bmatrix} \widehat{\boldsymbol{q_t}} \\ \widehat{\dot{\boldsymbol{q}}_t} \end{bmatrix}$.

For optimal design of observer as well as state feedback controller (based on observer state), three types of error are considered: $\boldsymbol{e_t}, \boldsymbol{f_t}$ and $\boldsymbol{k_t}$. The dynamics of these errors are obtained from the desired state dynamics, observer dynamics, and actual state dynamics. The error dynamics is shown in Fig. 3.2 and utilized in the succeeding sections for the design of state observer based control. In this system, the errors which are based on the observed state, $\widehat{\boldsymbol{X_t}}$:

the state estimation error, $\boldsymbol{e_t} = \boldsymbol{X_t} - \widehat{\boldsymbol{X}}_t$ and the state trajectory tracking error, $\boldsymbol{f_t} = \boldsymbol{X_{dt}} - \widehat{\boldsymbol{X}}_t$.

It is shown that the position measurements, $\boldsymbol{q_t}$ are taken by sensor and the state observer estimates the state $\widehat{\boldsymbol{X}}_t = [\widehat{\boldsymbol{q}}_t \quad \widehat{\dot{\boldsymbol{q}}}_t]^{\boldsymbol{T}}$ using EKF. These estimated states are compared with the desired states of the predefined time-varying trajectory, $\widehat{\boldsymbol{X}}_{dt} = [\widehat{\boldsymbol{q}}_{dt} \quad \widehat{\dot{\boldsymbol{q}}}_{dt}]^{\boldsymbol{T}}$ to get the error signal, $\boldsymbol{f_t}$ as shown in Fig. 3.1.

The closed-loop dynamics of the system when the the state observer is coupled to PD controller can be extended as

$$\left.\begin{aligned} &\boldsymbol{dX_t} = \boldsymbol{\psi(t, X_t)dt} + \widetilde{\boldsymbol{K}}_t(\boldsymbol{X_{dt}} - \widehat{\boldsymbol{X}}_t)\boldsymbol{dt} + \widetilde{\boldsymbol{G}}(\boldsymbol{q}_t)\boldsymbol{dB}_t \\ &\quad \text{where, } \boldsymbol{\psi(t, X_t)} = \begin{bmatrix} \dot{\boldsymbol{q}}_t \\ \boldsymbol{F(t, q_t, \dot{q}_t)} \end{bmatrix} \text{ and } \widetilde{\boldsymbol{G}}(\boldsymbol{q_t}) = \begin{bmatrix} \boldsymbol{0} \\ \boldsymbol{G(q_t)} \end{bmatrix} \end{aligned}\right\} \tag{3.3}$$

The general state dynamic equations of a nonlinear dynamical stochastic system are shown in equation(3.1) when the torque has a white Gaussian noise component without feedback. With feedback, equation (3.3) presents state dynamics of the system which has considered the estimated state for the controller design. The ability of an observer to estimate the state variables encourages its applications in the domain of control and monitoring of dynamical systems.

3.3 Estimation of state using EKF: State-observer

In the last section, it is clear that the admissible controls are now the functions of the estimate $\widehat{\boldsymbol{X}}_t$ and not the measured state $\boldsymbol{X_t}$. In this section, estimation process of the state vector of a stochastic system by EKF, using the noise-corrupted position measurements, $\boldsymbol{Z(t)}$ is discussed. The filtering algorithm, also called as state observer has used a driving force function same as that of the original state variable system without noise but with a feedback given by a linear transform '$\boldsymbol{L_t}$' of the output error between the original state variable system and the recommended output using the observer state (extended state). To implement the filtering algorithm, the nonlinear model of EKF based state

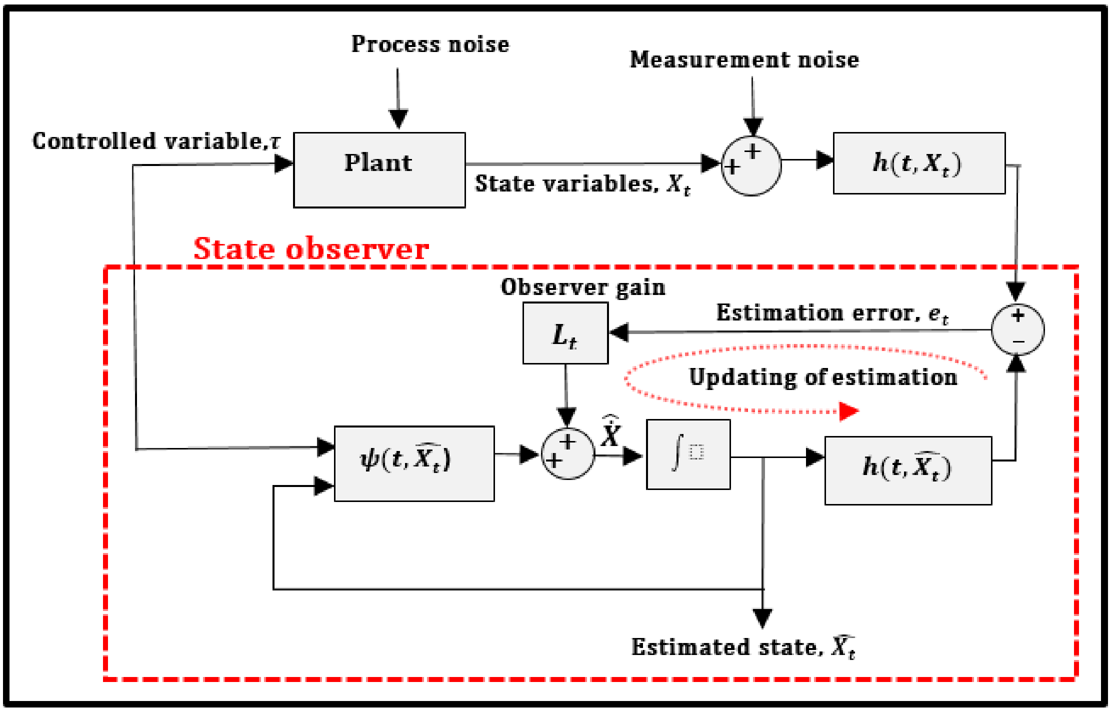

Figure 3.3: Block Diagram: State Estimation using EKF

observer is employed in which evolution of the state w.r.t. time is captured by equation (3.4). The observer is based on the measurement equation which is a noisy version of a function of the state expressed as in equation (3.5).

$$d\dot{\widehat{X}}_t = \psi(t, \widehat{X}_t) + L_t(dZ_t - h(t, \widehat{X}_t)dt) \tag{3.4}$$

$$dZ_t = h(t, X_t)dt + \sigma_v dV_t \tag{3.5}$$

where, $\widehat{X}_t$ is the vector of state estimate, $\psi(t, \widehat{X}_t)$ denotes n-dimensional vector of nonlinear function and L_t denotes output error feedback gain for the state observer. Also, $h(t, X_t)$ is m-dimensional vector and V_t denotes measurement noise respectively.

From Fig. 3.3, it is shown that EKF uses the nonlinear plant update and measurement function to compute a prediction error, which is then multiplied by the Kalman gain matrix, L_t derived from the linearized system and added to the state estimate.

3.3.1 Extended Kalman Filter

EKF is a nonlinear version of the Kalman filter as the estimation of states for a nonlinear dynamics is done by adapting the procedure of Kalman filter used for the linear system. It requires linearization of nonlinear dynamics of the system around the current estimated state. Further, the propagation of state vector and the covariance matrix is carried out differently due to nonlinearity present in the system.

3.3.2 Recursive computation of estimation of state, $\widehat{\boldsymbol{X}}_t$ and covariance, $\boldsymbol{P}_t$

The stochastic interpretation of the distribution of the actual state $\boldsymbol{X(t)}$ is Gaussian with mean $\widehat{\boldsymbol{X}}\boldsymbol{(t)}$ and covariance $\boldsymbol{P_t}$ and EKF based state observer is used to compute both of them. EKF carry out computations of both $\widehat{\boldsymbol{X}}_{\boldsymbol{t}}$ and $\boldsymbol{P_t}$ recursively as the time evolves in real-time as shown in Fig. 3.4. It is not possible to do recursive computation only for $\widehat{\boldsymbol{X}}_{\boldsymbol{t}}$ without considering $\boldsymbol{P_t}$. Also, $\widehat{\boldsymbol{X}}_{\boldsymbol{t}}$, $\boldsymbol{P_t}$ and $\boldsymbol{dZ_t}$ are required for the computation of $\widehat{\boldsymbol{X}}_{\boldsymbol{t+dt}}$ and $\boldsymbol{P_{t+dt}}$.

It should be noted that we have considered only the measurements of the angular position vector, $\boldsymbol{q_t}$ and estimated the state i.e. $\widehat{\boldsymbol{q}}_{\boldsymbol{t}}$ and $\widehat{\dot{\boldsymbol{q}}}_{\boldsymbol{t}}$. Further, the observer gain, $\boldsymbol{L_t}$ has been designed in accordance with the standard EKF algorithm i.e. $\boldsymbol{L_t} = \boldsymbol{\sigma_v^{-2} P H_t^T}$ is a special case of EKF which ensures suboptimality of the observer.

EKF Ricatti equation for observer error covariance matrix is represented as:

$$\left.\begin{aligned}
&\boldsymbol{P_{t+dt}} - \boldsymbol{P_t} = \frac{\boldsymbol{dP}}{\boldsymbol{dt}} = \frac{\boldsymbol{d}}{\boldsymbol{dt}}\begin{bmatrix} \boldsymbol{P_{qq}} & \boldsymbol{P_{q\dot{q}}} \\ \boldsymbol{P_{\dot{q}q}} & \boldsymbol{P_{\dot{q}\dot{q}}} \end{bmatrix} \\
&= \widehat{\boldsymbol{\psi}}'\boldsymbol{P} + \boldsymbol{P}\widehat{\boldsymbol{\psi}}'^{\boldsymbol{T}} - \boldsymbol{L_t H P} + \widehat{\widetilde{\boldsymbol{G}}}\widehat{\widetilde{\boldsymbol{G}}}^{\boldsymbol{T}} \\
&= \widehat{\boldsymbol{\psi}}'\boldsymbol{P} + \boldsymbol{P}\widehat{\boldsymbol{\psi}}'^{\boldsymbol{T}} - \boldsymbol{\sigma_v^{-2} P H^T H P} + \widehat{\widetilde{\boldsymbol{G}}}\widehat{\widetilde{\boldsymbol{G}}}^{\boldsymbol{T}} \\
&\text{where } \widetilde{\boldsymbol{G}} = \begin{bmatrix} \boldsymbol{0} \\ \boldsymbol{G} \end{bmatrix} = \begin{bmatrix} \boldsymbol{0} \\ \boldsymbol{\sigma_\omega M^{-1}(q_t)} \end{bmatrix} \\
&\text{and } \boldsymbol{H} = \begin{bmatrix} \boldsymbol{I_2} : \boldsymbol{O_2} \end{bmatrix} \text{ for } \boldsymbol{X_t} = \begin{bmatrix} \boldsymbol{q_t} \\ \dot{\boldsymbol{q}}_{\boldsymbol{t}} \end{bmatrix}
\end{aligned}\right\} \tag{3.6}$$

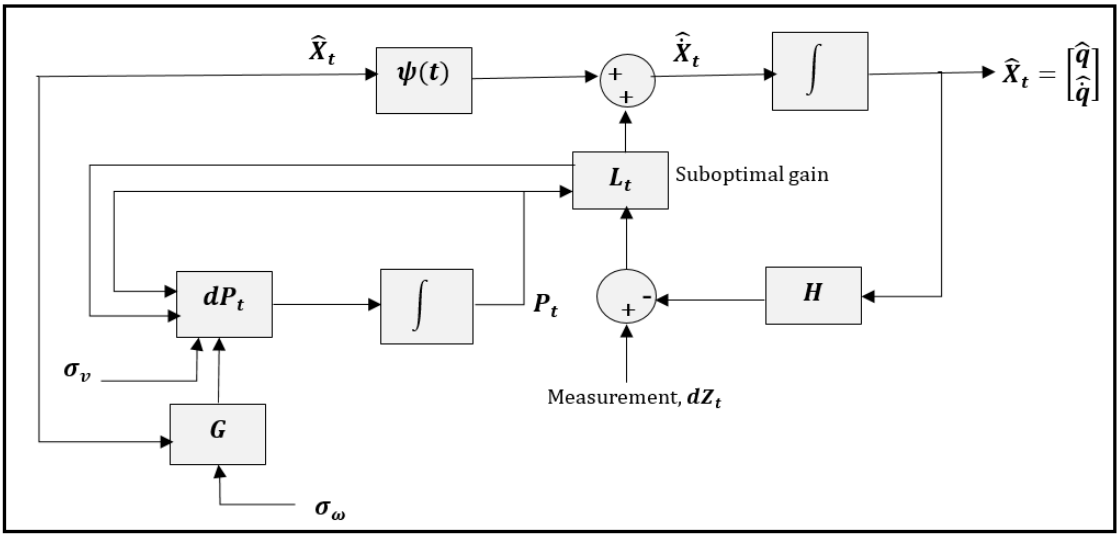

Figure 3.4: Recursive Computation of State Estimate and Covariance in EKF.

$$\left.\begin{aligned}
\psi(t, q, \dot{q}) = \psi &= \begin{bmatrix} \dot{q} \\ F(t, q_t, \dot{q}_t) \end{bmatrix} \\
&= \begin{bmatrix} \dot{q} \\ M(q_t)^{-1}(\tau(t) - N(q_t, \dot{q}_t)) \end{bmatrix} \\
\widehat{\psi}' &= \left[\frac{\partial \psi(t, \widehat{q}, \hat{\dot{q}})}{\partial q} \middle| \frac{\partial \psi(t, \widehat{q}, \hat{\dot{q}})}{\partial \dot{q}} \right] \\
\widehat{\psi}' &= \begin{bmatrix} 0 & I \\ \frac{\partial \widehat{f}}{\partial q} & \frac{\partial \widehat{f}}{\partial \dot{q}} \end{bmatrix}
\end{aligned}\right\} \tag{3.7}$$

Thus, the state dynamics of state observer from equation (3.4) can be written in the form as as

$$\frac{d}{dt}\begin{bmatrix} \widehat{q}_t \\ \hat{\dot{q}}_t \end{bmatrix} = \begin{bmatrix} \hat{\dot{q}}_t \\ M^{-1}(\widehat{q}_t)(\tau - N(\widehat{q}_t, \hat{\dot{q}}_t)) \end{bmatrix} + L_t(\dot{z}_t - \widehat{q}_t) \in \mathbb{R}^{4\times 2} \tag{3.8}$$

Kalman observer gain for EKF:

$$\left.\begin{aligned}
L_t &= \sigma_v^{-2} P H_t^T \\
i.e.\ L_t &= \sigma_v^{-2} \begin{bmatrix} P_{qq} & P_{q\dot{q}} \\ P_{\dot{q}q} & P_{\dot{q}\dot{q}} \end{bmatrix} \begin{bmatrix} I_2 \\ O_2 \end{bmatrix}
\end{aligned}\right\} \tag{3.9}$$

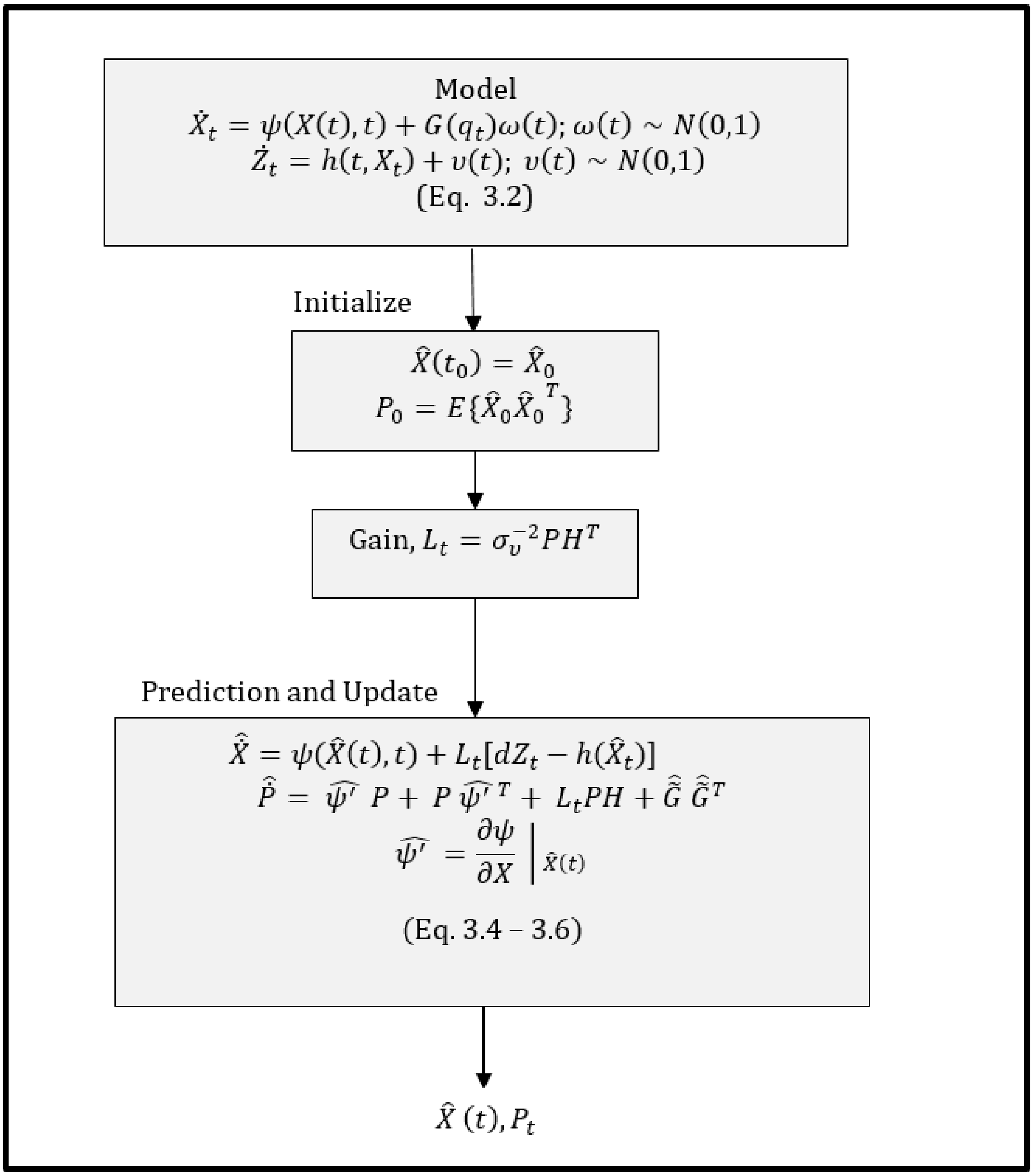

Figure 3.5: Estimation Process by EKF

$$\left.\begin{aligned} &\frac{d}{dt}\boldsymbol{P} = \widehat{\boldsymbol{\psi}}'\boldsymbol{P} + \boldsymbol{P}\widehat{\boldsymbol{\psi}}'^{\boldsymbol{T}} - \boldsymbol{\sigma}_v^{-2}\boldsymbol{P}\begin{bmatrix} \boldsymbol{I_2} & \boldsymbol{0} \\ \boldsymbol{0} & \boldsymbol{0} \end{bmatrix}\boldsymbol{P}^{\boldsymbol{T}} \\ &= \begin{bmatrix} \boldsymbol{P_{qq}} & \boldsymbol{P_{q\dot{q}}} \\ \boldsymbol{P_{\dot{q}q}} & \boldsymbol{P_{\dot{q}\dot{q}}} \end{bmatrix}\begin{bmatrix} \boldsymbol{P_{qq}} & \boldsymbol{P_{q\dot{q}}} \\ 0 & 0 \end{bmatrix} = \begin{bmatrix} \boldsymbol{P_{qq}^2} & \boldsymbol{P_{qq}P_{q\dot{q}}} \\ \boldsymbol{P_{\dot{q}q}P_{qq}} & \boldsymbol{P_{\dot{q}q}P_{q\dot{q}}} \end{bmatrix} \end{aligned}\right\} \tag{3.10}$$

The Ricatti equation (3.10) for updating covariance is solved on-line as it depends upon the estimated state, $\widehat{X}$.

In this chapter, state observer has estimated the states and a unified approach of filtering and control is developed to tackle the measurement noise along with reducing the cost and dimension of the sensor.

In section 3.4, the control law considers two types of error, namely the observer based tracking error, $\boldsymbol{f_t}$ and the observer estimation error, $\boldsymbol{e_t}$ to update the feedback coefficient matrix, $\boldsymbol{K_t}$ on a real-time basis. The proposed real-time stochastic approach computes the observer gain, $\boldsymbol{L_t}$ by EKF and updates the controller gain matrix, $\widetilde{\boldsymbol{K}}_{\boldsymbol{t}}$ continuously based on minimization of the tracking error energy increment that is computed using standard $It\hat{o}'s$ formulae for the Brownian motion. The minimization of the mean square tracking error is subjected to an energy constraint on the feedback matrix coefficient, $\boldsymbol{K_t}$. Such a constraint automatically guarantee the lesser energy, in implementing feedback.

3.4 Design of state-observer-based controller

In this section, implementation of a general algorithm for combining filtering and control of a noisy nonlinear state variable system with output measurements is investigated. The optimal PD controller with the controller input is designed based on the error between "the state-observer and the desired state." The possible uncertainty in the driving force parameter is assumed to obtain robust bounds. Further, feedback forcing term is incorporated into the original system by giving a linear transformation gain, $\boldsymbol{K_t}$ of the error between the desired trajectory, $\boldsymbol{X_{dt}}$ and the observed trajectory, $\widehat{\boldsymbol{X}}_{\boldsymbol{t}}$. The dynamics of the closed-loop system when the state- observer is coupled to the feedback PD controller (refer Fig.3.1) can be

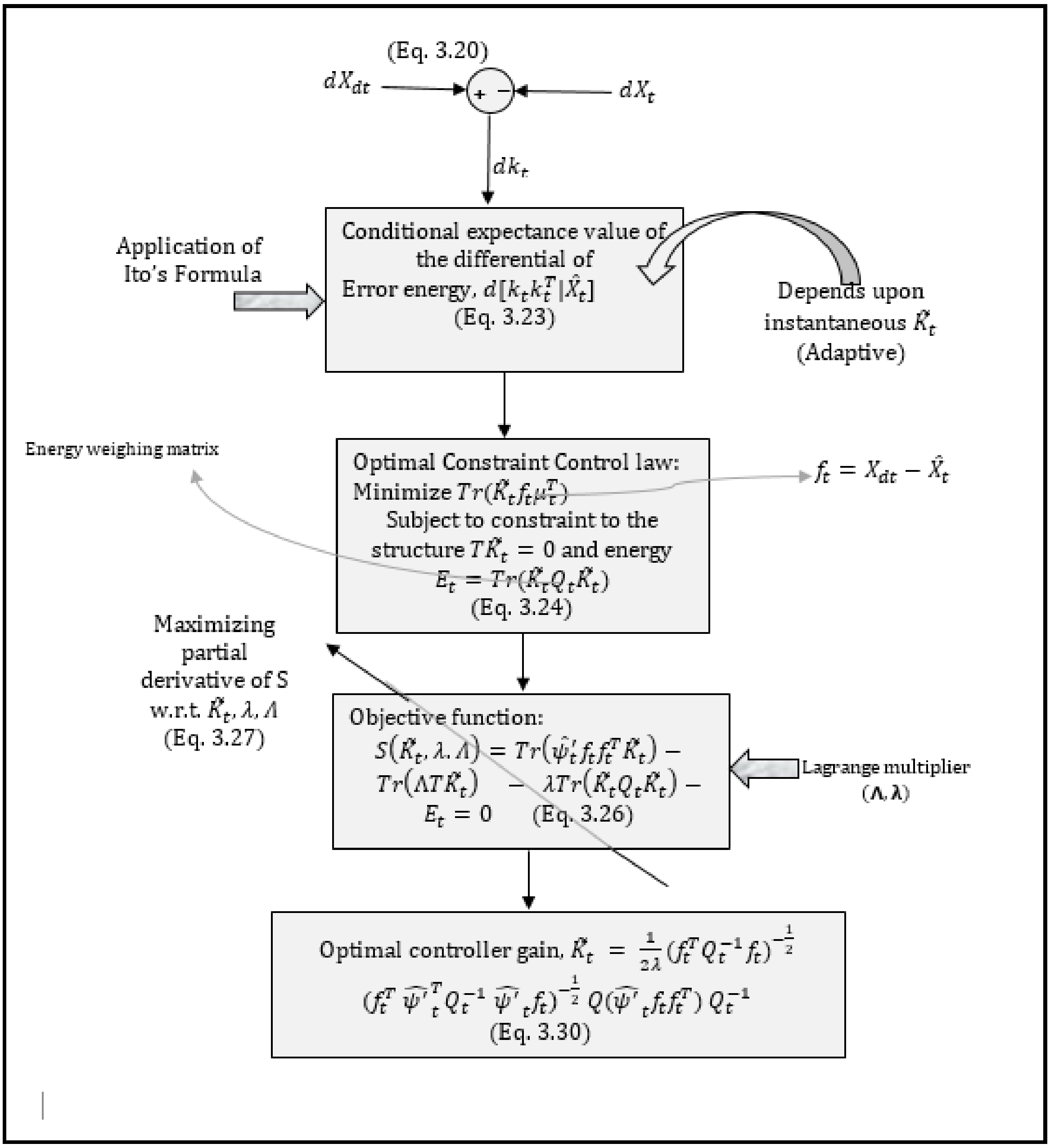

Figure 3.6: Process of Controller Design

extended as:

$$\boldsymbol{d}\begin{bmatrix}\boldsymbol{q}_t\\ \dot{\boldsymbol{q}}_t\end{bmatrix} = \begin{bmatrix}\dot{\boldsymbol{q}}_t\\ \boldsymbol{F}(\boldsymbol{t},\boldsymbol{q}_t,\dot{\boldsymbol{q}}_t)+\boldsymbol{K}_t(\begin{bmatrix}\boldsymbol{q}_{dt}\\ \dot{\boldsymbol{q}}_{dt}\end{bmatrix}-\begin{bmatrix}\widehat{\boldsymbol{q}}_t\\ \widehat{\dot{\boldsymbol{q}}}_t\end{bmatrix})\end{bmatrix}\boldsymbol{dt}+\begin{bmatrix}\boldsymbol{0}\\ \boldsymbol{G}(\boldsymbol{q}_t)\end{bmatrix}\boldsymbol{dB}_t \tag{3.11}$$

where feedback controller matrix gain is $\boldsymbol{K_t} = \boldsymbol{K}(\widehat{\boldsymbol{q}}_t, \widehat{\dot{\boldsymbol{q}}}_t) \in \mathbb{R}^{\mathbf{2\times 2}}$.

The special case of a diagonal block structure, $\boldsymbol{K_t} = \begin{bmatrix}\boldsymbol{K}_t^{(p)} & \boldsymbol{0}\\ \boldsymbol{0} & \boldsymbol{K}_t^{(d)}\end{bmatrix}$, reduces the decoupling of the position and velocity error feedback components.

It is clear from equation (3.11) that the controller gain matrix has a special block structure.

$$\text{Let } \widetilde{\boldsymbol{K}}_t = \begin{bmatrix}\boldsymbol{0}\\ \boldsymbol{K_t}\end{bmatrix}.$$

Thus special structure of the controller gain leads to the constraint block on $\widetilde{\boldsymbol{K}}_t$ characterized by

$$\boldsymbol{T}\widetilde{\boldsymbol{K}}_t = \boldsymbol{0}; \;\; \text{where } \boldsymbol{T} = [\boldsymbol{I_2}|\boldsymbol{O_2}] \leftarrow \mathbb{R}^{\mathbf{2\times 4}} \tag{3.12}$$

Initially, it was not assumed that controller gain $\widetilde{\boldsymbol{K}}_t$ has the block structure $\widetilde{\boldsymbol{K}}_t = \begin{bmatrix}\boldsymbol{0}\\ \boldsymbol{K_t}\end{bmatrix}$. Thus, we optimize the error energy over all $\boldsymbol{K}$. However, once we assume that $\widetilde{\boldsymbol{K}}_t$ has the above block structure, then we can still optimize over all $\boldsymbol{K}$ provided that we incorporates the constraints given in equation (3.12) using Lagrange multiplier.

The state tracking error SDE dynamic is obtained using the SDE's for the system state and the EKF observer for the estimated state.

In this system, two kinds of errors are taken into account:

The state estimation error, $\boldsymbol{e_t} = \boldsymbol{X_t} - \widehat{\boldsymbol{X}}_t$ and the state trajectory tracking error, $\boldsymbol{f_t} = \boldsymbol{X_{dt}} - \widehat{\boldsymbol{X}}_t$, which are based on the observed state, $\widehat{\boldsymbol{X}}_t$. Also, state estimation error covariance matrix is denoted by $\mathbb{E}(\boldsymbol{e_t e_t^T})$.

The dynamics of estimation error is represented by:

$$\boldsymbol{de_t} = \boldsymbol{dX_t} - \boldsymbol{d}\widehat{\boldsymbol{X}}_t$$

From equations (3.3), (3.4) and (3.5), we get:

$$\left.\begin{aligned} \boldsymbol{de_t = \psi(t, X_t)dt + \widetilde{K}_t f_t dt + \widetilde{G}_t dB_t - \psi(t, \widehat{X}_t)dt} \\ \boldsymbol{- L_t[h(t, X_t)dt + \sigma_v dV_t - h(t, \widehat{X}_t)dt]} \end{aligned}\right\} \tag{3.13}$$

It is intended for the controller to work around an operating point for the minimum deviation. Hence, the approximate linearization of the aforementioned nonlinear error equation is done around $\boldsymbol{\widehat{X}_t}$.
Linearization of a function $y = f(x)$ around a point 'a' is
$y \approx f(a)+f'(a)(x-a)+$higher order terms. As in this case, $a = \widehat{X}_t$ and $f(x) = de_t$

$$\left.\begin{aligned} f(\widehat{X}_t) &\approx \psi_t(t, \widehat{X}_t)dt + \widehat{\widetilde{K}}_t f_t dt + \\ &\qquad \widehat{\widetilde{G}}_t dB_t - \psi_t(t, \widehat{X}_t)dt - L_t[h(t, \widehat{X}_t)dt - h(t, \widehat{X}_t)dt + \sigma_v dV_t] \\ &\approx \widehat{\widetilde{K}}_t f_t dt + \widehat{\widetilde{G}}_t dB_t - \sigma_v L_t dV_t \\ f'(\widehat{X}_t) &\approx \frac{d}{dt}[\psi_t(t, X_t)dt + \widetilde{K}_t f_t dt + \widetilde{G}_t dB_t - \psi_t(t, \widehat{X}_t)dt - L_t[h(t, X_t)dt \\ &\qquad - h(t, \widehat{X}_t)dt + \sigma_v dV_t]_{X_t = \widehat{X}_t} \\ &\approx \widehat{\psi}'(t, \widehat{X}_t)dt - L_t[h(t, \widehat{X}_t)dt \end{aligned}\right\}$$

So, truncated linearization of de_t around $\widehat{X}_t$:

$$\boldsymbol{de_t \approx f(\widehat{X}_t) + f'(\widehat{X}_t)(X_t - \widehat{X}_t) \approx f(\widehat{X}_t) + f'(\widehat{X}_t)e_t} \tag{3.14}$$

From the above derivation, equation (3.14) is approximated as:

$$\left.\begin{aligned} &\boldsymbol{de_t \approx [(\widehat{\psi'}_t - L_t\widehat{H}_t)e_t + \widetilde{K}_t f_t]dt + \widehat{\widetilde{G}}_t dB_t - \sigma_v L_t dV_t} \\ &\text{Where, } \boldsymbol{\widehat{\psi}'_t = \psi'_t(t, \widehat{X}_t)}, \ \boldsymbol{\widehat{H}_t = h'(t, \widehat{X}_t)}\ , \boldsymbol{\widetilde{G}_t = G_t(q_t)} \ \text{ and } \ \boldsymbol{\widehat{\widetilde{G}}_t = G_t(\widehat{q}_t)} \end{aligned}\right\} \tag{3.15}$$

Although the approximate error is not directly considered, it can be evaluated by looking at term like $\mathbb{E}(\psi(X_t)) - (\psi(\mathbb{E}X_t)) = \frac{1}{2}\psi''(\mathbb{E}X_t)\mathbb{E}(X_t - \mathbb{E}X_t)^2 + O(|X_t - \mathbb{E}X_t|)^3 \approx \frac{1}{2}\psi''(\mathbb{E}X_t)P_t$ and evaluating $\sup_\xi |\psi''|$ and $|P_t|$ for bounding the error. Here $\mathbb{E}$ stands for conditional expectation w.r.t. X_t.

For any observable ξ_t , $\widehat{\xi_t}$ means $\mathbb{E}\left(\xi_t \,|Z_s,\, \forall\, s \leq t\right)$ i.e. the conditional mean of ξ_t at any time t, given all the measurements, Z_s up to time t. It should be noted that $\psi_t'(t,\widehat{X}_t) = \dfrac{\partial \psi_t(t,X_t)}{\partial t}|_{\widehat{X}_t}$ is the Jacobian matix of the map $\widehat{X} \to \psi(t,\widehat{X})$. Likewise $h'(t,\widehat{X}_t)$ is the Jacobian matix of the map $X \to h(t,X)$.

The total energy of a signal is equal to the sum of the eigen values of the covaiance matrix of the signal and the sum of the eigen values is nothing but the trace of the matrix. Thus, the aim is to find the trace of the covariance matrix of the error signal and minimizing it. The differential of covariance matrix is computed around $\widehat{\boldsymbol{X}_t}$ denoted as $\mathbb{E}(\boldsymbol{d(e_t e_t^T)|\widehat{X}_t})$.

Using $It\hat{o}'s$ calculus rule for SDE, the observer conditional error energy can be computed as: $\boldsymbol{d(e_t e_t^T) = de_t.e_t^T + e_t.de_t^T + de_t.de_t^T}$.

$$\left.\begin{aligned}\mathbb{E}(\boldsymbol{d(e_te_t^T)|\widehat{X}_t}) = (\boldsymbol{\widehat{\psi}_t' - L_t\widehat{H}_t})\mathbb{E}(\boldsymbol{d(e_te_t^T)|\widehat{X}_t})^{\boldsymbol{T}}\boldsymbol{dt} + \mathbb{E}(\boldsymbol{d(e_te_t^T)|\widehat{X}_t})^{\boldsymbol{T}}(\boldsymbol{\widehat{\psi}_t' - L_t\widehat{H}_t})\boldsymbol{dt}\\ + \boldsymbol{\widetilde{K}_t f_t}\mathbb{E}(\boldsymbol{(e_t^T)|\widehat{X}_t})\boldsymbol{dt} + \mathbb{E}(\boldsymbol{(e_t^T)|\widehat{X}_t})\boldsymbol{f_t^T K_t^T dt}\\ + (\boldsymbol{\widehat{\widetilde{G}}_t \widehat{\widetilde{G}}_t^T + \sigma_v^2 L_t L_t^T})\boldsymbol{dt}\end{aligned}\right\} \tag{3.16}$$

Substitute:

$$\left.\begin{aligned}\boldsymbol{\mu_t} &= \mathbb{E}(\boldsymbol{e_t|\widehat{X}_t})\\ \boldsymbol{P_t} &= \mathbb{E}(\boldsymbol{e_te_t^T|\widehat{X}_t})\end{aligned}\right\} \tag{3.17}$$

where, $\boldsymbol{\mu_t}$ is the conditional expectation of tracking error given observer state estimation at time t and $\boldsymbol{P_t}$ is conditional error covariance matrix.

Thus, equation (3.16) is presented as:

$$\left.\begin{aligned}\mathbb{E}[\boldsymbol{d(e_te_t^T)|\widehat{X}_t}] =& (\boldsymbol{\widehat{\psi}_t' - L_t\widehat{H}_t})\boldsymbol{P_t dt} + \boldsymbol{P_t}(\boldsymbol{\widehat{\psi}_t' - L_t H_T})^{\boldsymbol{T}}\boldsymbol{dt} + \boldsymbol{\widetilde{K}_t f_t \mu_t dt}\\ &+ \boldsymbol{\mu_t f_t^T \widetilde{K}_t^T dt} + (\boldsymbol{\widehat{\widetilde{G}}_t \widehat{\widetilde{G}}_t^T + \sigma_v^2 L_t L_t^T})\boldsymbol{dt^2}\end{aligned}\right\} \tag{3.18}$$

In the aforementioned equation, only terms having $\boldsymbol{\widetilde{K}_t}$ is controllable so, it is clear that in order to minimize $\mathbb{E}[d(e_te_t^T) \mid \widehat{X}_t]$, minimize the following expression to avoid overshooting provided we are interested only in designing optimal observer, i.e.

$$\left.\begin{aligned}&\text{Minimize}\ \boldsymbol{Tr}\ (\boldsymbol{\widetilde{K}_t f_t \mu_t^T}) = \boldsymbol{\mu_t^T \widetilde{K}_t f_t}\\ &\text{subject to constraint to the}\ \boldsymbol{T\,\widetilde{K}_t = 0}\ \text{and energy constraint,}\ \boldsymbol{E_t = Tr(\widetilde{K}_t Q_t \widetilde{K}_t^T)}\end{aligned}\right\} \tag{3.19}$$

Where, $\boldsymbol{Q_t}$ is feedback coefficient energy weighing matrix.

It is noted that the constraints given in the above equation corresponds to the fact that in the stochastic differential equation (3.11) of system for dX_t, feedback control has been applied only to the lower variable and nothing to the upper variable so that the feedback control has the special form $\begin{bmatrix} \mathbf{0} \\ \widehat{\boldsymbol{K}}_t \end{bmatrix}$ and this is accounted by the constraints $[\boldsymbol{I_2} : \mathbf{0}] \begin{bmatrix} \mathbf{0} \\ \widehat{\boldsymbol{K}}_t \end{bmatrix} = \mathbf{0}$

It is to be noted that state tracking error, $\boldsymbol{k_t}$, is defined as:

$$\boldsymbol{k_t} = \boldsymbol{X_t} - \boldsymbol{X_{dt}} = \boldsymbol{e_t} - \boldsymbol{f_t} \tag{3.20}$$

For optimal tracker, $\boldsymbol{k_t}$ must be made small and to meet the objective of having good tracking, we need to minimize $\boldsymbol{Tr}\mathbb{E}\boldsymbol{d}((\boldsymbol{k_t k_t^T})|\widehat{\boldsymbol{X}}_t)$, i.e. the conditional average tracking energy increments.

The approximate linearization of the nonlinear error equation is done around $\widehat{\boldsymbol{X}}_t$ so that controller can work with minimum deviation. Hence, the rate of increase of tracking error is approximated as the following:

$$\left.\begin{aligned} \boldsymbol{dk_t} &\approx \boldsymbol{dX_t} - \boldsymbol{dX_{dt}} \\ &= (\psi(\boldsymbol{t}, \boldsymbol{X_t}) - \psi(\boldsymbol{t}, \boldsymbol{X_{dt}}))\boldsymbol{dt} + \widetilde{\boldsymbol{K}}_t(\boldsymbol{X_{dt}} - \widehat{\boldsymbol{X}}_t)\boldsymbol{dt} + \widehat{\widehat{\boldsymbol{G}}}_t \boldsymbol{dB_t} \\ &\approx [\psi'(\boldsymbol{t}, \widehat{\boldsymbol{X}}_t)\boldsymbol{k_t} + \widetilde{\boldsymbol{K}}_t(\boldsymbol{X_{dt}} - \widehat{\boldsymbol{X}}_t)]\boldsymbol{dt} + \widehat{\widehat{\boldsymbol{G}}}_t \boldsymbol{dB_t} \end{aligned}\right\} \tag{3.21}$$

The conditional expectance value of the differential of tracking error energy is given as: $\mathbb{E}[\boldsymbol{d}(\boldsymbol{k_t k_t^T})|\widehat{\boldsymbol{X}}_t]$. It depends only on the instantaneous value of the $\boldsymbol{K_t}$ and hence, it is easy to minimize. The expectance value of the total error energy is $\mathbb{E}(\boldsymbol{k_t k_t^T}) = \mathbb{E}\int_0^t \mathbb{E}[\boldsymbol{d}(\boldsymbol{k_t k_t^T})|\widehat{\boldsymbol{X}}_t]\boldsymbol{dt}$ depends on all the past values of feedback coefficients, $\boldsymbol{K_s}, \boldsymbol{s} \leq \boldsymbol{t}$ and hence can't be carried out adaptively. Just as the least mean square (LMS) algorithm overcomes past values in comparison of recursive least-squares (RLS), the proposed algorithm overcomes past values making it adaptively implementable. The performance may not be as good as the optimal methods of minimizing $\mathbb{E}(\boldsymbol{k_t k_t^T})$ but like the suboptimal LMS or Widrow algorithm, its performance is good enough and has lesser computational complexity.

Using $It\hat{o}'s$ calculus rule in equation (3.21), the differential of tracking error energy is expressed as:

$$\left.\begin{aligned} \boldsymbol{d(k_t k_t^T)} =& \{[\psi'(\boldsymbol{t}, \widehat{\boldsymbol{X}}_t)\boldsymbol{k_t} + \widetilde{\boldsymbol{K}}_t(\boldsymbol{X_{dt}} - \widehat{\boldsymbol{X}}_t)]\boldsymbol{dt} + \widehat{\widehat{\boldsymbol{G}}}_t \boldsymbol{dB_t}\}\boldsymbol{k_t^T} \\ & .\boldsymbol{k_t}\{[\psi'(\boldsymbol{t}, \widehat{\boldsymbol{X}}_t)\boldsymbol{k_t} + \widetilde{\boldsymbol{K}}_t(\boldsymbol{X_{dt}} - \widehat{\boldsymbol{X}}_t)]\boldsymbol{dt} + \widehat{\widehat{\boldsymbol{G}}}_t \boldsymbol{dB_t}\}^{\boldsymbol{T}} \\ & + \{[\psi'(\boldsymbol{t}, \widehat{\boldsymbol{X}}_t)\boldsymbol{k_t} + \widetilde{\boldsymbol{K}}_t(\boldsymbol{X_{dt}} - \widehat{\boldsymbol{X}}_t)]\boldsymbol{dt} + \widehat{\widehat{\boldsymbol{G}}}_t \boldsymbol{dB_t}\} \\ & \{[\psi'(\boldsymbol{t}, \widehat{\boldsymbol{X}}_t)\boldsymbol{k_t} + \widetilde{\boldsymbol{K}}_t(\boldsymbol{X_{dt}} - \widehat{\boldsymbol{X}}_t)]\boldsymbol{dt} + \widehat{\widehat{\boldsymbol{G}}}_t \boldsymbol{dB_t}\}^{\boldsymbol{T}} \end{aligned}\right\} \tag{3.22}$$

The conditional expectation value of the differential of tracking error energy is obtained after simplifying the aforementioned expression by the use of $It\hat{o}'s$ formulae as:

$$\left.\begin{aligned} & \mathbb{E}(\boldsymbol{dB_t}) = \boldsymbol{0}; \\ & \mathbb{E}(\boldsymbol{e_t f_t}) = \boldsymbol{0}; \\ & (\boldsymbol{dB_t}.\boldsymbol{dB_t^T}) = \boldsymbol{1} \\ & \mathbb{E}(\widehat{\widehat{\boldsymbol{G}}}_t \boldsymbol{dB_t} \widehat{\widehat{\boldsymbol{G}}}_t^{\boldsymbol{T}} \boldsymbol{dB_t^T}) = \widehat{\widehat{\boldsymbol{G}}}_t \widehat{\widehat{\boldsymbol{G}}}_t^{\boldsymbol{T}} \end{aligned}\right\}$$

Thus, the resulting expression is approximated as:

$$\left.\begin{aligned} \mathbb{E}[\boldsymbol{d(k_t k_t^T)}|\widehat{\boldsymbol{X}}_t] \approx & \ \widehat{\psi}'_t \ \mathbb{E}(\boldsymbol{k_t k_t^T}|\widehat{\boldsymbol{X}}_t)\boldsymbol{dt} + \mathbb{E}(\boldsymbol{k_t k_t^T}|\widehat{\boldsymbol{X}}_t) \ \widehat{\psi'}_t^{\boldsymbol{T}} \boldsymbol{dt} \\ & - \widehat{\psi'}_t \ \boldsymbol{\nu_t}(\boldsymbol{X_{dt}} - \widehat{\boldsymbol{X}}_t)^{\boldsymbol{T}} \widetilde{\boldsymbol{K}}_t^{\boldsymbol{T}} \boldsymbol{dt^2} - \widetilde{\boldsymbol{K}}_t(\boldsymbol{X_{dt}} - \widehat{\boldsymbol{X}}_t)\boldsymbol{\nu_t^T} \ \widehat{\psi'}_t^{\boldsymbol{T}} \boldsymbol{dt^2} \\ & + \widetilde{\boldsymbol{K}}_t(\boldsymbol{X_{dt}} - \widehat{\boldsymbol{X}}_t)(\boldsymbol{X_{dt}} - \widehat{\boldsymbol{X}}_t)^{\boldsymbol{T}} \widetilde{\boldsymbol{K}}_t^{\boldsymbol{T}} \boldsymbol{dt^2} + \widehat{\widehat{\boldsymbol{G}}}_t \widehat{\widehat{\boldsymbol{G}}}_t^{\boldsymbol{T}} \boldsymbol{dt} \end{aligned}\right\} \tag{3.23}$$

Consider, $\boldsymbol{\nu_t} = -\mathbb{E}[\boldsymbol{k_t}|\widehat{\boldsymbol{X}}_t] \approx \boldsymbol{X_{dt}} - \widehat{\boldsymbol{X}}_t = \boldsymbol{f_t}$ and $\mathbb{E}(\boldsymbol{X_t}|\widehat{\boldsymbol{X}}_t) = \widehat{\boldsymbol{X}}_t$.

Minimizing the trace of the tracking-error-conditional-energy- increment thus amounts to

$$\left.\begin{aligned} \text{maximizing } & \boldsymbol{Tr}(\widehat{\psi}'_t(\boldsymbol{X_{dt}} - \widehat{\boldsymbol{X}}_t)(\boldsymbol{X_{dt}} - \widehat{\boldsymbol{X}}_t)^{\boldsymbol{T}} \widetilde{\boldsymbol{K}}_t^{\boldsymbol{T}}) = \boldsymbol{Tr}(\widehat{\psi}'_t \boldsymbol{f_t f_t^T} \widetilde{\boldsymbol{K}}_t^{\boldsymbol{T}}) \\ \text{subject to } & \boldsymbol{T}\widetilde{\boldsymbol{K}}_t = \boldsymbol{0} \ \text{ and } \ \boldsymbol{E_t} = \boldsymbol{Tr}(\widetilde{\boldsymbol{K}}_t \boldsymbol{Q_t} \widetilde{\boldsymbol{K}}_t^{\boldsymbol{T}}) \end{aligned}\right\} \tag{3.24}$$

where, $\boldsymbol{Q}_t$ denotes feedback coefficient energy weighing matrix and $\boldsymbol{E_t}$ refers to energy constraint.

Note that the quadratic in $\widetilde{\boldsymbol{K}}_t$ term $\boldsymbol{Tr}(\widetilde{\boldsymbol{K}}_t^{\boldsymbol{T}}(\boldsymbol{X_{dt}} - \widehat{\boldsymbol{X}}_t)(\boldsymbol{X_{dt}} - \widehat{\boldsymbol{X}}_t)^{\boldsymbol{T}} \widetilde{\boldsymbol{K}}_t)$ is taken care of by absorbing it into the constraints on $\boldsymbol{E_t}$. It is evident from expression (3.23) that the term in $Tr[\mathbb{E}(d(k_t k_t^T)|\widehat{X}_t)]$ containing $\widetilde{\boldsymbol{K}}_t$ (which is the only adjustable coefficient) is given by:

$$-2Tr\{\widehat{\psi}_t'\nu_t(X_{dt}-\widehat{X}_t)^T\widetilde{K}^T\} = -2Tr\{\widehat{\psi}_t'\nu_t{\nu_t}^T\widetilde{K}^T\} \tag{3.25}$$

The formation of objective function, $\boldsymbol{S}$, taking into account the constraints using Lagrange multiplier is presented as:

$$S(\widetilde{K}_t,\lambda,\Lambda) = Tr(\widehat{\psi}_t' f_t f_t^T \widetilde{K}_t^T) - \Lambda Tr(T\widetilde{K}_t) - \lambda(Tr(\widetilde{K}_t Q_t \widetilde{K}_t^T) - E_t) \tag{3.26}$$

The focus is on maximizing the objective function stated in equation (3.26), where the block structure of the controller along with the energy constraint on controller gain has been accounted for using Lagrange multiplier.

Standard matrix variational calculus is used for obtaining the optimum controller gain matrix. Lagrange multiplier is used to incorporate the constraint in the objective function. The calculations shown in (3.27) is carried out for the partial derivative of S with respect to the Lagrange multiplier involving $\boldsymbol{\Lambda}$, $\boldsymbol{\lambda}$ and the PD controller $\widetilde{\boldsymbol{K}}$, and equating to zero.

The results are shown in the following calculations as

$$\Lambda \in \mathbb{R}^{2\times 2} \tag{3.27a}$$

$$\delta_\Lambda S = 0 \implies T\widetilde{K}_t = 0 \tag{3.27b}$$

$$\delta_\lambda S = 0 \Rightarrow Tr(\widetilde{K}_t Q_t \widetilde{K}_t^T) = E_t \tag{3.27c}$$

Optimal selection of controller gain is presented as:

$$\delta_{\widetilde{K}_t} S = 0 \Rightarrow \widehat{\psi}_t' f_t f_t^T - T^T\Lambda^T - 2\lambda\widetilde{K}_t Q_t = 0 \tag{3.27d}$$

$$\text{Thus } \widetilde{K}_t = \frac{1}{2\lambda}(\widehat{\psi}_t' f_f f_t^T - T^T\Lambda^T)Q_t^{-1} \tag{3.27e}$$

It is to be noted that, $\boldsymbol{\Lambda}$ imposes constraints on block structure of PD gain as shown in (3.27b) , $\boldsymbol{\lambda}$ imposes error energy constraints on PD controller as shown in (3.27c). Combination of the results of block structure constraint (3.27b) and optimal selection of PD controller (3.27e) gives the following:

$$\left.\begin{aligned} \boldsymbol{T}(\widehat{\psi}'_t f_t f_t^T) - \boldsymbol{T}\boldsymbol{T}^T\Lambda^T = 0 \\ \implies \quad \Lambda^T = (\boldsymbol{T}\boldsymbol{T}^T)^{-1}\boldsymbol{T}(\widehat{\psi}'_t f_t f_t^T) \\ \text{So,}\ \ \Lambda^T = \boldsymbol{T}(\widehat{\psi}'_t f_t f_t^T) \\ \text{Note that}\ \ \boldsymbol{T} = [\boldsymbol{I_2} : \boldsymbol{0}] \implies \boldsymbol{T}\boldsymbol{T}^T = \boldsymbol{I_2} \end{aligned}\right\} \tag{3.27f}$$

The following expressions represent the procedure of determination of the Lagrange multiplier for PD energy constraint from prescribed energy after substituting (3.27e) into (3.27c) as:

$$\boldsymbol{E_t} = \frac{1}{4\lambda^2}\boldsymbol{Tr}\{(\widehat{\psi}'_t f_t f_t^T - \boldsymbol{T}^T\Lambda^T)\boldsymbol{Q}_t^{-1}(\widehat{\psi}'_t f_t f_t^T - \boldsymbol{T}^T\Lambda^T)^T\} \tag{3.28}$$

Further solving and rearranging the above equation, we get :

$$\begin{aligned} 4\lambda^2\boldsymbol{E_t} = (f_t^T\widehat{\psi}_t'^T\widehat{\psi}'_t f_t)(f_t^T\boldsymbol{Q}_t^{-1}f_t) - 2\boldsymbol{Tr}\{\widehat{\psi}'_t f_t f_t^T\boldsymbol{Q}_t^{-1}f_t f_t^T\widehat{\psi}_t'^T\boldsymbol{T}^T\boldsymbol{T}\} \\ + \boldsymbol{Tr}(\boldsymbol{T}^T\boldsymbol{T}\hat{\psi}_t'^T f_t f_t^T\boldsymbol{Q}_t^{-1}f_t f_t^T\hat{\psi}_t'^T\boldsymbol{T}^T\boldsymbol{T}) \end{aligned}$$

$$T^T T = \begin{bmatrix} I_2 & 0 \\ 0 & 0 \end{bmatrix} \quad \text{is a projection.}$$

$$\text{so}\ \ \lambda = \frac{1}{2\sqrt{\boldsymbol{E_t}}}\left[(f_t^T\boldsymbol{Q}_t^{-1}f_t)\left(f_t^T\widehat{\psi}_t'^T\begin{bmatrix} \boldsymbol{0} & \boldsymbol{0} \\ \boldsymbol{0} & \boldsymbol{I}_2 \end{bmatrix}\widehat{\psi}'_t f_t\right)\right]^{\frac{1}{2}} \tag{3.29}$$

Substituting Λ^T and λ from (3.27f) and (3.29) in (3.27e), the final form of controller gain, $\widetilde{K}_t$ for the given energy is presented as:

$$\begin{aligned} \widetilde{\boldsymbol{K}}_t &= \frac{1}{2\lambda}(\widehat{\psi}'_t f_t f_t^T - \boldsymbol{T}^T\boldsymbol{T}\widehat{\psi}'_t f_t f_t^T)\boldsymbol{Q}_t^{-1} \\ &= \frac{1}{2\lambda}\begin{bmatrix} \boldsymbol{0} & \boldsymbol{0} \\ \boldsymbol{0} & \boldsymbol{I_2} \end{bmatrix}\hat{\psi}'_t f_t f_t^T\boldsymbol{Q}_t^{-1} \\ &= \sqrt{\boldsymbol{E_t}}(f_t^T\boldsymbol{Q}_t^{-1}f_t)^{-\frac{1}{2}}(f_t^T\hat{\psi}'^T_t\boldsymbol{Q}\hat{\psi}' f_t)^{-\frac{1}{2}}\boldsymbol{Q}(\hat{\psi}'_t f_t f_t^T)\boldsymbol{Q}_t^{-1} \end{aligned} \tag{3.30}$$

The terms involved in equation (3.30) are represented in the form given as:

$$f_t = \begin{bmatrix} q_d(t) - \widehat{q}(t) \\ \dot{q}_d(t) - \hat{\dot{q}}(t) \end{bmatrix}$$

$$\boldsymbol{Q} = \begin{bmatrix} \boldsymbol{O_2} & \boldsymbol{O_2} \\ \boldsymbol{O_2} & \boldsymbol{I_2} \end{bmatrix} \in \mathbb{R}^{4\times 4}$$

$$\boldsymbol{Q_t} = \boldsymbol{I_4} \in \mathbb{R}^{4\times 4}$$

The primary feature of results obtained as shown in equation(3.30) is that the order of magnitude of the controller gain $\widetilde{\boldsymbol{K}}_{\boldsymbol{t}}$ is unity i.e. it is independent of the tracking error energy since

$$\begin{aligned}
&(\boldsymbol{f}_t^T \boldsymbol{Q}_t^{-1} \boldsymbol{f}_t)^{-\frac{1}{2}} = \boldsymbol{O}(||\boldsymbol{f}_t||^{-1}) \\
&(\boldsymbol{f}_t^T \widehat{\boldsymbol{\psi}'}_t^T \boldsymbol{Q} \widehat{\boldsymbol{\psi}'}_t \boldsymbol{f}_t)^{-\frac{1}{2}} = \boldsymbol{O}(||\boldsymbol{f}_t||)^{-1} \\
&\widehat{\psi}'_t \boldsymbol{f}_t \boldsymbol{f}_t^T = \boldsymbol{O}(||\boldsymbol{f}_t||^2)
\end{aligned}$$

Thus, our controller gain order of magnitude is likely to converge to a constant value irrespective of the initial errors.

The dynamics of the system with feedback for tracking as given in equation (3.3) is an $It\hat{o}'s$ SDE and wriiten as

$$\frac{\boldsymbol{d}}{\boldsymbol{dt}}\begin{bmatrix} \boldsymbol{q}_t \\ \dot{\boldsymbol{q}}_t \end{bmatrix} = \begin{bmatrix} \dot{\boldsymbol{q}}_t \\ \boldsymbol{M}(\boldsymbol{q}_t)^{-1}(\boldsymbol{\tau}(\boldsymbol{t}) - \boldsymbol{N}(\boldsymbol{q}_t, \dot{\boldsymbol{q}}_t)) \end{bmatrix} + \begin{bmatrix} \boldsymbol{0} \\ \boldsymbol{M}^{-1}(\boldsymbol{q}_t) \end{bmatrix} \left(\frac{d\boldsymbol{B}_t}{\boldsymbol{dt}}\right) + \widetilde{\boldsymbol{K}}_t \begin{bmatrix} \boldsymbol{q}_{dt} - \widehat{\boldsymbol{q}}_t \\ \dot{\boldsymbol{q}}_{dt} - \widehat{\dot{\boldsymbol{q}}}_t \end{bmatrix} \tag{3.31}$$

To implement the feedback controller, an estimate of system state, $\widehat{X_t}$ is required which is obtainted using state observer and shown in the previous section. The form of computed torque control (refer section 2.1) is represented as:

$$\boldsymbol{\tau} = \boldsymbol{M}(\widehat{\boldsymbol{q}})(\ddot{\boldsymbol{q}}_d + \boldsymbol{K}_d(\dot{\boldsymbol{q}}_d - \widehat{\dot{\boldsymbol{q}}}) + \boldsymbol{K}_p(\boldsymbol{q}_d - \widehat{\boldsymbol{q}})) + \boldsymbol{N}(\widehat{\boldsymbol{q}}, \widehat{\dot{\boldsymbol{q}}}) \tag{3.32}$$

Where, $\boldsymbol{K_p}$ and $\boldsymbol{K_d}$ are positive definite gain matrices.

In the design process of state observer based controller, the observer gain, $\boldsymbol{L_t}$ has been considered in accordance with the standard EKF algorithm. Although it could be designed by minimizing an appropriate weighted linear combination of the conditional tracking error energy and observer error energy. More accurate controllers and observers can be designed using Bellman's dynamic programming approach based on minimizing the expected value of the integral of a linear combination of the tracking error energy and the observer error energy over a time duration $[0, T]$.

The next chapter provides experience and insights into applying the theory of controller design to the realistic, practical problem of tracking control of a robot.

3.5 Conclusion

In this chapter, a stochastic model of the nonlinear dynamical system has been developed. The tracking control problem of the stochastic system has been resolved with state observer based control. This has resulted in an estimation of state from noisy position measurements. The optimal controller has been designed and tuned online considering the energy constraint. The adaptive feature of the control algorithm determines the gains automatically according to the current dynamics of the system. The proposed controller converges to constant value indicates the less complexity while employing in a practical system. The benefit of the proposed control method is that this applies to all kinds of state observer not necessarily EKF. Further, the general form of linear state feedback control technique provides a solution of tracking problems of the practical nonlinear dynamical system in the presence of noise.

The joint error dynamics of estimation error, e_t, and tracking error, k_t derived in this chapter is further utilized to analyze the effect of fluctuation in state tracking and state observer error energies due to parametric uncertainties and PD controller fluctuations. In short, analysis of sensitivity and robustness of the controller and observer is carried out in chapter 6. The theory investigated in this chapter derives the tools for the effective design of state estimation and stochastic control. The operational implementation of a state-observer-based controller to an n-link robot for tracking the desired trajectory is investigated in the next chapter systematically.

Chapter 4

Real-time Implementation of State-Observer-Based Controller to Robot

4.1 Introduction

In chapter 3, a stochastic optimal controller for the tracking control of a nonlinear dynamical system has been designed. This chapter presents a hardware platform for the validation of proposed state-observer based control on a robot in real-time. Real-time implementation refers to data processing, execution of the command derived from a software program and implementation on hardware within a given interval. The system is first simulated using the model of a robot, and then, the applicability of the control algorithm is verified on the experimental set up of Phantom Omni$^{\mathrm{TM}}$Bundle robot available in Industrial Automation laboratory, MPAE Department, NSUT (formerly NSIT), Delhi.

4.2 Mathematical model of robot

Mathematical model is the representation of physical system into the differential equations that provides essential premise for efficient controller designing followed by the simulations of the proposed control system. Here, the model of Phantom Omni$^{\mathrm{TM}}$Bundle robot is presented to describe the relationship between force and motion in joint space. It consists of six joints of which three are computer-controlled revolute joints energizes by DC motors. Other three joints are hand-actuated passive joints. Each joint has an optical encoder for position measurement.

The Lagrange model of n-dof robot is presented as:

$$\boldsymbol{M}(\boldsymbol{q_t})\ddot{\boldsymbol{q}} + \boldsymbol{N}(\boldsymbol{q_t}, \dot{\boldsymbol{q}}_t) = \boldsymbol{\tau} \tag{4.1}$$

Where, $M(q_t)$ is the moment of inertia $n \times n$ matrix ; $N(q_t, \dot{q}_t)$ represents $n \times 1$ coriolis-centrifugal-gravitational-frictional component of the torque and τ is the $n \times 1$ matrix of input control torque.

The forward kinematics using Denavit-Hartenberg (D-H) of Phantom Omni is given in Table 4.1.

The values of the physical parameters shown in Table 4.2 [178] are substituted for developing the dynamical model as represented by equation (4.1). The model considers only actuated joint 1 and joint 3 of the robot by locking actuated joint 2 at 0^o. The joint 2 is locked by providing it a steady trajectory. The Simulink model is developed for Omni robot, the terms in equation(4.1) has the following forms:

$$\boldsymbol{M}(\boldsymbol{q}) = \begin{bmatrix} \boldsymbol{M_{11}} & \boldsymbol{M_{31}} \\ \boldsymbol{M_{31}} & \boldsymbol{M_{33}} \end{bmatrix} \tag{4.2}$$

Also,

$$\boldsymbol{N}(\boldsymbol{q}, \dot{\boldsymbol{q}}) = \begin{bmatrix} \boldsymbol{N_1} & \boldsymbol{N_3} \end{bmatrix}^T \tag{4.3}$$

The inertia matrix of the robot, assuming $\boldsymbol{q_2 = 0}$, is

$$\boldsymbol{M}(\boldsymbol{q}) = \begin{bmatrix} (\boldsymbol{\alpha_1} + \boldsymbol{\alpha_2 C_{2,3}} + \boldsymbol{\alpha_3 S_{2,3}} + \boldsymbol{\alpha_4 C_3} + \boldsymbol{\alpha_5 S_3}) & \boldsymbol{0} \\ \boldsymbol{0} & \boldsymbol{\alpha_6} \end{bmatrix} \tag{4.4}$$

$$\text{and } \boldsymbol{N}(\boldsymbol{q}, \dot{\boldsymbol{q}}) = \begin{bmatrix} \boldsymbol{N_1} & \boldsymbol{N_3} \end{bmatrix}^T \tag{4.5}$$

Table 4.1: D-H Parameters of Phantom Omni™Robot

Joint q(rad)	Joint-Distance d(m)	Link-length a (rad)	Twist, α(rad)
q_1	0	0	$-\pi/2$
q_2	0	L_1	0
$q_3 - \pi/2$	0	L_2	0

Table 4.2: Parameters of Phantom Omni^{TM}Robot

Parameter	Value of α_i
α_1	$6.11 \times 10^{-3} \pm 0.9 \times 10^{-3}$
α_2	$-2.89 \times 10^{-3} \pm 0.43 \times 10^{-3}$
α_3	$-4.24 \times 10^{-3} \pm 1.01 \times 10^{-3}$
α_4	$3.01 \times 10^{-3} \pm 0.52 \times 10^{-3}$
α_5	$2.05 \times 10^{-3} \pm 0.15 \times 10^{-3}$
α_6	$1.92 \times 10^{-3} \pm 0.23 \times 10^{-3}$
α_7	$1.60 \times 10^{-1} \pm 0.05 \times 10^{-1}$
α_8	$-8.32 \times 10^{-3} \pm 2.78 \times 10^{-3}$

where,

$$\boldsymbol{N_1 = -2\alpha_2 \dot{q}_1 \dot{q}_3 S(2q_3) + 2\alpha_3 \dot{q}_1 \dot{q}_3 C(2q_3) + \alpha_4 \dot{q}_1 \dot{q}_3 C(q_3) - \alpha_5 \dot{q}_1 \dot{q}_3 S(q_3)} \tag{4.6}$$

$$\left.\begin{aligned} \boldsymbol{N_3 = 2\alpha_2 \dot{q}_1^2 C(q_3) S(q_3) - \alpha_3 \dot{q}_1^2 C(2q_3) - \frac{1}{2}\alpha_4 \dot{q}_1^2 C(q_3) +} \\ \boldsymbol{\frac{1}{2}\alpha_5 \dot{q}_1^2 S(q_3) + \alpha_7 S(q_3) + \alpha_8 C(q_3)} \end{aligned}\right\} \tag{4.7}$$

$$\begin{aligned} &\text{Also, } \boldsymbol{C_i = \cos(q_i)}, \\ &\boldsymbol{S_i = \sin(q_i)}, \\ &\boldsymbol{C_{2,i} = \cos(2q_i)}, \\ &\boldsymbol{S_{2,i} = \sin(2q_i)} \end{aligned} \tag{4.8}$$

Jacobian of the robot, when $q_2 = 0$ is as below:

$$\boldsymbol{J} = \begin{bmatrix} \boldsymbol{l_2 + l_3 S(q_3)} & \boldsymbol{0} \\ \boldsymbol{0} & \boldsymbol{l_2 S(q_3)} \end{bmatrix} \tag{4.9}$$

In the above equation, $\mathbf{l_2}$ and $\mathbf{l_3}$ denotes length of first link and third link respectively and is equal to **135** mm.

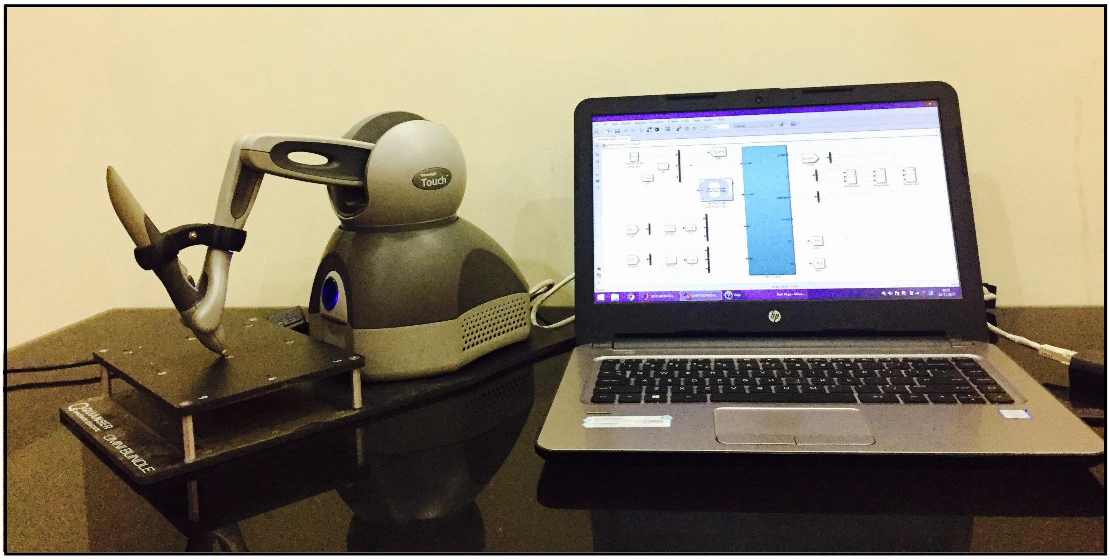

Figure 4.1: Experimental Set up of Phantom Omni™Robot.

4.3 Implementation of state-observer-based controller

The objective of this work is to implement the proposed observer-based feedback control system on a real device. Phantom Omni™Bundle robot is used with control software, QUARC® of "Quanser". QUARC provides useful tools capable of developing a Simulink model for real-time applications of the designed controller to the real system. So, without any digital signal processing or coding, the real-time code of Simulink-designed controllers can be run online directly on the Windows- target. Also, the parameters can be tuned for the running Simulink model with the facility to display the various signals and stream data to the workspace for further applications.

The following blocks are used from the Quarc library for the Simulink model and implementation of the proposed controller on the Phantom robot:

Phantom Block: This software solution includes a Phantom Omni block set for MATLAB's Simulink environment to control the Phantom haptic devices. After getting the successful simulation of the system, the dynamic forward block of a robot is replaced by Phantom block (shown in Fig. 4.3) of Quansar. In the block parameter dialog box, "Default device" is selected while using the Phantom Omni

Figure 4.2: Phantom Omni^{TM}Robot

Bundle robot so that SenSables Phantom Test program can recognize the device. The output type of this block is “Encoder values” of the joint sensors. As the controller is designed to control the joint angles of a robot, input type is selected as “Joint space”. Remaining parameters of the block are set to the default value as set by Quansar.

Smooth Signal Generator: This block is used for providing a continuous or discrete waveform with tunable amplitude and frequency online.

In the present Simulink model, it is used to provide a reference trajectory for each joint and the sample time is set to be Hz.

Sampling Time Block: This block outputs the time between samples, measured using an independent high-resolution time resource. During the experiment, the default command set for the sampling time of Phantom Omni ^{TM}Bundle device is **“qc-get-stepsize”** which automatically synchronizes the device to the workstation. The sampling time is generated automatically by the device and is equal to the refresh rate.

Bias removal: It calculates the initial position of joint of robot setting sampling time and stop time for the initial position to ”qc-get-stepsize”.

Second order low pass filter: This block is used to get the velocity signal from position signal to get velocity and to remove high-frequency noise.

Initially, Geomagic Touch software is used to pair the Phantom Omni device using LAN cable, i.e. interface IEEE-1394 FireWire (6-pin to 6-pin) port for communication. After pairing the device with the computer system, it is calibrated to remove any encoder error using Sensable phantom test. The calibration button is pressed so that the joints of a robot are physically arranged at zero configuration position as shown in Fig. 4.2. The C/C^{++} coding capability of Microsoft Visual

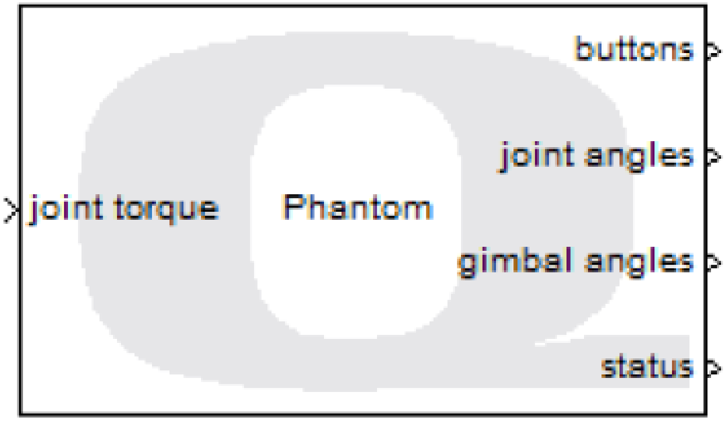

Figure 4.3: Phantom Block of Quansar

Table 4.3: Joint Parameters of Phantom Omni™Robot

Joint Position (rad)	$M(Kgm^2)$	$N(Nms/rad)$
Joint 1 ($q_2 = -\pi/4, q_3 = \pi$)	0.0031	0.0089
Joint 2 ($q_2 = 0, q_3 = \pi$)	0.0022	0.0170
Joint 3 ($q_2 = 0, q_3 = -\pi/4$)	0.0009	0.0058

basic tool or Microsoft redistributable has been used for building and compiling the code and loading it to hardware interface. After build and run command, the results of the experiments on the developed system are displayed on the scope of the Simulink. It is equipped with Open-Haptics toolkit that enables implementation and testing of the designed programming environment developed over MATLAB Simulink of controllers on the PHANToM devices easily. There is a facility to read each joint position (in radians) on the scope. Each joint is given control torque which in turn is the voltage to get the desired position which keeps on changing with time. Other three joints are hand actuated passive joints.

In the succeeding section, experiments are conducting to show the efficacy of the state observer design method and state observer- based control of a robot with stochastic noise, proposed in Chapter 3. The instruction workbook of the robot [179] used in this present study is provided by the manufacturer for conducting experiments, but some points are discussed while implementing the proposed controller on this robot.

4.4 Implementation of proposed controller

After the successful functioning of the Simulink model of a complete system, the model of the robot is replaced by "Phantom" block available in the toolbox of QUARC library so that controller can be implemented to a real device. The main difference between the available method of tracking control as given in the manual supplied by the manufacturer [179] and the proposed method are as follows:

(i) The velocity signal is obtained after feeding the position signal to second order low pass filter(refer Fig.4.4) which is supposed to reject the high-frequency noise after differentiation. Whereas in the present work, velocity is estimated using EKF state observer.

(ii) The available PID control block has Saturation blocks to limit the unsafe values for the proportional gains. However, no description is given about it. In the present work, Lagrange multiplier is used to constrain the error energy of controller to serve the same purpose.

(iii) Further, the maximum velocity of the device should not exceed by 20 rad/sec mentioned in the manual. Keeping this in mind the reference trajectory is designed.

(iv) The reference trajectory is chosen keeping in mind the maximum torque which the joints can bear as specified in the manual.

(v) In the available lab manual of this robot, K_p and K_d is computed for a fixed joint angle, friction force and mass of inertia (refer to Table 4.3). The value of proportional gain for Joint 1 is kept $K_p = 1.79Nm/rad$ and $K_d = 0.03Nms/rad$ and for Joint 3 is $K_p = 0.6Nm/rad$ and $K_d = 0.001Nms/rad$ that are fixed in the manual which we have to make varying or adaptive. However, in time-varying desired trajectory, values of parameters are changing w.r.t. joint angles so, the objective of work is to design an adaptive controller K_p and K_d according to the time-varying trajectory.

(vi) As the joint has a bias so in the desired trajectory of joint 3, π is added, joint 2 is kept fixed by providing step signal of 1.2 as it has the bias of $5\pi/12$.

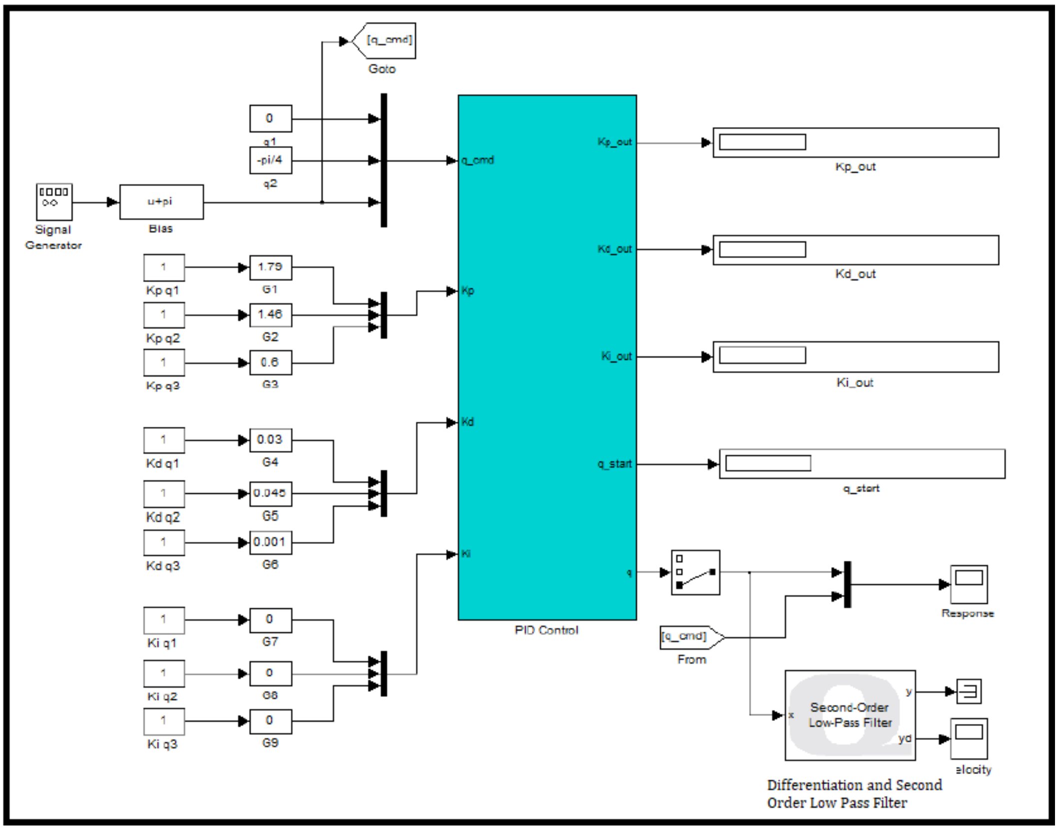

Figure 4.4: Controller Block

Fig. 4.2 shows the Joint 1, Joint 2 and Joint 3 of the Phantom robot and the zero configuration position means the Joint 1 and Joint 2 are set at 0 radian and Joint 3 at π radian respectively. The fixed sampling time in simulations (Δ) is replaced by variable sampling time of processor (taken from Quarc library block) to synchronize the program to get the accurate results. The variable sampling time is dependent upon the computational size of each loop/iteration.

4.5 EKF implementation

The system state vector ($\boldsymbol{X}$) is as below:

$$\boldsymbol{X} = [\ \boldsymbol{q_1},\ \ \boldsymbol{q_3},\ \ \dot{\boldsymbol{q}}_1,\ \ \dot{\boldsymbol{q}}_3]^{\boldsymbol{T}} \tag{4.10}$$

Thus, the system model in state space form can be represented as:

$$\left.\begin{aligned} \dot{\boldsymbol{X}} &= [\ \dot{\boldsymbol{q}}_1,\ \ \dot{\boldsymbol{q}}_3,\ \ \ddot{\boldsymbol{q}}_1,\ \ \ddot{\boldsymbol{q}}_3\ \ ]^{\boldsymbol{T}} \\ &= \boldsymbol{\psi(t, X) + G(q)W} \end{aligned}\right\} \tag{4.11}$$

$$\dot{\boldsymbol{X}} = \begin{bmatrix} \dot{\boldsymbol{q}}_1 \\ \\ \dot{\boldsymbol{q}}_3 \\ [\boldsymbol{M}(\boldsymbol{q})]^{-1}(-\boldsymbol{N}(\dot{\boldsymbol{q}}) + \boldsymbol{\tau}) \end{bmatrix} + \begin{bmatrix} \boldsymbol{0} \\ \\ \boldsymbol{0} \\ \boldsymbol{G}(\boldsymbol{q}) \end{bmatrix} \tag{4.12}$$

Where, $\boldsymbol{\tau}$ is the torque vector of joint 1 and joint 3 i.e. $\boldsymbol{\tau} = \begin{bmatrix} \boldsymbol{\tau}_1 \\ \boldsymbol{\tau}_2 \end{bmatrix}$ and also, $\boldsymbol{G}(\boldsymbol{q}) = \begin{bmatrix} \boldsymbol{G}(\boldsymbol{q}_1) \\ \boldsymbol{G}(\boldsymbol{q}_2) \end{bmatrix}$

To proceed with the experimental verification of the proposed control algorithm on hardware, first of all, modeling of the Phantom robot is done in Simulink. The information about the dynamics of this robot is inferred from the available literature [178] and illustrated in section 4.2.

The Simulink block of EKF observer is also developed using the model of the robot and including process and measurement noise. Simulations testing is done to ensure the proper estimations of states using position signal in the presence of reasonable noises (assuming Gaussian White noise) as shown in Fig.4.3.

By defining the state vector

$$\widehat{\boldsymbol{X}} = [\widehat{\boldsymbol{q}}_1, \widehat{\boldsymbol{q}}_3, \widehat{\dot{\boldsymbol{q}}}_1, \widehat{\dot{\boldsymbol{q}}}_3]^{\boldsymbol{T}} \tag{4.13}$$

From equations (3.6) and (3.8), extended non-linear state observer is represented as:

$$\left.\begin{aligned} \dot{\widehat{\boldsymbol{X}}} &= \boldsymbol{\psi}(\boldsymbol{t}, \widehat{\boldsymbol{X}}) + \boldsymbol{P}\boldsymbol{H}^{\boldsymbol{T}}\boldsymbol{\sigma}_{\boldsymbol{v}}^{-2}(\dot{\boldsymbol{z}} - \widehat{\boldsymbol{q}}) \\ \dot{\boldsymbol{P}} &= \widehat{\boldsymbol{\psi}}'\boldsymbol{P} + \boldsymbol{P}\widehat{\boldsymbol{\psi}}'^{\boldsymbol{T}} + \widehat{\boldsymbol{g}}\boldsymbol{\sigma}_{\boldsymbol{w}}^2\widehat{\boldsymbol{g}}^{\boldsymbol{T}} - \boldsymbol{P}\boldsymbol{H}^{\boldsymbol{T}}\boldsymbol{\sigma}_{\boldsymbol{v}}^{-2}\boldsymbol{H}\boldsymbol{P} \end{aligned}\right\} \tag{4.14}$$

$$\left.\begin{aligned} \boldsymbol{\sigma}_\nu &= \begin{bmatrix} \boldsymbol{cov.}(\boldsymbol{w}) & \boldsymbol{0} \\ \boldsymbol{0} & \boldsymbol{cov.}(\boldsymbol{w}) \end{bmatrix} \\ \boldsymbol{P} &= \begin{bmatrix} \boldsymbol{P}_{\boldsymbol{qq}} & \boldsymbol{P}_{\boldsymbol{q},\dot{\boldsymbol{q}}} \\ \boldsymbol{P}_{\dot{\boldsymbol{q}}\boldsymbol{q}} & \boldsymbol{P}_{\dot{\boldsymbol{q}}\dot{\boldsymbol{q}}} \end{bmatrix} \\ \widehat{\boldsymbol{g}} = \boldsymbol{g}(\widehat{\boldsymbol{q}}) &= \begin{bmatrix} \boldsymbol{0} \\ \boldsymbol{G}(\widehat{\boldsymbol{q}}) \end{bmatrix} \end{aligned}\right\} \tag{4.15}$$

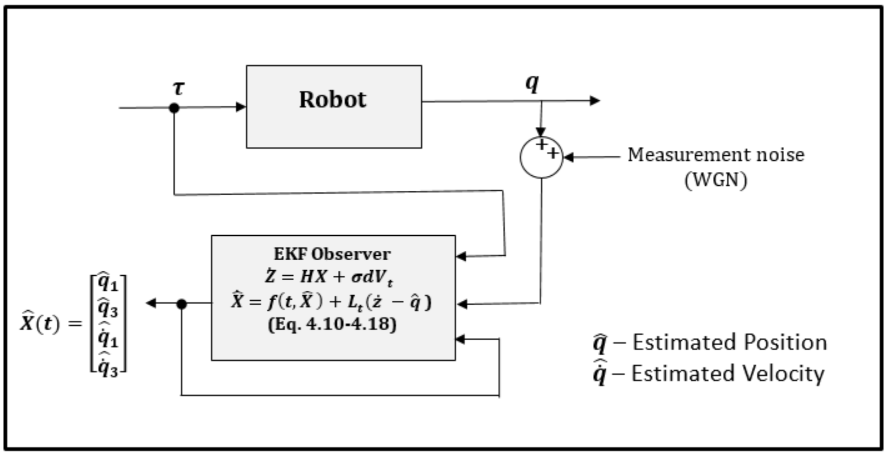

Figure 4.5: EKF Implementation

$\boldsymbol{\sigma_v}$, $\boldsymbol{\sigma_w}$, $\boldsymbol{P}$ and $\widehat{\boldsymbol{g}}$ are defined above and for the present measurement linear system

$$\left.\begin{aligned} \dot{\boldsymbol{z}} = \boldsymbol{HX} + \boldsymbol{\sigma_v dV_t} = [\boldsymbol{q_1}, \boldsymbol{q_3}]^{\boldsymbol{T}} \\ \text{Here,} \quad \boldsymbol{H} = \begin{bmatrix} \mathbf{1} & \mathbf{0} & \mathbf{0} & \mathbf{0} \\ \mathbf{0} & \mathbf{1} & \mathbf{0} & \mathbf{0} \end{bmatrix} \end{aligned}\right\} \tag{4.16}$$

$$\widehat{\boldsymbol{\psi}}' = \frac{\partial \boldsymbol{\psi}}{\partial \widehat{\boldsymbol{X}}} = \begin{bmatrix} \frac{\partial \psi_1}{\partial \widehat{q}_1} & \frac{\partial \psi_1}{\partial \widehat{q}_3} & \frac{\partial \psi_1}{\partial \widehat{\dot{q}}_1} & \frac{\partial \psi_1}{\partial \widehat{\dot{q}}_3} \\ \frac{\partial \psi_2}{\partial \widehat{q}_1} & \frac{\partial \psi_2}{\partial \widehat{q}_3} & \frac{\partial \psi_2}{\partial \widehat{\dot{q}}_1} & \frac{\partial \psi_2}{\partial \widehat{\dot{q}}_3} \\ \frac{\partial \psi_3}{\partial \widehat{q}_1} & \frac{\partial \psi_3}{\partial \widehat{q}_3} & \frac{\partial \psi_3}{\partial \widehat{\dot{q}}_1} & \frac{\partial \psi_3}{\partial \widehat{\dot{q}}_3} \\ \frac{\partial \psi_4}{\partial \widehat{q}_1} & \frac{\partial \psi_4}{\partial \widehat{q}_3} & \frac{\partial \psi_4}{\partial \widehat{\dot{q}}_1} & \frac{\partial \psi_4}{\partial \widehat{\dot{q}}_3} \end{bmatrix} \tag{4.17}$$

$$= \begin{bmatrix} \mathbf{0}^{2\times2} & \boldsymbol{I}^{2\times2} \\ \frac{\partial \widehat{\boldsymbol{F}}}{\partial \widehat{\boldsymbol{q}}} & \frac{\partial \widehat{\boldsymbol{F}}}{\partial \widehat{\dot{\boldsymbol{q}}}} \end{bmatrix} \tag{4.18}$$

In Simulink block of EKF, Fourth-order Rung Kutta method is used to perform the algorithm. The estimated values of one iteration are stored in the memory for the further use of the next iteration for time value updation with the help of a fast processor.

4.6 Computed torque ontrol

The implementation of a state observer based computed torque control (CTC) for the n-link robot has been done in this section. CTC provides linear feedback to the non-linear robotic system as discussed in section 2.2. For a given current position and velocity, CTC cancels out the nonlinearities and provides exactly the torque required to overcome the inertia of the actuator.

$$\boldsymbol{\tau} = \boldsymbol{M}(\boldsymbol{q})\ddot{\boldsymbol{q}}_{\boldsymbol{d}} + \boldsymbol{N}(\boldsymbol{q}_{\boldsymbol{d}}, \dot{\boldsymbol{q}}_{\boldsymbol{d}}) \tag{4.19}$$

Also, $M(q_t)$ is the moment of inertia matrix and $N(q_t, \dot{q}_t)$ represents the coriolis-centrifugal-gravitational-frictional component of the torque.
Substitution of control law results:

$$\boldsymbol{M}(\boldsymbol{q})\ddot{\boldsymbol{q}}_{\boldsymbol{d}} = \boldsymbol{M}(\boldsymbol{q})\ddot{\boldsymbol{q}} \tag{4.20}$$

The property of inertia matrix implies that $\boldsymbol{M}(\boldsymbol{q})$ is positive definite in $\ddot{\boldsymbol{q}}_{\boldsymbol{d}}\forall\ddot{\boldsymbol{q}}$. State feedback is added to inertial acceleration to get the corrected acceleration to get the tracking property. Thus, to get the linear form of (4.19), the form of control law is :

$$\boldsymbol{\tau} = \boldsymbol{M}(\boldsymbol{q})(\ddot{\boldsymbol{q}}_{\boldsymbol{d}} + \boldsymbol{K}_{\boldsymbol{p}}\boldsymbol{e} + \boldsymbol{K}_{\boldsymbol{d}}\dot{\boldsymbol{e}}) + \boldsymbol{N}(\boldsymbol{q}_{\boldsymbol{d}}, \dot{\boldsymbol{q}}_{\boldsymbol{d}}) \tag{4.21}$$

The term with inertia matrix is termed as feedback component and rest is feedforward component of control. Inverse dynamic block computes the feedforward component while the computation of feedback component is done according to the actual trajectory. Thus, the computation of control torque signal is done at each sample period in real time.

4.7 Results and comparison

In this section, the performance of the proposed method is analyzed by conducting Test A, and Test B. Tests are performed by applying:

(i) Test signal-I: Signal with white Gaussian measurement noise of covariance 10^{-7}

(ii) Test signal-II: Signal with white Gaussian measurement noise of covariance 10^{-5}.

The results of both tests carried on joint 1 and joint3 have been illustrated in Fig.4.6 to Fig.4.13 for joint1 and joint3. The performance is analyzed regarding desired, estimated and actual trajectory tracking for the proposed approach.

The following observations have been recorded:

- From Fig.4.6 to Fig.4.13, it is observed that there will be spikes in the initial process of results as seen in the zoomed section (a) but later on responses settle down and converge and can be seen in the zoomed section (b) of every figure.

- The experimental results as shown in Fig.4.6 to Fig.4.13 for desired trajectory ($\boldsymbol{q}_d$), actual trajectory and estimated trajectory ($\widehat{\boldsymbol{q}}$) for joint 1 and joint 3 respectively validate the good performance of the proposed technique.

- Fig.4.14 and Fig.4.17 indicates the position tracking error and velocity tracking error of joint 1 and joint3 with noises having covariance 10^{-7} and 10^{-5} respectively in the system.

- Fig.4.6-Fig.4.7 show position and Fig.4.10-Fig.4.11 show velocity tracking of joint 1. What is surprising that although there are small ripples in the position estimate $\widehat{q}$, there are no large ripples in $\widehat{\dot{q}}$. If we had used derivative of estimated postion i.e. $\dot{\widehat{q}}$ in place of estimated velocity, $\widehat{\dot{q}}$, we would have got sharp spikes. Thus, the EKF overcomes the velocity tracking problem successfully.

- Every joint has specific limits of motion. This can be seen in Fig.4.9(b). During the initial process of estimation, joint 3 rotates to its lower limit and thus encounters saturation. Also, joint 2 is made fixed to 1.2 radians and the motion of joint 3 depends upon joint 2.

- Joint 1 has a lesser error magnitude than joint 3 (refer Fig.4.14-Fig.4.17). This could be explained by the fact that the errors propagate from joint1 to

Table 4.4: Experiment Results: Position Tracking RMS Error ($\times 10^{-3}$)

Work	[117]	[100]	Proposed Test A	Proposed Test B
Noise	Not Consider	Not Consider	cov. (10^{-7})	cov. (10^{-5})
Joint-1	11.9	9.98	6.09	8.34
Joint-3	76.9	33.1	13.09	15.76

joint 3. Specifically, if the position of joint 1 is $\mathbf{r_1}$ and the position of joint3 is $(\mathbf{r_1} + \mathbf{r_3})$, then the respective error variances are $\mathbb{E}[||\delta\mathbf{r_1}||^\mathbf{2}]$ and $\mathbb{E}[||\delta\mathbf{r_1}||^\mathbf{2}] + \mathbb{E}[||\delta\mathbf{r_3}||^\mathbf{2}$, assuming $\delta\mathbf{r_1}$ and $\delta\mathbf{r_3}$ are uncorrelated i.e. $\mathbb{E}(\delta\mathbf{r_1^T}\delta\mathbf{r_3}) = \mathbf{0}$.

The comparison of performance of proposed method and techniques employed by [100] and [117] is shown in Table 4.4. This indicates better results in the presence of measurement noises. Also, with the increase in the noise, as shown in the column of Test B, RMS error is increased, but even then the performance is better as compared to previous work [100] and [117]. The reason is that the Kushner filter is optimal but the EKF is suboptimal so many authors try to implement the EKF closer to optimal by replacing the Kalman gain $\boldsymbol{\sigma_v^{-2} P_t H^T}$ by a gain matrix $\boldsymbol{L_t}$, designed to minimize the mean square observer error.

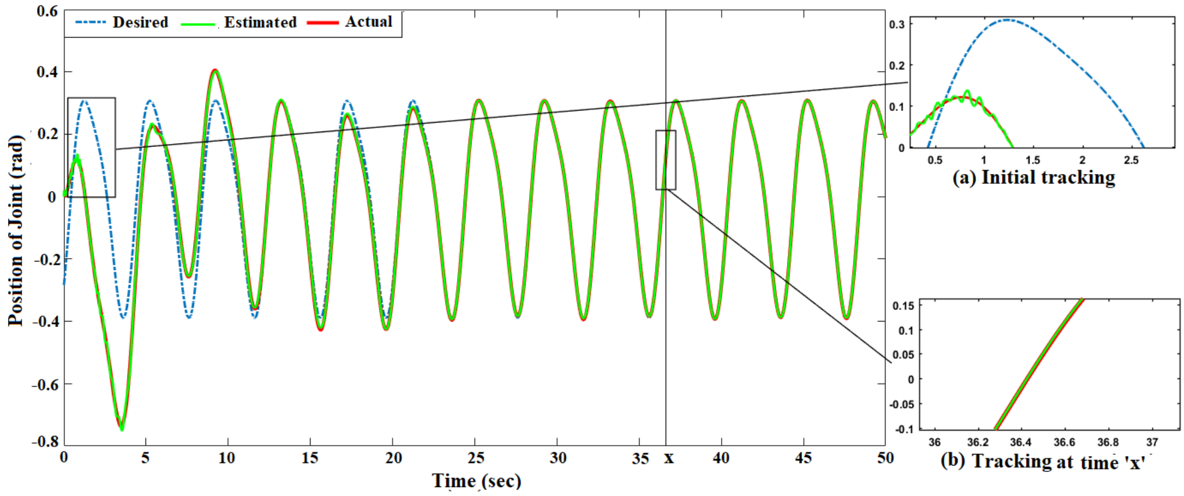

Figure 4.6: Position Tracking of Joint 1 with Measurement Noise of Covariance 10^{-7} at Different Time Slots.

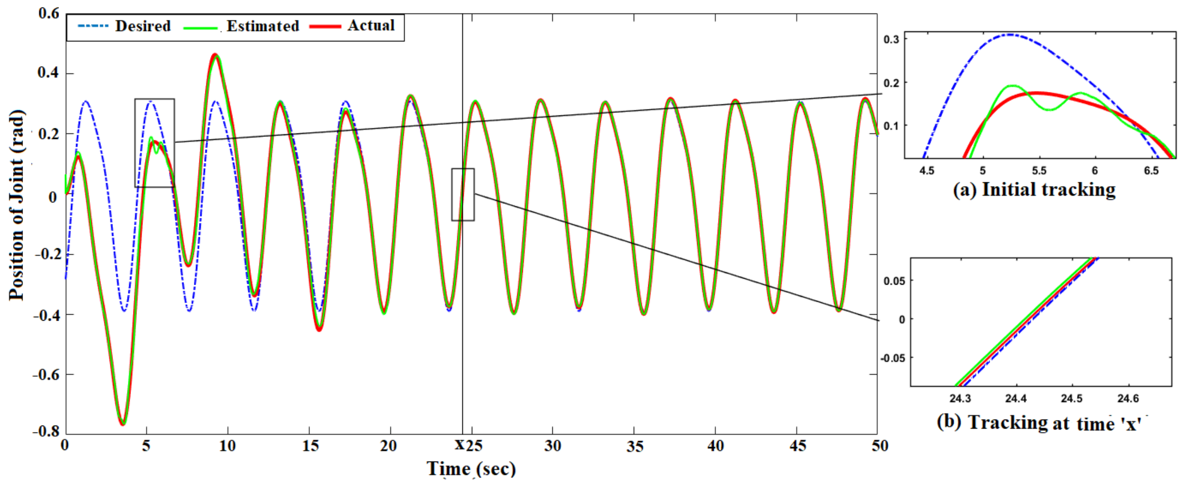

Figure 4.7: Position Tracking of Joint 1 with Measurement Noise of Covariance 10^{-5} at Different Time Slots.

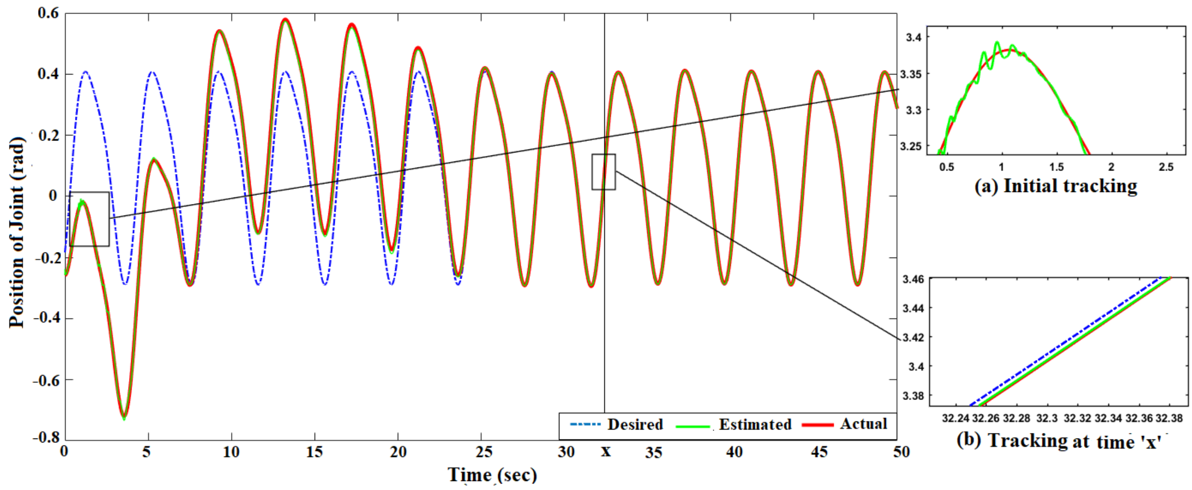

Figure 4.8: Position Tracking of Joint3 with Measurement Noise of covariance 10^{-7} at Different Time Slots.

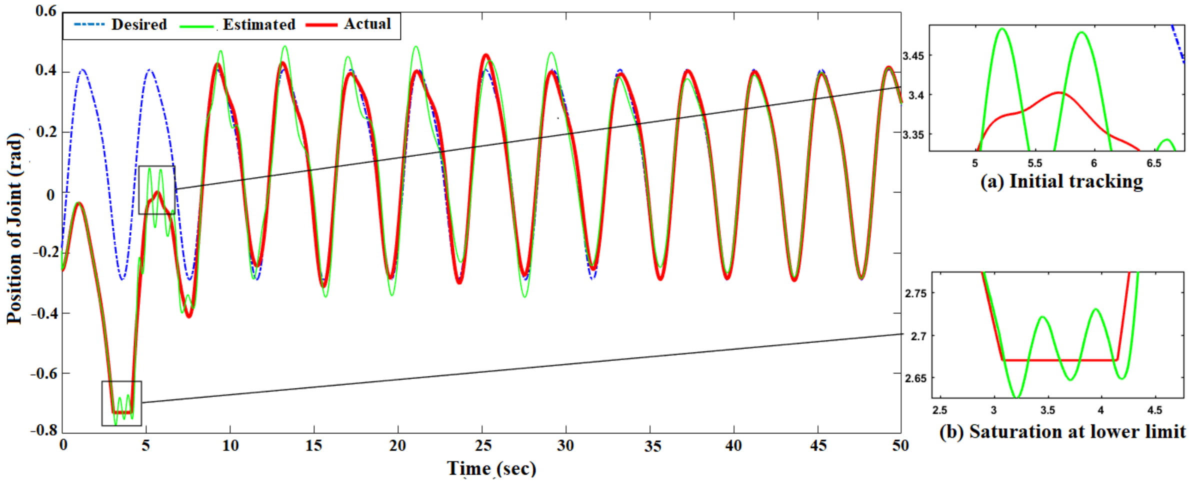

Figure 4.9: Position Tracking of Joint 3 with Measurement Noise of Covariance 10^{-5} at Different Time Slots.

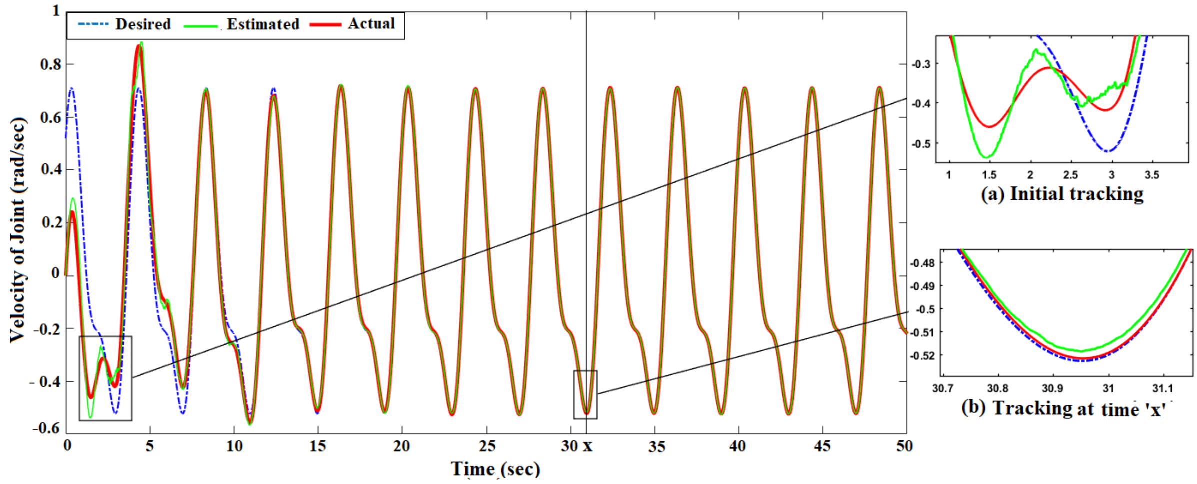

Figure 4.10: Velocity Tracking of Joint 1 with Measurement Noise of Covariance 10^{-7} at Different Time Slots.

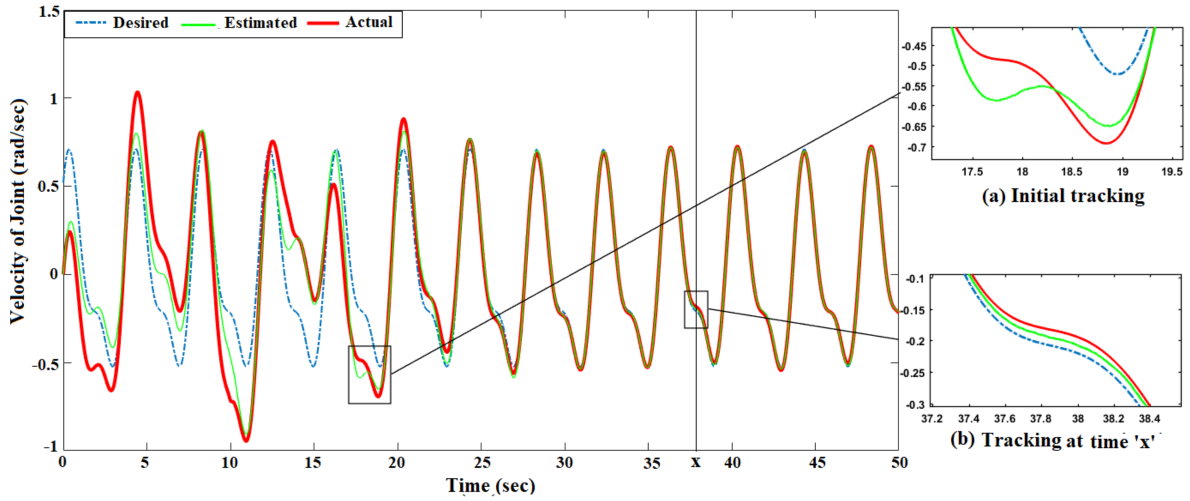

Figure 4.11: Velocity Tracking of Joint 1 with Measurement Noise of Covariance 10^{-5} at Different Time Slots.

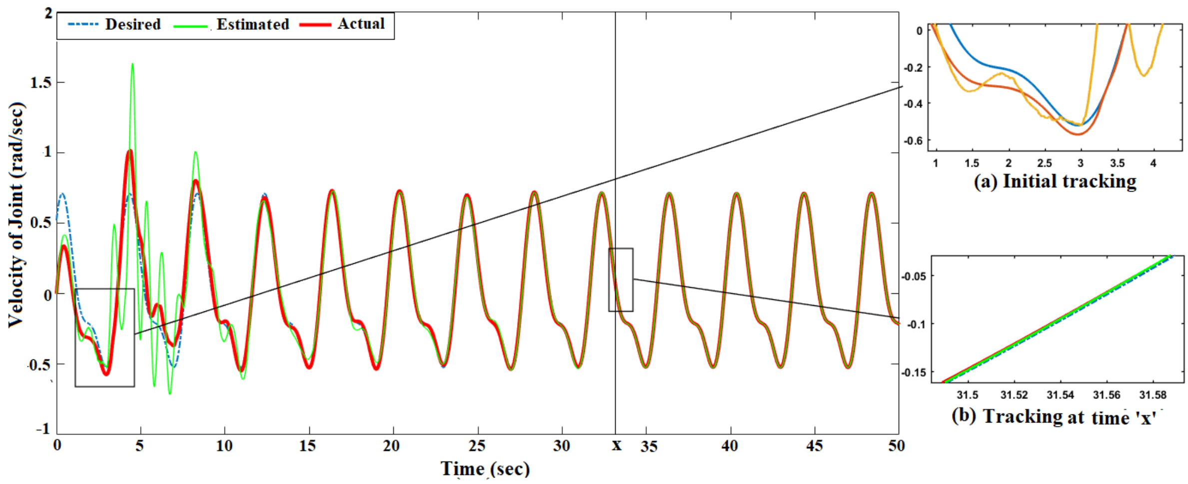

Figure 4.12: Velocity tracking of joint 3 with Measurement Noise of Covariance 10^{-7} at Different Time Slots.

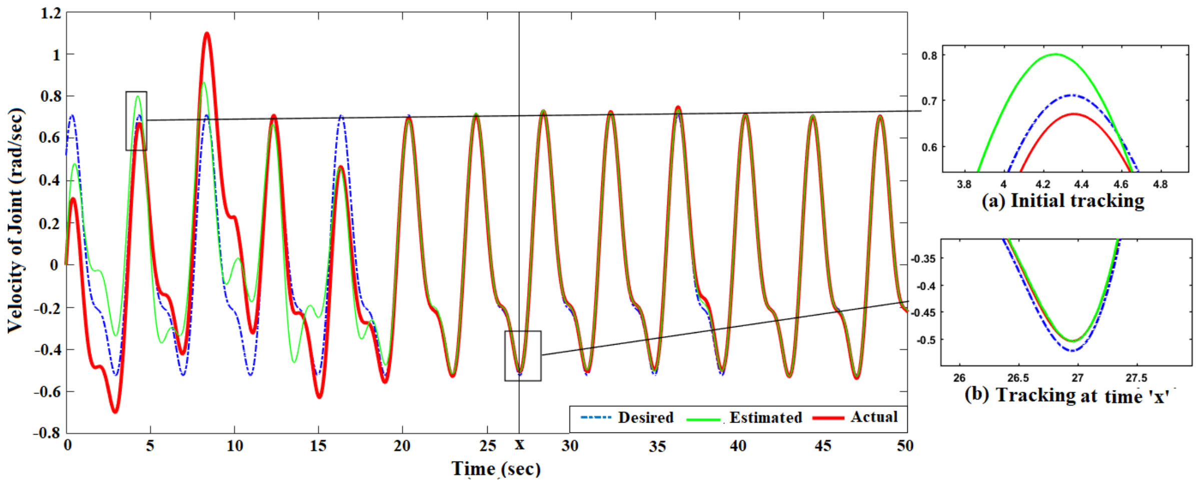

Figure 4.13: Velocity Tracking of Joint 3 with Measurement Noise of Covariance 10^{-5} at Different Time Slots.

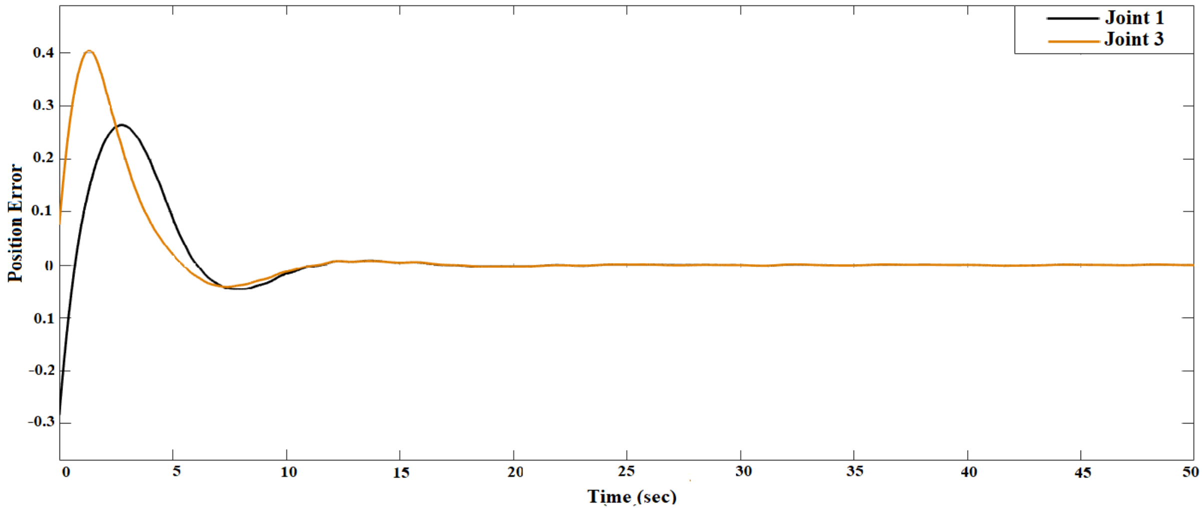

Figure 4.14: Position Error of Joints with Measurement Noise of Covariance 10^{-7}.

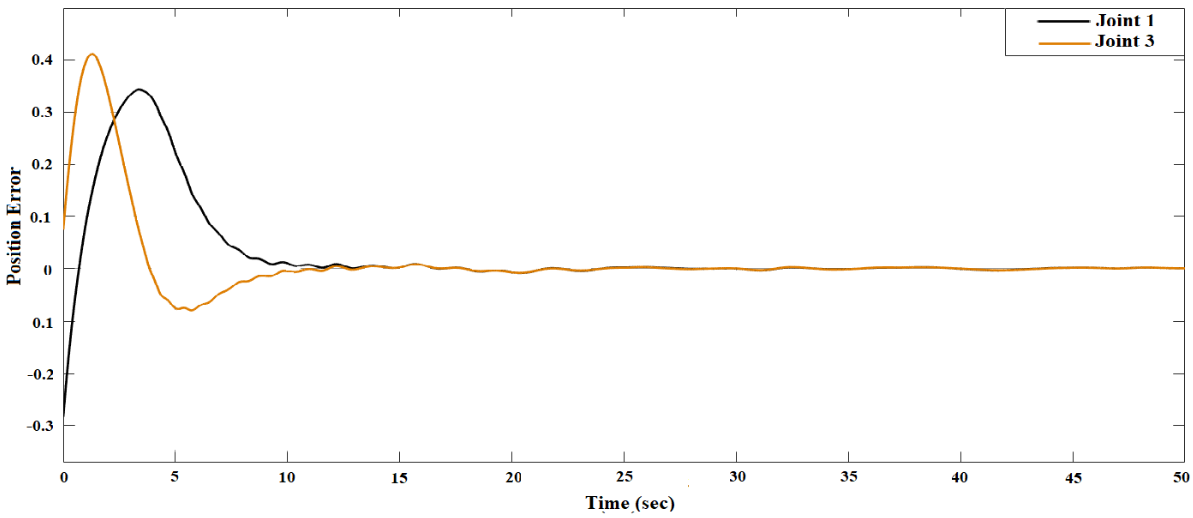

Figure 4.15: Position Error of Joints with Measurement Noise of Covariance 10^{-5}.

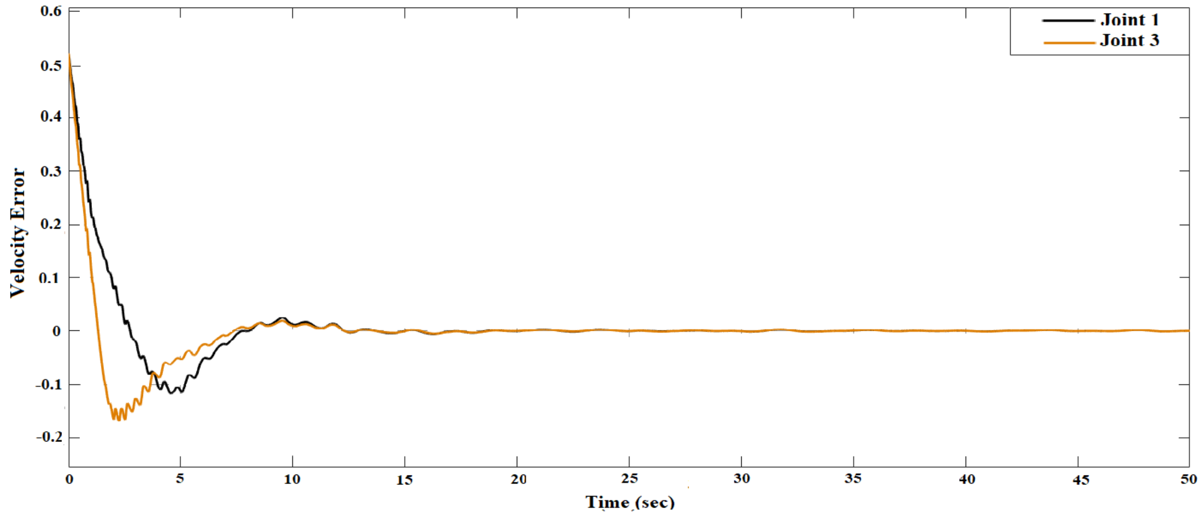

Figure 4.16: Velocity Error of Joints with Measurement Noise of Covariance 10^{-7}.

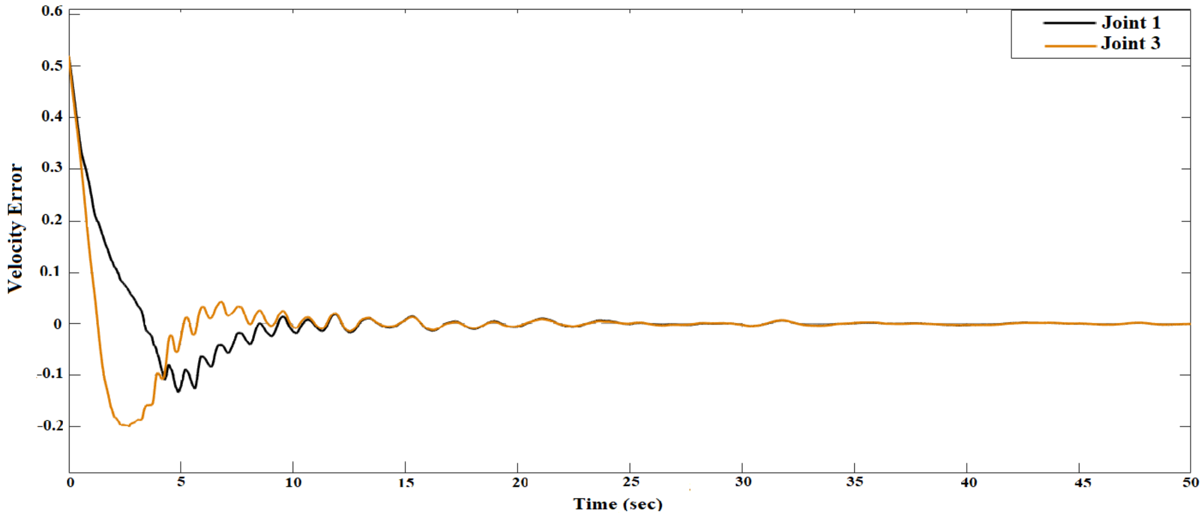

Figure 4.17: Velocity Error of Joints with Measurement Noise of Covariance 10^{-5}.

4.8 Conclusion

The proposed algorithm has successfully been implemented for a generalized controller of a robot based on observer derived state error feedback. State-observer-based control has utilized only the position measurement from the encoder and relives the system from using velocity sensor or traditional way of differentiation of position signal to get the velocity. Hence, with the use of observer, estimated position and velocity signals without measurement noise have effectively improved the performance of the feedback control system to track the desired trajectory in real-time. Further, the developed optimal controller subjected to energy constraint has restricted the actuator saturation.

The proposed control algorithm with adaptive features has been successfully used for tracking of the robotic manipulator in this chapter. The experimental results conducted using the Phantom Omni^{TM} Bundle robot manipulator has demonstrated and validated the potential application of the proposed control algorithm on a real system.

Experimental results have indicated excellent tracking as compared to standard PD or P-controllers used in literature. Further, efforts have been seeking to minimize a linear combination of the tracking error energy and the observer error energy simultaneously by choosing the PD controller gain, $\boldsymbol{K_t}$ and the observer gain, $\boldsymbol{L_t}$ appropriately. The prime feature of this work is that the real-time feedback coefficients have been designed for very general nonlinear systems described by a stochastic differential equation and later on specialized to robot dynamics and control problems.

This chapter has implemented on-line observer and qualify the robust controller through experimentation done on the real device. Further, recommendations are made to expand the theoretical results in a direction to a specific measure of the robustness of controller and establishing a relation between model accuracy along with variation in the system variables with the dynamics of the system in the next chapter.

Chapter 5

Sensitivity Analysis and Robustness

5.1 Introduction

Sensitivity analysis is done to study the system's behavior corresponding to fluctuations in some variables or parameters of the system which are supposed to ultimately affect the performance of the system. The impact of fluctuations in parameters can be reflected in the state transition matrix, Eigenvalues, state variables and ultimately stability and performance of the system. This analysis helps to test the robustness of a system in the presence of uncertainty. The aim of the robustness property for the controller in the presence of uncertain dynamic is to render the system insensitive to parameter fluctuations that may be caused due to disturbances, e.g. joint interactions, measurement noises, and noises affecting the system itself. A dynamic system is robust if it tolerates fluctuations in the parts of the system without exceeding predefined tolerance bounds in the vicinity of some nominal dynamic behavior.

In this chapter, sensitivity analysis of state observer based control designed for a nonlinear dynamical system having uncertainties in the system parameter, $\boldsymbol{\theta}$ and controller parameter, $\boldsymbol{K_t}$ is investigated. Extended the results of section 3.4, the joint error dynamics of estimation error, $\boldsymbol{e(t)}$ and tracking error, $\boldsymbol{k(t)}$ is utilized in section 5.2. The analysis is based on linearizing the dynamics of the system satisfied by errors with respect to the parameter, and controller gain fluctuations in section 5.3. Finally, the variation of the energies both in state estimation error and tracking error with respect to the fluctuations in the system parameters and the feedback coefficients are investigated in section 5.4.

Robustness of the system ensures that one can meet tracking and stability objectives through the design of controller provided the changes occur within the plant remain within certain bounds. As long as uncertainties stay within bounds, there will be a guarantee of stable control of the system. This results to investigate the conditions that guarantee bound on mean square error energies of the system. With the use of the formulae of variation of parameters and norms as candidates, the general inequalities are derived that impose an upper bound on the tracking error and observer error in a mean square sense. This investigation checks the property of robustness for the proposed stochastic control design as presented in section 5.5.

5.2 System dynamics with parametric uncertainty

From section 3.3, consider the closed-loop dynamics of the system that takes into account the observer model. To examine the sensitivity, assume this model is influenced by parametric uncertainty and controller adjustment. So, in the state model, the fixed parameter, $\boldsymbol{\theta}$ appearing in the drift term is replaced with an unknown parameter, $\boldsymbol{\theta_0}$ as shown in equation (5.1).

$$\left.\begin{aligned} \boldsymbol{X_t} &= \begin{bmatrix} \boldsymbol{q}_t \\ \dot{\boldsymbol{q}}_t \end{bmatrix} \\ \boldsymbol{dX_t} &= \boldsymbol{\psi(t, X_t, \theta_0)dt + \widetilde{K}_t(X_{dt} - X_t)dt + \widetilde{G}_t dB_t} \end{aligned}\right\} \tag{5.1}$$

Recalling in a SDE, the coefficient of $\boldsymbol{dt}$ is called the drift coefficient while the coefficient of $\boldsymbol{dB(t)}$ is called the diffusion coefficient.

The observer model is the same as the state model but without the state noise term and it uses a given parameter $\boldsymbol{\theta}$ in place of the unknown parameter $\boldsymbol{\theta_0}$ appearing in the drift term of the state model. It also uses an output error feedback via an observer gain $\boldsymbol{L_t}$ which is assumed not to fluctuate.

$$\boldsymbol{d\widehat{X}_t = \psi(t, \widehat{X}_t, \theta)dt + L_t(dZ_t - H\widehat{X}_t dt)} \tag{5.2}$$

The measurement model is

$$\boldsymbol{dZ_t = HX_tdt + \sigma_v dV_t} \tag{5.3}$$

Where $\boldsymbol{dZ_t}$ is the measurement from the plant and $\boldsymbol{H}$ is the state observation matrix given as $\boldsymbol{H} = [\boldsymbol{I_2} : \boldsymbol{0}]$. This form of matrix $\boldsymbol{H}$ accounts to measure $\boldsymbol{q_t}$ and not $\boldsymbol{\dot{q}_t}$.

The controller gain $\boldsymbol{\widetilde{K}_t}$ has the special block form as:

$$\boldsymbol{\widetilde{K}_t} = \begin{bmatrix} \boldsymbol{0} \\ \boldsymbol{K_t} \end{bmatrix} \tag{5.4}$$

The derived state $\boldsymbol{X_{dt}}$ follows the same dynamics as the actual state $\boldsymbol{X_t}$ but without the state noise term and controller.

$$\boldsymbol{dX_{dt} = \psi(t, X_{dt}, \theta_0)dt} \tag{5.5}$$

5.3 Error dynamics, $\boldsymbol{\xi_t}$

Consider the different types of errors (refer Section 3.2) involved in the closed loop nonlinear dynamical system defined as:

$$\left.\begin{aligned} \text{Observer error, } \boldsymbol{e_t} &= \boldsymbol{X_t - \hat{X}_t} \\ \text{Tracking error using observer state as true state , } \boldsymbol{f_t} &= \boldsymbol{X_{dt} - \hat{X}_t} \\ \text{and tracking error, } \boldsymbol{k_t} &= \boldsymbol{e_t - f_t = X_t - X_{dt}} \end{aligned}\right\}$$

After linearizing with respect to the parameter fluctuation, $\boldsymbol{\delta\theta}$, the approximate dynamics of the state observer error and the tracking error process are represented as:

$$\left.\begin{aligned} \boldsymbol{de_t} &= \boldsymbol{\widehat{\psi}'_t e_t dt +\ \widetilde{K}_t k_t dt + \widehat{\widehat{G}}_t dB_t - L_t(He_t dt + \sigma_v dV_t)} \\ \boldsymbol{dk_t} &= \boldsymbol{-\widehat{\psi}'_t k_t dt - \widetilde{K}_t k_t - \widehat{\psi}_{\theta t}\delta\theta - \widehat{\widehat{G}}_t dB_t} \end{aligned}\right\} \tag{5.6}$$

The above equations can be arranged in the following form as:

$$\boldsymbol{d}\begin{bmatrix} \boldsymbol{e}_t \\ \boldsymbol{k}_t \end{bmatrix} = \begin{bmatrix} \boldsymbol{\widehat{\psi'}_t - L_t H} & \boldsymbol{\widetilde{K}_t} \\ \boldsymbol{0} & \boldsymbol{-\widehat{\psi'} - \widetilde{K}_t} \end{bmatrix} \begin{bmatrix} \boldsymbol{e}_t \\ \boldsymbol{k}_t \end{bmatrix} \boldsymbol{dt} + \begin{bmatrix} \boldsymbol{\widehat{\widehat{G}}_t} & \boldsymbol{-\sigma_v L_t} \\ \boldsymbol{-\widehat{\widehat{G}}_t} & \boldsymbol{0} \end{bmatrix} \boldsymbol{d} \begin{bmatrix} \boldsymbol{B}_t \\ \boldsymbol{V}_t \end{bmatrix} - \begin{bmatrix} \boldsymbol{0} \\ \boldsymbol{\widehat{\psi}_{\theta t}} \end{bmatrix} \boldsymbol{\delta\theta} \tag{5.7}$$

$$\text{Putting } \boldsymbol{\xi_t} = \begin{bmatrix} \boldsymbol{e_t} \\ \boldsymbol{k_t} \end{bmatrix} \tag{5.8}$$

where, $\boldsymbol{\xi_t}$ is complete model of error process taking in to account of state estimation error and tracking error and the drift matrix, $\boldsymbol{A_t}$ for the stochastic differential equation of error process is defined as:

$$\boldsymbol{A}_t = \begin{bmatrix} \widehat{\boldsymbol{\psi}}'_t - \boldsymbol{L}_t\boldsymbol{H} & \widetilde{\boldsymbol{K}}_t \\ \boldsymbol{0} & -\widehat{\boldsymbol{\psi}}'_t - \widetilde{\boldsymbol{K}}_t \end{bmatrix} \tag{5.9}$$

5.4 Sensitivity analysis

In this section, sensitivity analysis is carried out to check the effect on error-dynamics by varying the values of controller gain and parameter. The steps involved in carrying out the analysis is outline in the flow diagram as shown in Fig. 5.1.

In the following derivation, it is inferred that the fluctuations in the feedback gain $\widetilde{\boldsymbol{K}}_{\boldsymbol{t}}$ by $\boldsymbol{\delta}\widetilde{\boldsymbol{K}}_{\boldsymbol{t}}$ will affect the drift matrix $\boldsymbol{A_t}$ to fluctuate by $\boldsymbol{\delta A_t}$ and subsequently lead to fluctuate the state transition matrix $\boldsymbol{\phi(t,\tau)}$ by $\boldsymbol{\delta\phi(t,\tau)}$.

The fluctuations of controller gain matrix $\widetilde{\boldsymbol{K}}_{\boldsymbol{t}}$ is expressed as:

$$\begin{aligned} \widetilde{\boldsymbol{K}}_t + \boldsymbol{\delta}\widetilde{\boldsymbol{K}}_t &= \begin{bmatrix} \boldsymbol{0} \\ \boldsymbol{K_t} + \boldsymbol{\delta K_t} \end{bmatrix} = \begin{bmatrix} \boldsymbol{0} \\ \boldsymbol{K_t} \end{bmatrix} + \begin{bmatrix} \boldsymbol{0} \\ \boldsymbol{\delta K_t} \end{bmatrix} \\ \text{so, } \boldsymbol{\delta}\widetilde{\boldsymbol{K}}_t &= \begin{bmatrix} \boldsymbol{0} \\ \boldsymbol{\delta K_t} \end{bmatrix} \end{aligned} \tag{5.10}$$

The fluctuations in controller gain matrix, $\boldsymbol{\delta}\widetilde{\boldsymbol{K}}_{\boldsymbol{t}}$ will result in the fluctuations of drift matrix , $\boldsymbol{\delta A_t}$ which is shown as:

$$\left.\begin{aligned} \boldsymbol{A_t} &\implies \boldsymbol{A_t} + \boldsymbol{\delta A_t} \\ \boldsymbol{\delta A_t} &= \begin{bmatrix} 0 & \boldsymbol{\delta}\widetilde{\boldsymbol{K}}_t \\ 0 & -\boldsymbol{\delta}\widetilde{\boldsymbol{K}}_t \end{bmatrix} = \begin{bmatrix} 0 & 0 \\ 0 & \boldsymbol{\delta K_t} \\ 0 & 0 \\ 0 & -\boldsymbol{\delta K_t} \end{bmatrix} \end{aligned}\right\} \tag{5.11}$$

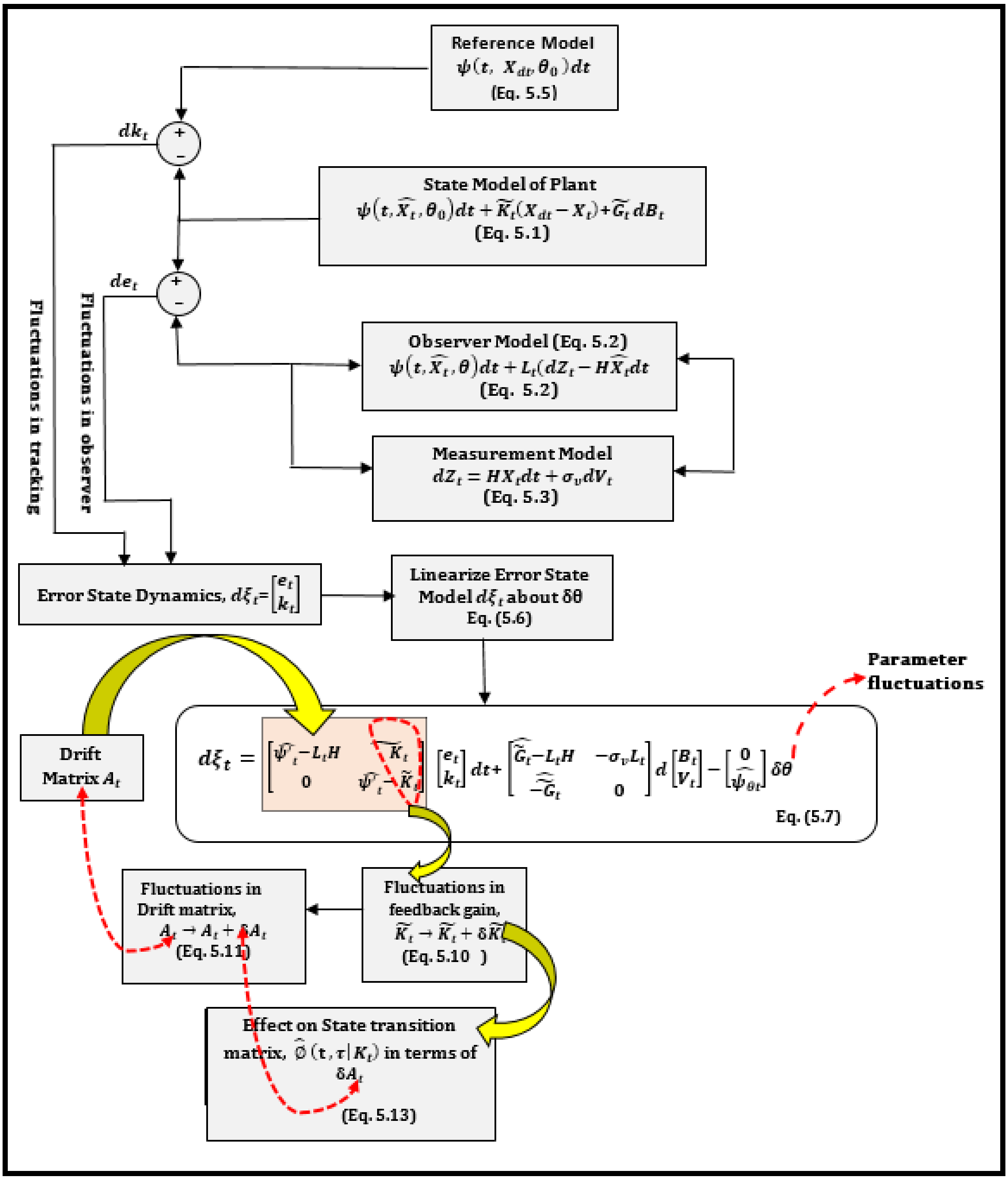

Figure 5.1: Flow Diagram of Sensitivity Analysis.

In the prceeding numerical analysis, we can infer that sensitivity relies upon fluctuations in the parameters as well as on the controller gain which in term depends upon the drift matrix as discussed in equation (5.11).

The complete evolution of the error process taken into account controller gain fluctuations and parametric fluctuations can be expressed as:

$$\left.\begin{aligned} d\boldsymbol{\xi}_t &= (\boldsymbol{A}_t + \boldsymbol{\delta A}_t)\boldsymbol{\xi}_t dt + \widetilde{\boldsymbol{G}}_t d\begin{bmatrix}\boldsymbol{B}_t\\ \boldsymbol{V}_t\end{bmatrix} - \widetilde{\boldsymbol{\psi}}_{\boldsymbol{\theta} t}\boldsymbol{\delta\theta} \\ \text{where } \widetilde{\boldsymbol{G}_t} &= \begin{bmatrix}\widehat{\boldsymbol{G}}_t & -\boldsymbol{\sigma}_v \boldsymbol{L}_t\\ -\widehat{\boldsymbol{G}}_t & \boldsymbol{0}\end{bmatrix} \text{ and } \widetilde{\boldsymbol{\psi}}_{\boldsymbol{\theta} t} = \begin{bmatrix}\boldsymbol{0}\\ \hat{\boldsymbol{\psi}}_{\boldsymbol{\theta} t}\end{bmatrix}\end{aligned}\right\} \tag{5.12}$$

As seen in equation (5.12), $\boldsymbol{\delta A}_t$ form a component of the drift coefficient and since $\boldsymbol{\delta A}_t$ is defined in terms of $\boldsymbol{\delta K}_t$ (as shown in equation 5.11), $\boldsymbol{\delta K}_t$ form a component of the drift coefficient. $\boldsymbol{A}_t$ is the drift matrix since $\boldsymbol{A}_t\boldsymbol{\xi}_t$ is the drift coefficient and $\boldsymbol{\delta A}_t$ is therefore, the drift matrix fluctuations.

The property of state transition matrix is applied i.e. it satisfy the system differential equation, we have, $\dfrac{\boldsymbol{\partial\hat{\phi}(t,\tau)}}{\boldsymbol{\partial t}} = \boldsymbol{A}_t\boldsymbol{\hat{\phi}(t,\tau), t \geq \tau}$; and $\boldsymbol{\hat{\phi}(\tau,\tau) = I}$.

The effect of controller gain fluctuations on the state transition matrix fluctuations is represented as:

$$\left.\begin{aligned} \boldsymbol{\hat{\phi}(t,\tau)} &= \boldsymbol{\phi(t,\tau|K_t)} \\ \boldsymbol{\delta\hat{\phi}(t,\tau)} &= \frac{\boldsymbol{\partial\phi(t,\tau|K_t)}}{\boldsymbol{\partial Vec(K_t)}}\boldsymbol{\delta Vec(K_t)} \\ \frac{\boldsymbol{\partial\delta\hat{\phi}}}{\boldsymbol{\partial t}}\boldsymbol{(t,\tau)} &= \boldsymbol{\delta A_t\hat{\phi}(t,\tau) + A_t\delta\hat{\phi}(t,\tau)} \\ \boldsymbol{\delta\hat{\phi}(t,\tau)} &= \int_{\boldsymbol{\tau}}^{\boldsymbol{t}} \boldsymbol{\hat{\phi}(t,\tau')\delta A_{\tau'}\hat{\phi}(\tau',\tau)d\tau'}\end{aligned}\right\} \tag{5.13}$$

Essentially, after forming the differentiation of the state equations for the error, $\boldsymbol{\xi}_t$ with respect to the feedback parameters and solving for the resulting differentiated change in the state transition matrix would enable to calculate the effect of fluctuations in feedback coefficients on the tracking and observer state error which is shown below.

The error evolution is expressed in terms of state transition matrix fluctuation (or equivalently controller-gain fluctuation) and the parameter fluctuation, $\boldsymbol{\delta\theta}$, and presented as:

$$\boldsymbol{\xi}_t = \int_0^t (\boldsymbol{\phi}(\boldsymbol{t},\boldsymbol{\tau}) + \boldsymbol{\delta\phi}(\boldsymbol{t},\boldsymbol{\tau})) \left(\widetilde{\boldsymbol{G}}_{\boldsymbol{\tau}} \boldsymbol{d} \begin{bmatrix} \boldsymbol{B}_\tau \\ \boldsymbol{V}_\tau \end{bmatrix} + \widetilde{\boldsymbol{\psi}}_{\boldsymbol{\theta\tau}} \boldsymbol{\delta\theta} \right) \boldsymbol{d\tau} \tag{5.14}$$

Remark

As $\boldsymbol{\delta K_t} = \boldsymbol{\delta K}$ is constant in time over a sufficiently long time interval, then from equation (5.11), it is evident that $\boldsymbol{\delta A_t} = \boldsymbol{\delta A}$ is also constant in time. This can be justified with the help of following discussion:

After a long time, when steady state is reached, it is expected that the desired state, $\boldsymbol{X_{dt}}$ converge to a constant DC value plus some minor oscillations about the equilibrium. Likewise, the actual state, $\boldsymbol{X_t}$ should also converge to a constant DC value plus small oscillations. Thus, the feedback force, $\boldsymbol{K_t(X_{dt} - X_t)}$ must be nearly constant which imply that the gain, $\boldsymbol{K_t}$ should converge to a constant value. For the sake of simplicity, let us consider an observer given as:

$$\dot{\boldsymbol{X}}_{\boldsymbol{t}} = \boldsymbol{A X_t} + \boldsymbol{K(X_{dt} - X_t)} + \boldsymbol{L_t(Y_t - H\widehat{X_t})} \tag{5.15}$$

The above equation is considered at equilibrium in the absence of noise.

Thus, if $X_t \rightarrow X_\infty$ becomes a constant vector then the above equation can be shown as

$$AX_\infty + K(X_{d\infty} - \widehat{X}_\infty) = 0 \tag{5.16}$$

If the observer is good, the $\widehat{X}_\infty \approx X_\infty$ and then,

$$AX_\infty + K_\infty(X_{d\infty} - \widehat{X}_\infty) + L_t(H(X_\infty - \widehat{X}_\infty)) = 0 \tag{5.17}$$

$$\left.\begin{aligned} \text{consider, } e_\infty &= X_\infty - \widehat{X}_\infty \\ f_\infty &= X_{d\infty} - \widehat{X}_\infty \end{aligned}\right\}$$

The following is obtained:

$$AX_\infty + K_\infty(f_\infty) + L_t(e_\infty) = 0 \tag{5.18}$$

If e_∞, X_∞ and f_∞ are random vectors, then K becomes the value at which

$$\mathbb{E}[\, || \, AX_\infty + Kf_\infty + L_tHe_\infty||^2 \,] \text{ is a minimum.} \tag{5.19}$$

Minimizing this with respect to K gives

$$\left.\begin{aligned} &\mathbb{E}\,[(\, AX_\infty + Kf_\infty + L_tHe_\infty).f_\infty^T] \;= 0 \\ &\text{So, } A\,\mathbb{E}(X_\infty f_\infty^T) + L_tH\,\mathbb{E}(e_\infty f_\infty^T) + K_\infty\,\mathbb{E}(f_\infty.f_\infty^T) = 0 \\ &\text{or } K_\infty = -[A\,\mathbb{E}(X_\infty f_\infty^T) + L_tH\,\mathbb{E}(e_\infty f_\infty^T)]\,(\mathbb{E}(f_\infty f_\infty^T))^{-1} \end{aligned}\right\} \tag{5.20}$$

From the above equation, it is to be noted that $\boldsymbol{K}$ is constant after a sufficient long time.

5.5 Ensuring Robustness-boundness of mean-square error

As it can be infered from the above subsection that the parameter vector, $\boldsymbol{\theta}$ fluctuates by $\boldsymbol{\delta\theta}$ and so the resulting change in the dynamics of $\boldsymbol{\xi_t}$ receives contributions from both $\boldsymbol{\delta\widetilde{K}}$ and $\boldsymbol{\delta\theta}$. Taking both of these into account, the state dynamics of error is derived in equation (5.14). It can be further solve as:

$$\boldsymbol{\xi_t} = \int_{0}^{t} \boldsymbol{\phi(t,\tau)\widetilde{G}_\tau d}\begin{bmatrix}\boldsymbol{B_\tau}\\ \boldsymbol{V_\tau}\end{bmatrix} + \int_{0}^{t} \boldsymbol{\delta\phi(t,\tau)\widetilde{G}_\tau d}\begin{bmatrix}\boldsymbol{B_\tau}\\ \boldsymbol{V_\tau}\end{bmatrix} + \left(\int_{0}^{t} \boldsymbol{\phi(t,\tau)\widetilde{\psi}_{\theta\tau} d\tau}\right)\boldsymbol{\delta\theta} \tag{5.21}$$

The dynamics of mean square tracking error and observer error is presented as:

$$\begin{aligned}\mathbb{E}\{\|\boldsymbol{\xi_t}\|^2\} = \boldsymbol{Tr}\{\mathbb{E}\int_{0}^{t}(\boldsymbol{\phi(t,\tau)\widetilde{G}_\tau\widetilde{G}_\tau^T(\phi^T(t,\tau)} + \boldsymbol{\delta\phi(t,\tau)}) + \boldsymbol{\delta\phi^T(t,\tau))d\tau}\}+\\ \boldsymbol{\delta\theta^T}\left(\int_{0}^{t}\boldsymbol{\phi(t,\tau)\widetilde{\psi}_{\theta\tau}d\tau}\right)^{\boldsymbol{T}}\left(\int_{0}^{t}\boldsymbol{\phi(t,\tau)\widetilde{\psi}_{\theta\tau}d\tau}\right)\boldsymbol{\delta\theta}\\ = \boldsymbol{X_1(t)} + \boldsymbol{X_2(t)} + \boldsymbol{X_3(t)} + \boldsymbol{X_4(t)}\end{aligned} \tag{5.22}$$

The mean square error process, $\mathbb{E}\{\|\boldsymbol{\xi_T}\|^2\}$ is expressed in term of the parametric fluctuation, $\boldsymbol{\delta\theta}$ and controller fluctuation, $\boldsymbol{\delta K_t}$ (which manifest itself in the form of state transition matrix fluctuation) and neglecting $\boldsymbol{O(\delta K \otimes \delta\theta)}$).

From equation (5.22), the values of $\boldsymbol{X_1(t), X_2(t), X_3(t), X_4(t)}$ are given as:

$$
\begin{aligned}
X_1(t) &= Tr\left\{\int_0^t \phi(t,\tau)\widetilde{G}_\tau\widetilde{G}_\tau^T\phi^T(t,\tau)d\tau\right\};\\
X_2(t) &= 2\,Tr\left\{\int_0^t \delta\phi(t,\tau)\widetilde{G}_\tau\widetilde{G}_\tau^T\phi^T(t,\tau)d\tau\right\};\\
X_3(t) &= Tr\left\{\int_0^t \delta\phi(t,\tau)\widetilde{G}_\tau\widetilde{G}_\tau^T\delta\phi^T(t,\tau)d\tau\right\};\\
X_4(t) &= \delta\theta^T\left(\int_0^t \phi(t,\tau)\widetilde{\psi}_{\theta\tau}d\tau\right)^T\left(\int_0^t \phi(t,\tau)\widetilde{\psi}_{\theta\tau}d\tau\right)\delta\theta.
\end{aligned}
\tag{5.23}
$$

It is to be noted that term $\boldsymbol{X_1(t)}$ has only noise fluctuations, $\boldsymbol{X_2(t), X_3(t)}$ terms have contributed to drift matrix fluctuations and term $\boldsymbol{X_4(t)}$ reflects fluctuations in parameters.

The system is robust if it is possible to determine the bounds on the system uncertainties, which guarantees robust control of the system as long as the uncertainties stay within these bounds. An upper bound can be imposed on the mean square tracking and observer errors by putting the upper bound on the various terms given in equation (5.23) as follows:

The objective of robustness of system is ensured in terms of the size of error energy signals. A quantitative treatment of the performance of control systems requires the introduction of appropriate norms, which give measurements of the sizes of the signals considered.

Let the largest real part of the Eigen values of $\boldsymbol{A_t}$ be bounded by $\boldsymbol{-\alpha_0 < 0}$.

Consider $\boldsymbol{\sup_\tau \|\widetilde{G}_\tau\| = g_0 < \infty}$ and size of matrix $\boldsymbol{A_t}$ i.e. of $\boldsymbol{\psi(t,\tau)}$ to be $\boldsymbol{(d\times d)}$, then

$$
\left.
\begin{aligned}
\|\ \phi(t,\tau)\ \| &\le e^{-\alpha_0(t-\tau)},\ \ \left[\phi(t,\tau) \approx e^{(t-\tau)A}\right]\\
\text{thus,}\ \ \|\ X_1(t)\ \| &\le d^2\int e^{-2\alpha_0(t-\tau)}\ \|\ \widetilde{G}_\tau\ \|^2\ d\tau\\
&\le d^2\left(\sup_\tau \|\ \widetilde{G}\ \|^2\right)\left(\frac{1-e^{-2\alpha_0 t}}{2\alpha_0}\right)\\
\lim_{t\to\infty} X_1 &\le \frac{d^2 g_0^2}{2\alpha_0}
\end{aligned}
\right\}
\tag{5.24}
$$

Likewise, the limiting values for $\boldsymbol{X_2, X_3}$ and $\boldsymbol{X_4}$ are evaluated as:

$$\left.\begin{aligned} &\boldsymbol{X_2 = 2Tr\left\{\int\limits_{0<\tau<\tau'<t} \Phi(t,\tau')\delta A\Phi(\tau',\tau)\widetilde{G}_\tau\widetilde{G}_\tau\Phi^T(t,\tau)d\tau' d\tau\right\}}, \\ &\overline{\lim_{t\to\infty}}\,|\boldsymbol{X_2}| \leq \frac{\|\boldsymbol{\delta A}\|^2\boldsymbol{d^3 g_0^2}}{\boldsymbol{\alpha_0^2}} \end{aligned}\right\} \tag{5.25}$$

$$\left.\begin{aligned} &\boldsymbol{X_3 = Tr\left\{\int\limits_{0<\tau<\tau',\tau''<<t} \phi(t,\tau'|\delta A(\tau',\tau)\widetilde{G}_\tau\widetilde{G}_\tau^T\phi^T(\tau'',\tau)\delta A\phi^T(t,\tau'')d\tau' d\tau'' d\tau)\right\}} \\ &\overline{\lim_{t\to\infty}}\,\boldsymbol{X_3} \leq \frac{\|\boldsymbol{\delta A}\|^2\boldsymbol{g_0^2}}{\boldsymbol{\alpha_0^3}} \end{aligned}\right\} \tag{5.26}$$

$$\overline{\lim_{t\to\infty}}\,\boldsymbol{X_4} \leq \frac{\|\boldsymbol{\delta\theta}\|^2}{\boldsymbol{\alpha_0^2}}\boldsymbol{\psi_0^2 d^2}; \text{ where } \boldsymbol{\psi_0 = \sup_\tau \|\widetilde{\psi}_{\theta\tau}\|} \tag{5.27}$$

Thus, the upper bound on the tracking and observer error energy is presented as:

$$\overline{\lim_{t\to\infty}}\,\mathbb{E}\|\boldsymbol{\xi}^2\| \leq \frac{\boldsymbol{d^2 g_0}}{\boldsymbol{2\alpha_0}} + \boldsymbol{d^3 g_0^2}\frac{\|\boldsymbol{\delta A}\|^2}{\boldsymbol{\alpha_0^2}} + \frac{\|\boldsymbol{\delta A}\|^2\boldsymbol{g_0^3}}{\boldsymbol{\alpha_0^2}} + \frac{\|\boldsymbol{\delta\theta}\|^2\boldsymbol{\psi_0^2 d^2}}{\boldsymbol{\alpha_0^2}} \tag{5.28}$$

further, using the property of norm,

$$\|\ \boldsymbol{\delta A_t}\ \|^2 \leq \boldsymbol{2}\ \|\ \boldsymbol{\delta K_t}\ \|_F^2 \tag{5.29}$$

From equations (5.24) to (5.27), it is shown that the term, $\lim\limits_{t\to\infty}\boldsymbol{X_1}$ gives the limiting tracking error and observer error energies in the absence of parameter and feedback coefficients uncertainties while the sum of different terms i.e. $\boldsymbol{X_2 + X_3 + X_4}$ express the limiting tracking error and observer error energies in the presence of parameter and feedback coefficients uncertainties. Further, $\boldsymbol{X_2, X_3}$ depend on $\boldsymbol{\delta\phi}$ which in turn depends on $\boldsymbol{\delta K}$ while $\boldsymbol{X_4}$ depends on $\boldsymbol{\delta\theta}$, so the upper bounds on $\boldsymbol{X_2 + X_3 + X_4}$ depends on $\|\ \boldsymbol{\delta K}\ \|$ and $\|\ \boldsymbol{\delta\theta}\ \|$, which therefore, determines the sensitivity and robustness of the tracking error energy w.r.t. parameter and feedback coefficients fluctuations.

Limiting mean square fluctuation in the tracking error depends upon parameter fluctuation as well as fluctuations in drift matrix. The limiting mean square fluctuations in observer error and tracking error are upper bounded by a noise contribution which depends upon square of maximum eigen value of drift matrix, $\boldsymbol{A}$ i.e. $\boldsymbol{\lambda_1}$ plus fluctuation in energy of drift matrix plus energy of parameter as shown in equation (5.28).

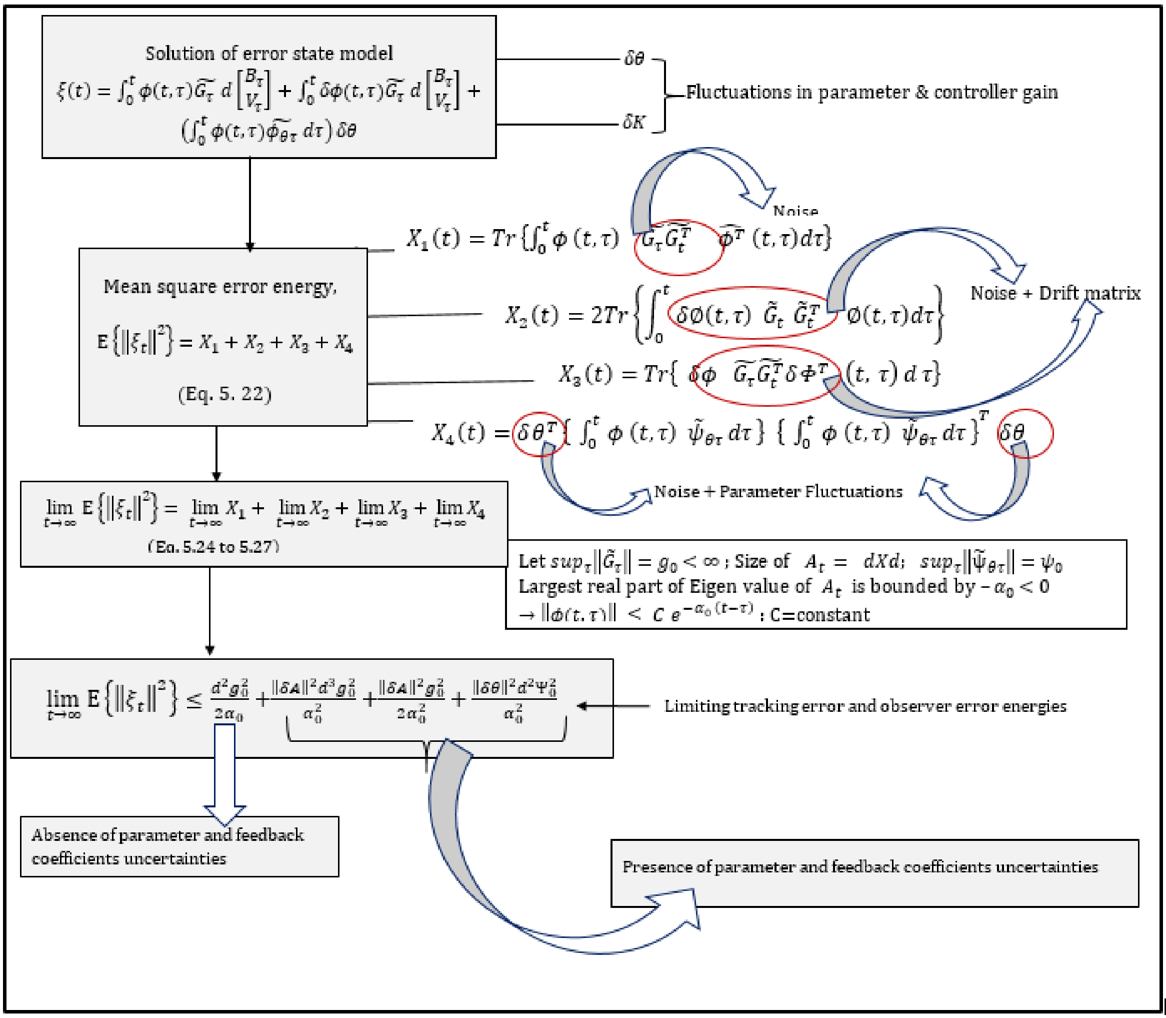

Figure 5.2: Analysis of Robustness.

5.6 Conclusion

An interpretation on the effect of fluctuations in parameter and controller gain on the error dynamics of observer based feedback system has been presented through sensitivity analysis. The study infers that these fluctuations affect state transition matrix of the system and an expression of deviation in this matrix is derived. The derivation of general inequality giving an upper bound on the mean-square tracking error and observer error is presented. The robustness of the proposed control solution is ensured by tracking of a stochastic system to a sufficiently smooth reference signal with an error norm smaller than a prescribed value. Finally, we have obtained explicit upper bounds on the tracking and state estimation error energies as quadratic functions of the feedback coefficient. These upper bounds are expressed as quadratic functions of the parameter and controller gain as well as the state noise and observer noise gain fluctuations. The system matrices $\boldsymbol{M(q)}, \boldsymbol{N(q, \dot{q})}$ as well as the controller gain $\boldsymbol{K_t}$ and observer gain $\boldsymbol{L_t}$ determine the sensitivity of the mean square errors to the parameter and controller gain fluctuations while the state noise and observer gain obtained from the matrices $\boldsymbol{G_t}, \boldsymbol{L_t}$, determine the noise contributions to the mean square error upper bounds as analyzed in this chapter. These formulae involve the process noise and measurement noise covariance and lend novelty to this paper.

Chapter 6

Estimation of Controller-gain and Stochastic Environment Force of Master-slave Robotic System

6.1 Introduction

This chapter addresses the design of controller-gain parameters, $\widehat{\boldsymbol{K}}$ of slave robot in a master-slave robotic system when a slave is interacting with a stochastic environment. The slave robot aims to follow the time-varying trajectory of the master robot in a situation when the environment is modelled as a zero-mean white Gaussian random process. This randomness is introduced into slave dynamics, adding formidable complexity to the dynamics of a robotic system. The stochastic dynamics of the system is modelled in section 6.3. Further, for a known master torque, $\boldsymbol{\tau_{mo}}$, the joint positions of master and noisy slave is measured to compute the joint probability distribution function (pdf) of angle error over a given time duration as a function of the unknown parameters '**K**'. Maximizing the conditional pdf of the slave error angles vector, $\boldsymbol{p(\delta q_s[.]|K)}$ over a duration of time w.r.t. **K** is equivalent to minimizing the negative likelihood function $\boldsymbol{\mathcal{L}((\delta q_s[.]|K)}$ w.r.t. **K** to obtain the Maximum likelihood estimation (MLE) of controller-gain parameters as presented in section 6.4. Further to back substitute these controller estimates, $\widehat{\boldsymbol{K}}$ into the dynamics and thereby estimate the sample trajectory of the environmental noise process, $\boldsymbol{(W[n])_{n=0}^{N}}$. The validation of estimation performance is carried out (a) through simulations done on a 2-link master-slave

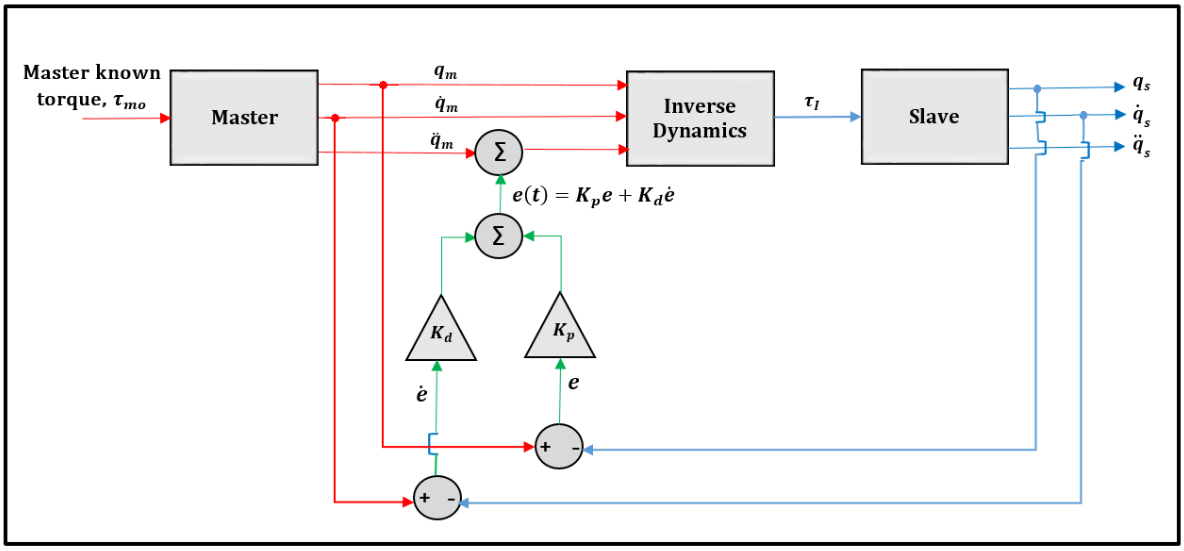

Figure 6.1: Controller Design of Slave Robot for Master-Slave Trajectory Tracking Without Environment Interaction.

robotic system in section 6.5 and (b) analytically in section 6.6. Convergence analysis of error in the estimates is performed, and subsequently, an expression of the Cramer Rao Lower Bound (CRLB) is derived to measure the accuracy of the estimation.

6.2 Graphical representation of robot tracking

Consider the situation when slave robot has to follow the master trajectory in the absence of environmental force as shown in Fig. 6.1. The master robot controls the slave robot by inverse dynamics computation. The slave dynamics do not influence the master dynamics as no feedback from the slave is given to master. For a known master torque, τ_{mo}, the inverse dynamics computation block takes the master angles, $q_m(t)$ and angular velocities $\dot{q}_m(t)$, as its other two variables and generates a torque, τ_I that is used as input to the slave so that the states of slave track the states of master i.e. $q_s(t) = q_m(t)$ and $\dot{q}_s(t) = \dot{q}_m(t)$. The torque control law is computed using the angular acceleration of master, $\ddot{q}_m$ plus an error torque, $e(t)$ obtained by passing the position and velocity error through a PD controller. This error feedback guarantees that if the slave robot lags the master robot either in position or in velocity, then the acceleration input to the

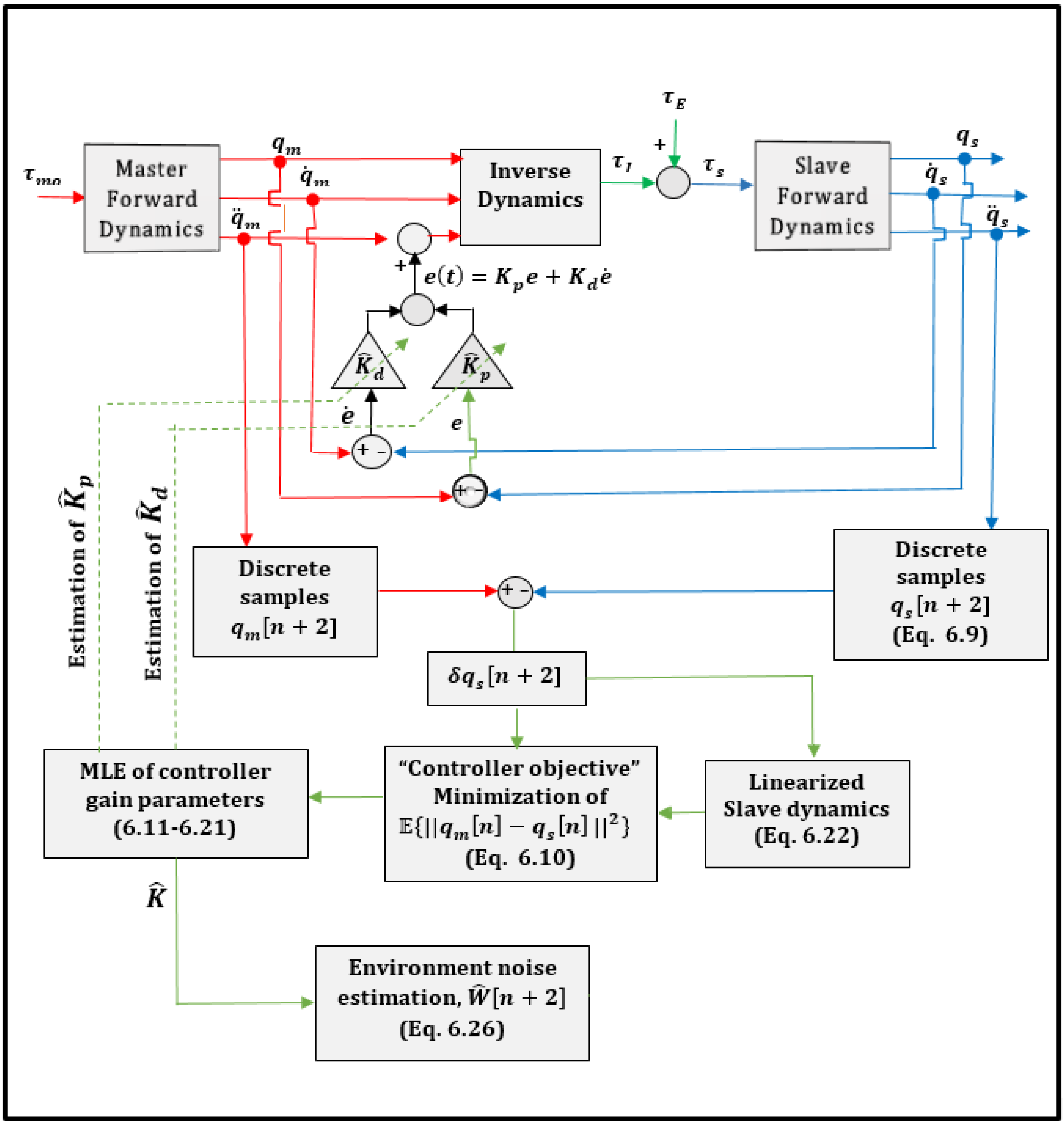

Figure 6.2: Block Diagram for Estimation Process of PD controller Gain Parameters and Environment Force for Master-slave System.

inverse dynamics block increases thus, causing the torque applied to the slave to increase so that its position and velocity approach more closely the master position and velocity respectively. In response to the deviation from the desired trajectory, the controller gains $\boldsymbol{K_p}$ and $\boldsymbol{K_d}$ are tuned that are required to minimize the position and velocity tracking error.

Assuming zero environmental torque, the PD feedback coefficients are designed based on optimal control theory to minimize the error energy between the Master and Slave angles for a known master torque. This system is then handed over to the user who does not know the exact values of the PD control gain parameters but wishes to use the system to determine the torque generated by a rapidly vibrating environment considered as environmental uncertainty. This is done by causing the slave robot to act on the environment. In this situation, measurement of angles of master and slave for a given master torque, $\boldsymbol{\tau_{mo}}$ and random environmental torque $(\boldsymbol{\tau_E})$ is taken. The process illustrating the proposed design of the PD controller's parameters and environment noise estimation is shown in the block diagram of Fig. 6.2 and explained in the following sections. The error feedback from slave to master is not given; hence, the slave motion does not influence the master dynamics in this model. However, the slave dynamics is determined by (a) the environmental torque, $\boldsymbol{\tau_E(t)}$, (b) the Master process, $\boldsymbol{q_m(t)}$ and (c) the PD controller coefficients $\boldsymbol{K_p}$, $\boldsymbol{K_d}$ which affect the error process, $\boldsymbol{e(t)}$ that gets fed into the slave torque i.e. $\boldsymbol{\tau_s = \tau_I + \tau_E}$ as shown in the Fig. 6.2.

In the presence of environmental noise, it is proposed to reconfigure the available PD controller gain parameters of the master-slave robotic system by exploiting estimation methods. Here, Maximum likelihood technique is used for estimation of controller gain parameters and then to back substitute these controller estimates into the dynamics and thereby estimate the sample trajectory of the environmental noise process as discussed in section 6.4. The process of MLE utilizes the slave dynamics which is influenced by master dynamics and environment interaction and presented in the next section.

6.3 Master-slave dynamics

The dynamic equations of both two link master and slave robot are identical except for the input torques. The master equation is represented as:

$$\boldsymbol{M_m(q_m)\ddot{q}_m + N_m(q_m, \dot{q}_m) = \tau_{mo}(t)} \tag{6.1}$$

Where, $\boldsymbol{M_m}$ represents the moment of inertia matrix, $\boldsymbol{N_m}$ combines the effects of damping-coriolis-centrifugal-gravitation force and $\boldsymbol{\tau_{mo}(t)}$ is torque. The master equation (6.1) can be rearranged as

$$\boldsymbol{\ddot{q}_m = \psi_1(q_m, \dot{q}_m) + \psi_2(q_m)\tau_{mo}(t)} \tag{6.2a}$$

$$\boldsymbol{\psi_1(q_m, \dot{q}_m) = -M_m(q_m)^{-1}N_m(q_m, \dot{q}_m)} \tag{6.2b}$$

and

$$\boldsymbol{\psi_2(q_m) = M_m(q_m)^{-1}} \tag{6.2c}$$

For a given torque process in discrete time $\tau_{mo}[n] = \tau_{mo}[n\Delta]$ (Δ being the discretization step size), the master robot angular position can be simulated as

$$\left.\begin{aligned} &\boldsymbol{(q_m[n+1] - 2q_m[n] + q_m[n-1])/\Delta^2} \\ &\boldsymbol{= \psi_1(q_m[n], (q_m[n] - q_m[n-1])/\Delta) + \psi_2(q_m[n]).\tau_{mo}[n+1]} \end{aligned}\right\} \tag{6.3}$$

The torque from error dynamics is represented as:

$$\boldsymbol{e(t) = K_p(q_m - q_s) + K_d(\dot{q}_m - \dot{q}_s)} \tag{6.4}$$

In the presence of environment torque, $\boldsymbol{\tau_E}$, the total torque applied to the slave robot is $\boldsymbol{\tau_s = \tau_E + \tau_I}$, where, $\boldsymbol{\tau_I}$ is the torque computed from inverse dynamics. Also. $\boldsymbol{\tau_I}$ is represented as

$$\left.\begin{aligned} &\boldsymbol{\tau_I(t) = F(q_I, \dot{q}_I, \ddot{q}_I)} \\ \text{Where,} \quad &\boldsymbol{q_I = q_m}; \\ &\boldsymbol{\dot{q}_I = \dot{q}_m}; \\ &\boldsymbol{\ddot{q}_I = \ddot{q}_m + \ e(t)} \end{aligned}\right\} \tag{6.5}$$

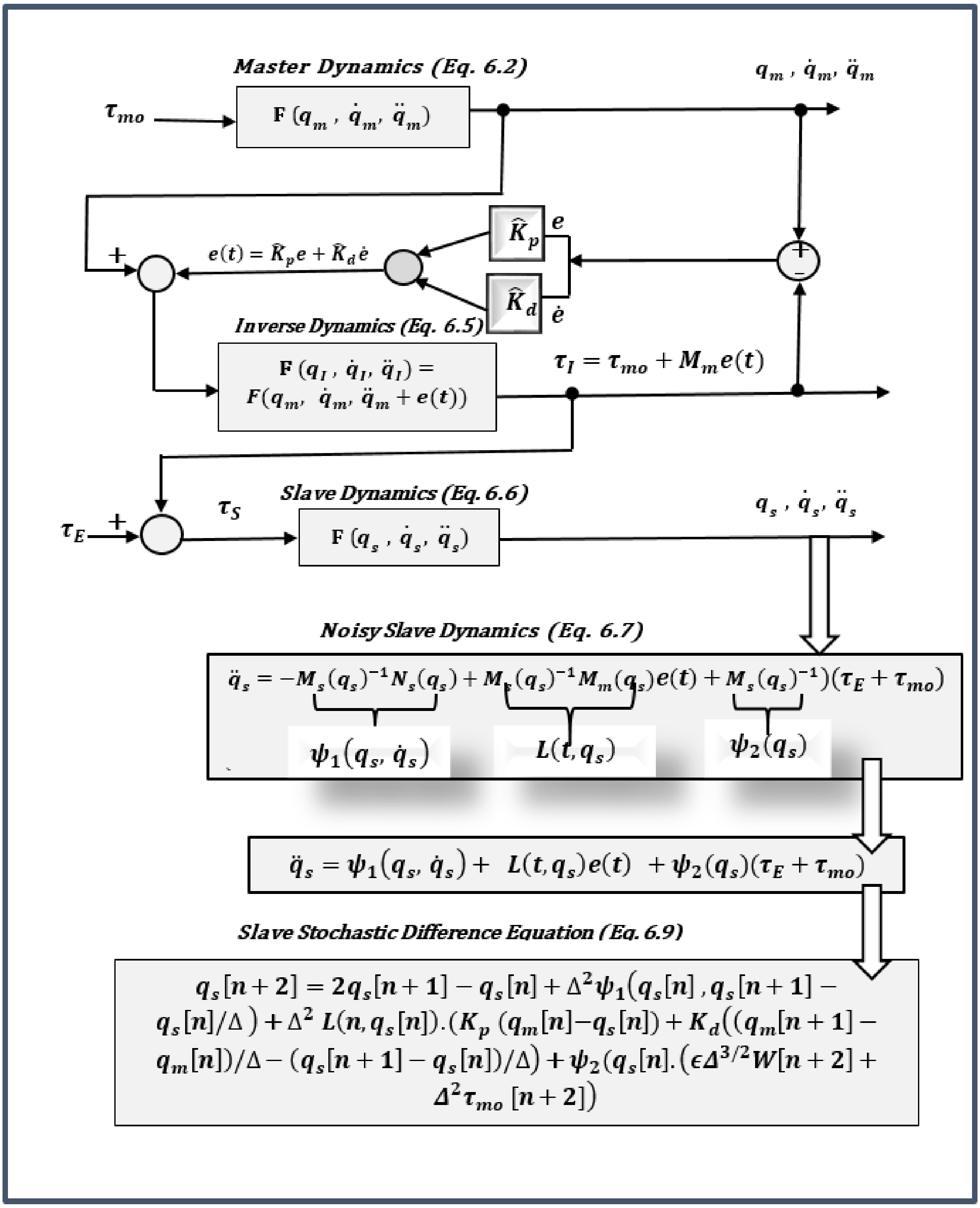

Figure 6.3: Master-slave Dynamics.

The slave equations are represented as:

$$\left.\begin{aligned}\boldsymbol{M_s(q_s)\ddot{q}_s + N_s(q_s,\dot{q}_s) = \tau_s}\\ \boldsymbol{F(q_s,\dot{q}_s,\ddot{q}_s) = \tau_s = \tau_E + \tau_I}\\ \boldsymbol{\tau_s = \tau_E + F(q_m,\dot{q}_m,\ddot{q}_m + e(t))}\\ \boldsymbol{= \tau_E + \tau_{mo} + M(q_m)e(t)}\end{aligned}\right\} \tag{6.6}$$

or equivalently the dynamics of slave robot interacting with environment is

$$\left.\begin{aligned}&\boldsymbol{\ddot{q}_s = -M_s(q_s)^{-1}N_s(q_s,\dot{q}_s) + M_s(q_s)^{-1}M_m(q_m)e(t) + M_s(q_s)^{-1}(\tau_E + \tau_{mo})}\\ &\boldsymbol{= \psi_1(q_s,\dot{q}_s) + L(t,q_m,q_s)e(t) + \psi_2(q_s)(\tau_E + \tau_{mo})}\\ &\text{where, } \boldsymbol{L(t,q_m,q_s) = M_s(q_s)^{-1}M_m(q_m)}\end{aligned}\right\} \tag{6.7}$$

In Fig. 6.3, the block diagram describes the contribution of master dynamics, noise component and controller gain parameters in the closed-loop dynamics of slave robot.

Suppose $\boldsymbol{\tau_E}$ is small, i.e. $\boldsymbol{\tau_E(t) = \epsilon W(t)}$, where $\boldsymbol{W(t)}$ is a standard 2-dimensional zero mean White Gaussian random process and ϵ is a perturbation parameter attached to the noise term in the slave dynamics to keep track of terms having different order of smallness in the dynamics. This amounts to assuming that the noise term is of first order of smallness and enables to expand the solution in the powers of $\boldsymbol{\epsilon}$. Thus the solution of the dynamical system to any degree of smallness (i.e. power of ϵ) can be achieved by this process. At the end of the calculation, we may let $\epsilon = 1$. This appears when the slave robot hits a randomly vibrating wall. Then, from (6.7), the stochastic difference equation representing the discretized dynamical model of slave can be expressed as:

$$\left.\begin{aligned}&\boldsymbol{(q_s[n+2] - 2q_s[n+1] + q_s[n])/\Delta^2 = \psi_1(q_s[n],(q_s[n+1] - q_s[n])/\Delta)}\\ &\quad\boldsymbol{+ L(n,q_m[n],q_s[n])e[n] + \psi_2(q_s[n])(\epsilon W[n+2]/\sqrt{\Delta} + \tau_{mo}[n+2])}\end{aligned}\right\} \tag{6.8}$$

where, $\boldsymbol{L[n,q_m,q_s] = L[n\Delta,q_m,q_s]}$ and $\boldsymbol{W[n]}$ is an independent and identically distributed (i.i.d.) $N(0,\sigma_w^2 I_2)$ sequence.

The factor of $\dfrac{1}{\sqrt{\Delta}}$ is attached to W[n+2] is based on the fact that if B(t) is standard Brownian motion, then $\dfrac{dB(t)}{dt}$ is standard White Gaussian noise and in discrete time, can be approximated by $\dfrac{B(t+\Delta)-B(t)}{\Delta}$ which is a Gaussian random variable having zero mean and variance $\dfrac{1}{\Delta}$.

Equation (6.8) can be arranged as

$$\left.\begin{aligned} \boldsymbol{q_s[n+2]} = \quad & \boldsymbol{2q_s[n+1] - q_s[n] + \Delta^2\psi_1(q_s[n],(q_s[n+1]-q_s[n])/\Delta)} \\ & \boldsymbol{+ \Delta^2 L(n, q_m[n]q_s[n]).(K_p(q_m[n]-q_s[n])} \\ & \boldsymbol{+ (K_d/\Delta)(q_m[n+1]-q_m[n]-q_s[n+1]+q_s[n])} \\ & \boldsymbol{+ \psi_2(q_s[n].(\epsilon\Delta^{3/2}W[n+2]+\Delta^2\tau_{mo}[n+2])} \end{aligned}\right\} \tag{6.9}$$

The aforementioned equation represents the sample data of slave position upto time $(N+2)$ which is utilized to get the estimation of controller gain parameters and environment force in the following sections.

6.4 Estimation of controller's gain parameters with stochastic environment force

6.4.1 Controller design

It is assumed that designing of controller parameters i.e. $\boldsymbol{K_p}$ and $\boldsymbol{K_d}$ is done so that $\boldsymbol{\{\sum_{n=0}^{N-1}||q_m[n]-q_s[n]||^2\}}$ is a minimum in the presence of noise. Direct minimization of $\boldsymbol{\{\sum_{n=0}^{N-1}||q_m[n]-q_s[n]||^2\}}$ w.r.t. $\boldsymbol{K_p}$ and $\boldsymbol{K_d}$ is equivalent to a Maximum Likelihood problem since the noise has been considered to be White Gaussian. This design can be achieved by using stochastic optimal control methods like Bellman's stochastic dynamic programming method.

Having designed $\boldsymbol{K_p}$ and $\boldsymbol{K_d}$, noise is introduced through the environment in the slave dynamics and the robot is handed over to a user who does not know values of gain parameters and the environment. This user takes measurements of noisy slave position $\boldsymbol{\delta q_s[n] = q_s[n] - q_m[n]}$ over a finite time duration. Noisy slave position means difference of master and slave position with noise or noise present in slave dynamics as $\boldsymbol{K_p}$ and $\boldsymbol{K_d}$ have already taken care of tracking error. Using MLE, he estimates the unknown controller's gain parameters and after that estimates to determine the environmental noise.

The aim is to design $\boldsymbol{K_p}$ and $\boldsymbol{K_d}$ (2×2) matrices so that

$$\mathbb{E}\{\sum_{n=0}^{N-1} ||\boldsymbol{q_m}[\boldsymbol{n}] - \boldsymbol{q_s}[\boldsymbol{n}]||^2\} \text{ is minimum;} \tag{6.10}$$

where $\boldsymbol{q_s}[\boldsymbol{n}] - \boldsymbol{q_m}[\boldsymbol{n}] \approx \boldsymbol{\delta q_s}[\boldsymbol{n}]$ is of $\boldsymbol{O(\epsilon)}$.

The slave dynamics given in equation (6.9) is linearized about $\boldsymbol{q_s^{(0)}}[\boldsymbol{n}] = \boldsymbol{q_m}[\boldsymbol{n}]$. This is presented as:

As $f(x) = f(a) + f'(a)(x-a) +$ higher order terms. Assuming $a = 0, f(a) = 0$ and neglecting higher order terms.

$$\left.\begin{aligned}
&\boldsymbol{\delta q_s}[\boldsymbol{n}+2] = \\
&\quad 2\boldsymbol{\delta q_s}[\boldsymbol{n}+1] - \boldsymbol{\delta q_s}[\boldsymbol{n}] + \boldsymbol{\Delta^2 \Psi_{1,1}}[\boldsymbol{n}]\boldsymbol{\delta q_s}[\boldsymbol{n}] + \boldsymbol{\Delta^2 \Psi_{1,2}}[\boldsymbol{n}](\boldsymbol{\delta q_s}[\boldsymbol{n}+1] - \boldsymbol{\delta q_s}[\boldsymbol{n}])/\boldsymbol{\Delta} \\
&\quad + \boldsymbol{\Delta^2 L}[\boldsymbol{n}]\left(\boldsymbol{K_p \delta q_s}[\boldsymbol{n}] + \boldsymbol{K_d/\Delta}(\boldsymbol{\delta q_s}[\boldsymbol{n}+1] - \boldsymbol{\delta q_s}[\boldsymbol{n}])\right) \\
&\quad + \boldsymbol{\Delta^2 \Psi_{2,1}}[\boldsymbol{n}](\boldsymbol{\delta q_s}[\boldsymbol{n}] \otimes \boldsymbol{\tau_{mo}}[\boldsymbol{n}+2]) + \boldsymbol{\Delta^{3/2} \Psi_2}[\boldsymbol{n}]\boldsymbol{W}[\boldsymbol{n}+2]
\end{aligned}\right\} \tag{6.11}$$

where,

$$\left.\begin{aligned}
&\boldsymbol{\psi_1}[\boldsymbol{n}] = \boldsymbol{\psi_1}(\boldsymbol{q_s}[\boldsymbol{n}], \boldsymbol{\dot{q}_s}[\boldsymbol{n}]) \\
&\boldsymbol{\psi_2}[\boldsymbol{n}] = \boldsymbol{\psi_1}(\boldsymbol{q_s}[\boldsymbol{n}], \boldsymbol{\dot{q}_s}[\boldsymbol{n}]) \\
&\text{Where } \boldsymbol{\psi_{1,1}}[\boldsymbol{n}] = \frac{\boldsymbol{\partial \psi_1}(\boldsymbol{q_s}[\boldsymbol{n}], \boldsymbol{\partial \dot{q}_s}[\boldsymbol{n}])}{(\boldsymbol{\partial q_s}[\boldsymbol{n}])} \\
&\text{Where } \boldsymbol{\psi_{2,1}}[\boldsymbol{n}] = \frac{\boldsymbol{\partial \psi_1}(\boldsymbol{q_s}[\boldsymbol{n}], \boldsymbol{\partial \dot{q}_s}[\boldsymbol{n}])}{(\boldsymbol{\partial \dot{q}_s}[\boldsymbol{n}])} \\
&\text{also, } \boldsymbol{\dot{q}_s}[\boldsymbol{n}] = \frac{\boldsymbol{q_s}[\boldsymbol{n}] - \boldsymbol{q_s}[\boldsymbol{n}-1]}{\boldsymbol{\Delta}} \\
&\text{similary,} \\
&\boldsymbol{\psi_{2,1}}[\boldsymbol{n}] = \frac{\boldsymbol{\partial \psi_2}(\boldsymbol{q_s}[\boldsymbol{n}], \boldsymbol{\partial \dot{q}_s}[\boldsymbol{n}])}{(\boldsymbol{\partial q_s}[\boldsymbol{n}])} \\
&\boldsymbol{\psi_{2,2}}[\boldsymbol{n}] = \frac{\boldsymbol{\partial \psi_2}(\boldsymbol{q_s}[\boldsymbol{n}])}{(\boldsymbol{\partial \dot{q}_s}[\boldsymbol{n}])} = \boldsymbol{0}
\end{aligned}\right\} \tag{6.12}$$

$q_m[n] = \theta_m[n\Delta]$ is obtained by sampling the continuous time master trajectory.

$q_s[n] = q_s[n\Delta]$ is obtained by sampling the continuous time slave trajectory.

Also, $\boldsymbol{L}[\boldsymbol{n}] = \boldsymbol{L}(\boldsymbol{n}, \boldsymbol{q_m}[\boldsymbol{n}], \boldsymbol{q_s}[\boldsymbol{n}]) = \boldsymbol{I_2}$.

Elementary linear algebra techniques involving Kronecker product in equation

(6.11) is applied and after linearizing, the approximated linear time-varying stochastic difference equation is represented as:

$$\left.\begin{aligned}\boldsymbol{\delta q_s[n+2]} = \quad & [\boldsymbol{2I_2} + \boldsymbol{\Delta\Psi_{1,2}[n]} - \boldsymbol{\Delta K_d}]\,\boldsymbol{\delta q_s[n+1]} \\ & - [\boldsymbol{I_2} - \boldsymbol{\Delta^2\Psi_{1,1}[n]} + \boldsymbol{\Delta\Psi_{1,2}[n]} - (\boldsymbol{\Delta^2 K_p} - \boldsymbol{\Delta K_d}) \\ & - \boldsymbol{\Delta\Psi_{2,1}[n]}(\boldsymbol{I_2} \otimes \boldsymbol{\tau_{mo}[n+2]})]\boldsymbol{\delta q_s[n]} \\ & + \boldsymbol{\Delta^{3/2}\Psi_2[n]W[n+2]}\end{aligned}\right\} \tag{6.13}$$

The partial derivative in the aforementioned equation take place w.r.t. each element of $q[n]$ thus, kronecker operation is performed. The terms involving in equation (6.13) can be defined as:

$$\left.\begin{aligned}&\boldsymbol{\Delta K_d} = \boldsymbol{\alpha_d} \in \mathbb{R}^{\boldsymbol{2\times 2}}, \\ &\boldsymbol{\Delta^2 K_p} - \boldsymbol{\Delta K_d} = \boldsymbol{\beta_d} \in \mathbb{R}^{\boldsymbol{2\times 2}} \\ &\boldsymbol{A[n]} = \boldsymbol{2I_2} + \boldsymbol{\Delta\Psi_{1,2}[n]} \\ &\boldsymbol{B[n]} = -\boldsymbol{I_2} + \boldsymbol{\Delta^2\Psi_{1,1}[n]} - \boldsymbol{\Delta\Psi_{1,2}[n]} + \boldsymbol{\Delta\Psi_{2,1}[n]}(\boldsymbol{\tau_{mo}[n+2]} \otimes \boldsymbol{I_2}) \\ &\boldsymbol{C[n]} = \boldsymbol{\Delta^{3/2}\Psi_2[n]}\end{aligned}\right\} \tag{6.14}$$

Equation (6.13) can be rearranged as

$$\boldsymbol{\delta q_s[n+2]} = [\boldsymbol{A[n]} - \boldsymbol{\alpha_d}]\boldsymbol{I_2\delta q_s[n+1]} + [\boldsymbol{B[n]} - \boldsymbol{\beta_d}]\boldsymbol{I_2\delta q_s[n]} + \boldsymbol{C[n]W[n+2]} \tag{6.15}$$

This equation is now in the right form required for applying the ML method to estimate $\boldsymbol{\alpha_d}$ and $\boldsymbol{\beta_d}$ or equivalently $\boldsymbol{K_p}$ and $\boldsymbol{K_d}$.

As $\{\boldsymbol{\delta q_s[n]}\}$ follows 2^{nd} order difference equation with white noise driving term, the pdf of $\{\boldsymbol{\delta q_s[n]}\}$ parameterized by $\boldsymbol{\alpha_d}$ and $\boldsymbol{\beta_d}$ can be calculated by the following process based on second order Markov model [Laurence Smith 2006].

$$\left.\begin{aligned}&\boldsymbol{p(\delta q_s[n+2]|\delta q_s[n+1], \delta q_s[n])} = \boldsymbol{1/2\pi|C[n]|exp\{-1/2(\delta q_s[n+2]} \\ &\qquad - \boldsymbol{(A[n]-\alpha_d)\delta q_s[n+1]} - \boldsymbol{(B[n]-\beta_d)\delta q_s[n]|^T} \\ &\quad \boldsymbol{(C[n]C[n]^T)^{-1}(\delta q_s[n+2]} - \boldsymbol{(A[n]-\alpha_d)\delta q_s[n+1]} - \boldsymbol{(B[n]-\beta_d)\delta q_s[n])\}}\end{aligned}\right\} \tag{6.16}$$

The above expression represents a time series model which contains controller parameters, $\boldsymbol{\alpha_d}$ and $\boldsymbol{\beta_d}$ as static variable, known as parameter, which parametrizes

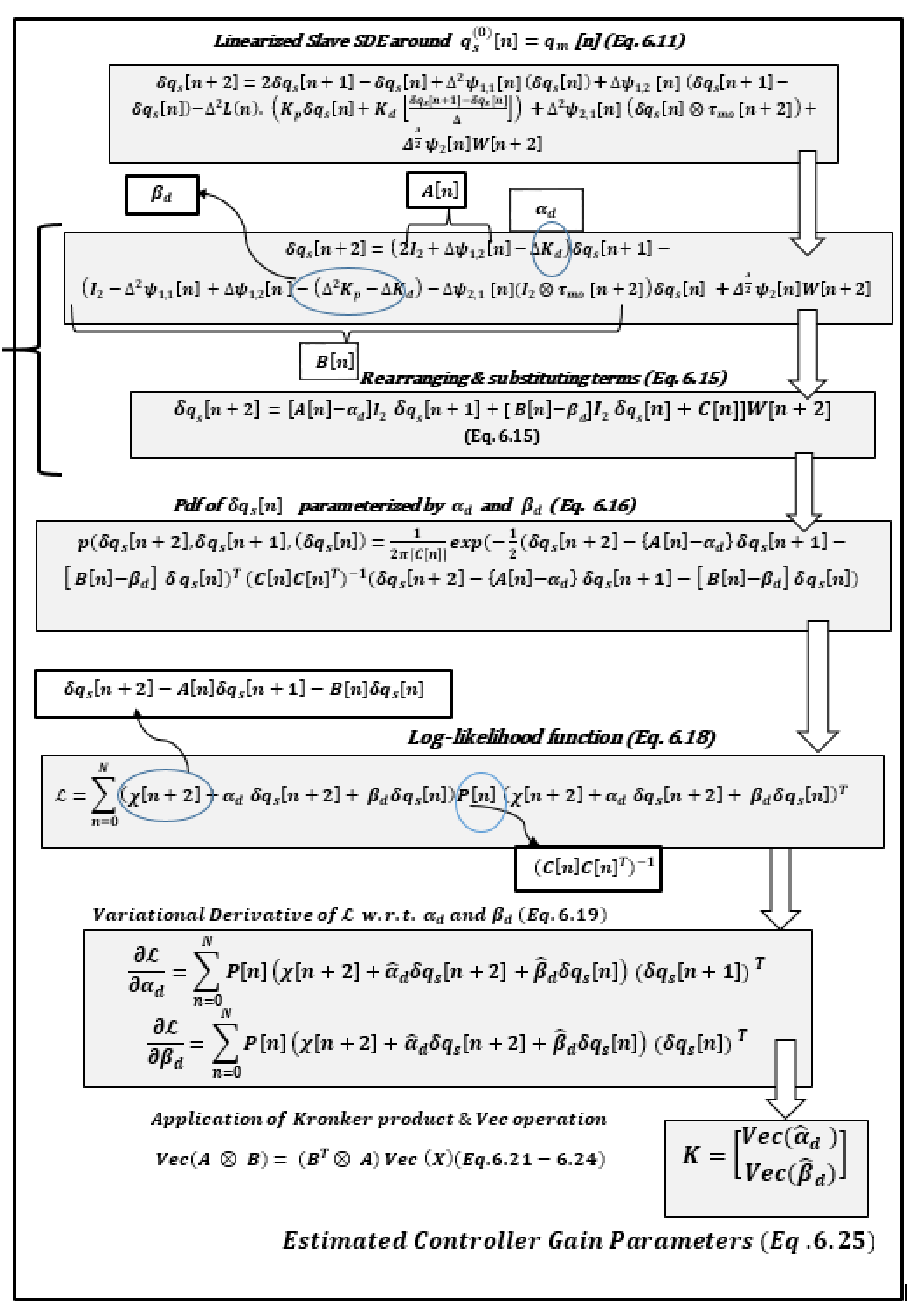

Figure 6.4: Process of Estimation of Controller Gain Parameters for Tracking Control.

the joint law of the random variables (here, q and $\dot{q}$) involved in the dynamics of the model. A log- likelihood function is formed which is equivalent to pdf function as given above. The technique of maximum likelihood choose the set of values of the model parameters that maximizes the likelihood function. After forming log-likelihood of equation (6.16) and substituting the terms as follows:

$$\left.\begin{aligned}\boldsymbol{\chi}[\boldsymbol{n}+2] =& \boldsymbol{\delta q_s}[\boldsymbol{n}+2] - \boldsymbol{A}[\boldsymbol{n}]\boldsymbol{\delta q_s}[\boldsymbol{n}+1] - \boldsymbol{B}[\boldsymbol{n}]\boldsymbol{\delta q_s}[\boldsymbol{n}] \\ \boldsymbol{P}[\boldsymbol{n}] =& (\boldsymbol{C}[\boldsymbol{n}]\boldsymbol{C}[\boldsymbol{n}]^{\boldsymbol{T}})^{-1}\end{aligned}\right\} \tag{6.17}$$

The log-likelihood function is represented as:

$$\left.\begin{aligned}\boldsymbol{\mathcal{L}} = \sum_{\boldsymbol{n}=0}^{\boldsymbol{N}} (\boldsymbol{\chi}[\boldsymbol{n}+2] + \boldsymbol{\alpha_d}\boldsymbol{\delta q_s}[\boldsymbol{n}+1] + \boldsymbol{\beta_d}\boldsymbol{\delta q_s}[\boldsymbol{n}])\, \boldsymbol{P}[\boldsymbol{n}] \\ \left(\boldsymbol{\chi}[\boldsymbol{n}+2] + \widehat{\boldsymbol{\alpha}}_{\boldsymbol{d}}\boldsymbol{\delta q_s}[\boldsymbol{n}+1] + \widehat{\boldsymbol{\beta}}_{\boldsymbol{d}}\boldsymbol{\delta q_s}[\boldsymbol{n}]\right)^{\boldsymbol{T}}\end{aligned}\right\} \tag{6.18}$$

Thus, the Maximum Likelihood estimates of $\boldsymbol{\alpha_d}$ and $\boldsymbol{\beta_d}$ based on the measurements of $\{\boldsymbol{\delta q_s}[\boldsymbol{n}] : \boldsymbol{0} \leq \boldsymbol{n} \leq \boldsymbol{N}\}$ are given by setting the $0 \leq n \leq N$ w.r.t. $\boldsymbol{\alpha_d}$ and $\boldsymbol{\beta_d}$ to zero.

$$\left.\begin{aligned}\frac{\partial \boldsymbol{\mathcal{L}}}{\partial \boldsymbol{\alpha_d}} &= \sum_{\boldsymbol{n}=0}^{\boldsymbol{N}} \boldsymbol{P}[\boldsymbol{n}] \left(\boldsymbol{\chi}[\boldsymbol{n}+2] + \widehat{\boldsymbol{\alpha}}_{\boldsymbol{d}}\boldsymbol{\delta q_s}[\boldsymbol{n}+1] + \widehat{\boldsymbol{\beta}}_{\boldsymbol{d}}\boldsymbol{\delta q_s}[\boldsymbol{n}]\right) \boldsymbol{\delta q_s}[\boldsymbol{n}+1]^{\boldsymbol{T}} = \boldsymbol{0} \\ \frac{\partial \boldsymbol{\mathcal{L}}}{\partial \boldsymbol{\beta_d}} &= \sum_{\boldsymbol{n}=0}^{\boldsymbol{N}} \boldsymbol{P}[\boldsymbol{n}] \left(\boldsymbol{\chi}[\boldsymbol{n}+2] + \widehat{\boldsymbol{\alpha}}_{\boldsymbol{d}}\boldsymbol{\delta q_s}[\boldsymbol{n}+1] + \widehat{\boldsymbol{\beta}}_{\boldsymbol{d}}\boldsymbol{\delta q_s}[\boldsymbol{n}]\right) \boldsymbol{\delta q_s}[\boldsymbol{n}]^{\boldsymbol{T}} = \boldsymbol{0}\end{aligned}\right\} \tag{6.19}$$

Further simplification gives the following expressions:

$$\left.\begin{aligned}\sum_{\boldsymbol{n}=0}^{\boldsymbol{N}} (\boldsymbol{P}[\boldsymbol{n}]\boldsymbol{\chi}[\boldsymbol{n}+2]\boldsymbol{\delta q_s}[\boldsymbol{n}+1]^{\boldsymbol{T}}) + \sum_{\boldsymbol{n}=0}^{\boldsymbol{N}} (\boldsymbol{P}[\boldsymbol{n}]\widehat{\boldsymbol{\alpha}}_{\boldsymbol{d}}\boldsymbol{\delta q_s}[\boldsymbol{n}+1]\boldsymbol{\delta q_s}[\boldsymbol{n}+1]^{\boldsymbol{T}}) \\ \sum_{\boldsymbol{n}=0}^{\boldsymbol{N}} \left(\boldsymbol{P}[\boldsymbol{n}] + \widehat{\boldsymbol{\beta}}_{\boldsymbol{d}}\boldsymbol{\delta q_s}[\boldsymbol{n}]\boldsymbol{\delta q_s}[\boldsymbol{n}+1]^{\boldsymbol{T}}\right) = \boldsymbol{0}\end{aligned}\right\} \tag{6.20}$$

$$\left.\begin{aligned}\sum_{\boldsymbol{n}=0}^{\boldsymbol{N}} (\boldsymbol{P}[\boldsymbol{n}]\boldsymbol{\chi}[\boldsymbol{n}+2]\boldsymbol{\delta q_s}[\boldsymbol{n}]^{\boldsymbol{T}}) + \sum_{\boldsymbol{n}=0}^{\boldsymbol{N}} (\boldsymbol{P}[\boldsymbol{n}]\widehat{\boldsymbol{\alpha}}_{\boldsymbol{d}}\boldsymbol{\delta q_s}[\boldsymbol{n}+1]\boldsymbol{\delta q_s}[\boldsymbol{n}]^{\boldsymbol{T}}) \\ \sum_{\boldsymbol{n}=0}^{\boldsymbol{N}} \left(\boldsymbol{P}[\boldsymbol{n}] + \widehat{\boldsymbol{\beta}}_{\boldsymbol{d}}\boldsymbol{\delta q_s}[\boldsymbol{n}]\boldsymbol{\delta q_s}[\boldsymbol{n}]^{\boldsymbol{T}}\right) = \boldsymbol{0}\end{aligned}\right\} \tag{6.21}$$

Elementary properties of the kronecker tensor product is applied in equations (6.20) and (6.21), especially $\boldsymbol{Vec(A \times B)} = \boldsymbol{(B^T \otimes A)Vec(X)}$ so that the resulting expression can be arranged in the form as shown in equation (6.23). The property is used by substituting $\boldsymbol{B} = \boldsymbol{\delta q_s}[\boldsymbol{n}+1]\boldsymbol{\delta q_s}[\boldsymbol{n}+1]^{\boldsymbol{T}}$; $\boldsymbol{A} = \boldsymbol{P}[\boldsymbol{n}]$; $\boldsymbol{X} = \widehat{\boldsymbol{\alpha}}_{\boldsymbol{d}}$ in the second term and $\boldsymbol{B} = \boldsymbol{\delta q_s}[\boldsymbol{n}]\boldsymbol{\delta q_s}[\boldsymbol{n}+1]^{\boldsymbol{T}}$; $\boldsymbol{A} = \boldsymbol{P}[\boldsymbol{n}]$, $\boldsymbol{X} = \widehat{\boldsymbol{\beta}}_{\boldsymbol{d}}$ in the third term of equation (6.20).

$$\boldsymbol{Vec}\{\sum_{n}\boldsymbol{P}[\boldsymbol{n}]\boldsymbol{\chi}[\boldsymbol{n}+2]\boldsymbol{\delta q_s}[\boldsymbol{n}+1]^{\boldsymbol{T}}\} + \left(\sum_{n=0}^{N}(\boldsymbol{\delta q_s}[\boldsymbol{n}+1]\boldsymbol{\delta q_s}[\boldsymbol{n}+1]^{\boldsymbol{T}}) \otimes \boldsymbol{P}[\boldsymbol{n}])\boldsymbol{Vec}(\widehat{\boldsymbol{\alpha}}_{\boldsymbol{d}})\right) + \left(\sum_{n=0}^{N}(\boldsymbol{\delta q_s}[\boldsymbol{n}+1]\boldsymbol{\delta q_s}[\boldsymbol{n}]^{\boldsymbol{T}}) \otimes \boldsymbol{P}[\boldsymbol{n}])\boldsymbol{Vec}(\widehat{\boldsymbol{\beta}}_{\boldsymbol{d}})\right) = 0 \tag{6.22}$$

Similar, the property is used by substituting $\boldsymbol{B} = \boldsymbol{\delta q_s}[\boldsymbol{n}]\boldsymbol{\delta q_s}[\boldsymbol{n}]^{\boldsymbol{T}}$; $\boldsymbol{A} = \boldsymbol{P}[\boldsymbol{n}]$; $\boldsymbol{X} = \widehat{\boldsymbol{\alpha}}_{\boldsymbol{d}}$ in the second term and $\boldsymbol{B} = \boldsymbol{\delta q_s}[\boldsymbol{n}]\boldsymbol{\delta q_s}[\boldsymbol{n}]^{\boldsymbol{T}}$; $\boldsymbol{A} = \boldsymbol{P}[\boldsymbol{n}]$, $\boldsymbol{X} = \widehat{\boldsymbol{\beta}}_{\boldsymbol{d}}$ of equation (6.23).

$$\left.\begin{aligned}&\boldsymbol{Vec}\{\sum_{n}\boldsymbol{P}[\boldsymbol{n}]\boldsymbol{\chi}[\boldsymbol{n}+2]\boldsymbol{\delta q_s}[\boldsymbol{n}]^{\boldsymbol{T}}\} + \left(\sum_{n=0}^{N}(\boldsymbol{\delta q_s}[\boldsymbol{n}]\boldsymbol{\delta q_s}[\boldsymbol{n}+1]^{\boldsymbol{T}} \otimes \boldsymbol{P}[\boldsymbol{n}])\boldsymbol{Vec}(\widehat{\boldsymbol{\alpha}}_{\boldsymbol{d}})\right)\\ &\quad + \left(\sum_{n=0}^{N}(\boldsymbol{\delta q_s}[\boldsymbol{n}]\boldsymbol{\delta q_s}[\boldsymbol{n}]^{\boldsymbol{T}} \otimes \boldsymbol{P}[\boldsymbol{n}])\boldsymbol{Vec}(\widehat{\boldsymbol{\beta}}_{\boldsymbol{d}})\right) = 0\end{aligned}\right\} \tag{6.23}$$

Equations (6.22) and (6.23) form a set of eight simultaneous linear equations for the unknown parameter vector $\begin{bmatrix}\boldsymbol{Vec}(\boldsymbol{\alpha_d})\\ \boldsymbol{Vec}(\boldsymbol{\beta_d})\end{bmatrix} \in \mathbb{R}^8$.
These can be expressed as following and can be inverted immediately.

$$\left.\begin{aligned}&\begin{bmatrix}\sum_{n=0}^{N}\boldsymbol{\delta q_s}[\boldsymbol{n}+1]\boldsymbol{\delta q_s}[\boldsymbol{n}+1]^{\boldsymbol{T}} \otimes \boldsymbol{P}[\boldsymbol{n}] & \sum_{n=0}^{N}\boldsymbol{\delta q_s}[\boldsymbol{n}+1]\boldsymbol{\delta q_s}[\boldsymbol{n}]^{\boldsymbol{T}} \otimes \boldsymbol{P}[\boldsymbol{n}]\\ \sum_{n=0}^{N}\boldsymbol{\delta q_s}[\boldsymbol{n}]\boldsymbol{\delta q_s}[\boldsymbol{n}+1]^{\boldsymbol{T}} \otimes \boldsymbol{P}[\boldsymbol{n}] & \sum_{n=0}^{N}\boldsymbol{\delta q_s}[\boldsymbol{n}]\boldsymbol{\delta q_s}[\boldsymbol{n}]^{\boldsymbol{T}} \otimes \boldsymbol{P}[\boldsymbol{n}]\end{bmatrix}\begin{bmatrix}\boldsymbol{Vec}(\hat{\boldsymbol{\alpha}}_{\boldsymbol{d}})\\ \boldsymbol{Vec}(\hat{\boldsymbol{\beta}}_{\boldsymbol{d}})\end{bmatrix}\\ &\quad = -\begin{bmatrix}\boldsymbol{Vec}(\sum_{n=0}^{N}\boldsymbol{P}[\boldsymbol{n}]\boldsymbol{\xi}[\boldsymbol{n}+2]\boldsymbol{\delta q_s}[\boldsymbol{n}+1]^{\boldsymbol{T}})\\ \boldsymbol{Vec}(\sum_{n=0}^{N}\boldsymbol{P}[\boldsymbol{n}]\boldsymbol{\xi}[\boldsymbol{n}+2]\boldsymbol{\delta q_s}[\boldsymbol{n}]^{\boldsymbol{T}})\end{bmatrix}\end{aligned}\right\} \tag{6.24}$$

Equation (6.24) can be solved for the 4×1 vectors i.e. $\boldsymbol{Vec}(\widehat{\boldsymbol{\alpha}}_{\boldsymbol{d}})$ *and* $\boldsymbol{Vec}(\widehat{\boldsymbol{\beta}}_{\boldsymbol{d}})$

$$\boldsymbol{K} = \begin{bmatrix}\boldsymbol{Vec}(\widehat{\boldsymbol{\alpha}}_d)\\ \boldsymbol{Vec}(\widehat{\boldsymbol{\beta}}_d)\end{bmatrix} \text{ or equivalently for the } 8 \times 1 \text{ vector.} \tag{6.25}$$

The ML estimate of $\boldsymbol{K}$ is based upon samples upto time (N+2). The complete process of MLE of controller gain parameters for slave robot interacting with stochastic environment is summerized in Fig. 6.4.
In the next subsection, the procedure of back substituting these controller estimates into the dynamics leads to estimation of the sample trajectory of the environmental noise process.

6.4.2 Environment noise estimation

The general nonlinear dynamical model of Slave is presented in equation (6.9).

$$\left.\begin{aligned} \boldsymbol{q_s[n+2]} = \quad & \boldsymbol{2q_s[n+1] - q_s[n] + \Delta^2\psi_1(q_s[n], (q_s[n+1] - q_s[n])/\Delta)} \\ & \boldsymbol{+ \Delta^2 L(n, q_m[n]q_s[n]).(K_p(q_m[n] - q_s[n])} \\ & \boldsymbol{+ (K_d/\Delta)(q_m[n+1] - q_m[n] - q_s[n+1] + q_s[n])} \\ & \boldsymbol{+ \psi_2(\theta_s[n].(\epsilon\Delta^{3/2}W[n+2] + \Delta^2\tau_{mo}[n+2])} \end{aligned}\right\}$$

The terms in the aforemention expression can be defined as:

$$\left.\begin{aligned} & \boldsymbol{\xi[n+2] = q_s[n+2] - 2q_s[n+1] + q_s[n] - \Delta^2\Psi_1(q_s[n]q_s[n+1) - q_s[n]/\Delta} \\ & \qquad\qquad \boldsymbol{- \Delta^2\Psi_2(q_s[n]\tau_{mo}[n+2])} \\ & \quad \boldsymbol{X[n] = -\Delta^2 L[n, q_m[n], q_s[n]](\delta q[n]^T \otimes I_2)} \\ & \quad \boldsymbol{Y[n] = \epsilon\Delta^{3/2}\psi_2(q_s[n])} \\ & \quad \boldsymbol{K = (K_p(q_m[n] - q_s[n]) + (K_d/\Delta)(q_m[n+1] - q_m[n] - q_s[n+1] + q_s[n])} \end{aligned}\right\} \tag{6.26}$$

Thus, the equation (6.26) can be be written in the linear form as:

$$\boldsymbol{\xi[n+2] = X[n]K + Y[n]W[n+2]} \tag{6.27}$$

$$\left.\begin{aligned} & \text{Recall that } \boldsymbol{L[n, q_m[n], q_s[n]] = M_s(q_s[n])^{-1}M_m(q_m[n])}; \\ & \boldsymbol{\delta q[n]} = \begin{bmatrix} \boldsymbol{\delta q_s[n]} \\ \boldsymbol{\delta \dot{q}_s[n]} \end{bmatrix} \\ & \boldsymbol{\delta q_s[n] = q_s[n] - q_m[n]} \text{ and } \boldsymbol{\delta \dot{q}_s[n] = \dot{q}_s[n] - \dot{q}_m[n]} \end{aligned}\right\}$$

Substitute $\boldsymbol{L[n, q_s[n]] = I_2}$ since $\boldsymbol{q_s \approx q_m}$ and $\boldsymbol{M_m \approx M_s}$, The aim is to minimize noise i.e. $\boldsymbol{W[n+2]}$ w.r.t. $\boldsymbol{K}$, thus,

$$\boldsymbol{\widehat{K}[N] = argmin_K \sum_{n=0}^{N} ||Y^{-1}[n](\xi[n+2] - X[n]K)||^2} \tag{6.28}$$

If $\boldsymbol{K}$ is unknown and environment is considered as white-Gaussian noise (WGN), then the MLE of $\boldsymbol{K}$ based on data $\boldsymbol{q_s}(.)$ collected upto sample, **N** is least square and is given by

$$\left.\begin{aligned} -2\sum_{n=0}^{N}\boldsymbol{Y}^{-1}[n](\boldsymbol{\xi}[n+2]-\boldsymbol{X}[n]\widehat{\boldsymbol{K}})\boldsymbol{X}[n]=0 \\ -\left(\sum_{n=0}^{N}(\boldsymbol{Y}[n]\boldsymbol{Y}^{T}[n])^{-1}\boldsymbol{\xi}[n+2]\boldsymbol{X}[n]\right)+\left(\sum_{n=0}^{N}(\boldsymbol{Y}[n]\boldsymbol{Y}^{T}[n])^{-1}\boldsymbol{X}[n]\boldsymbol{X}^{T}[n]\widehat{\boldsymbol{K}}\right)=0 \\ \left(\sum_{n=0}^{N}\boldsymbol{X}^{T}[n]\left((\boldsymbol{Y}[n]\boldsymbol{Y}^{T}[n])^{-1}\boldsymbol{X}[n]\right)\right)\widehat{\boldsymbol{K}}=\left(\sum_{n=0}^{N}\boldsymbol{X}^{T}[n]((\boldsymbol{Y}[n]\boldsymbol{Y}^{T}[n])^{-1}\boldsymbol{\xi}[n+2]\right) \end{aligned}\right\}$$

The estimates of $\boldsymbol{K}$ is

$$\widehat{\boldsymbol{K}}=\left(\sum_{n=0}^{N}\boldsymbol{X}^{T}[n](\boldsymbol{Y}[n]\boldsymbol{Y}^{T}[n])^{-1}\boldsymbol{X}[n]\right)^{-1}\left(\sum_{n=0}^{N}\boldsymbol{X}[n](\boldsymbol{Y}[n]\boldsymbol{Y}^{T}[n])^{-1}\boldsymbol{\xi}[n+2]\right) \tag{6.29}$$

After substituting the value of $\boldsymbol{\xi}[n+2]$ from equation (6.27), the aforemention equation (6.29) can be represented as:

$$\left.\begin{aligned} \widehat{\boldsymbol{K}}=\boldsymbol{K}+\boldsymbol{H}[N]^{-1}\sum_{n=0}^{N}\boldsymbol{F}[n]\boldsymbol{W}[n+2] \\ \text{Where, }\ \boldsymbol{H}[N]=\sum_{n=0}^{N}\boldsymbol{X}[n]^{T}(\boldsymbol{Y}[n]\boldsymbol{Y}[n]^{T})^{-1}\boldsymbol{X}[n] \\ \boldsymbol{F}[n]=\boldsymbol{X}[n]^{T}(\boldsymbol{Y}[n]\boldsymbol{Y}[n]^{T})^{-1}\boldsymbol{Y}[n] \end{aligned}\right\} \tag{6.30}$$

The noise estimates is obtained by substituting the estimates of $\boldsymbol{K}$ i.e. $\widehat{\boldsymbol{K}}$ in place of $\boldsymbol{K}$ in equation (6.27)

$$\left.\begin{aligned} \widehat{\boldsymbol{W}}[n+2]=\boldsymbol{Y}[n]^{-1}(\boldsymbol{\xi}[n+2]-\boldsymbol{X}[n]\widehat{\boldsymbol{K}}) \\ =\boldsymbol{Y}[n]^{-1}(\boldsymbol{X}[n]\boldsymbol{K}+\boldsymbol{Y}[n]\boldsymbol{W}[n+2]-\boldsymbol{X}[n]\widehat{\boldsymbol{K}}) \\ \widehat{\boldsymbol{W}}[n+2]-\boldsymbol{W}[n+2]=\boldsymbol{Y}[n]^{-1}\boldsymbol{X}[n](\boldsymbol{K}-\widehat{\boldsymbol{K}}) \end{aligned}\right\} \tag{6.31}$$

Up to $O(||\delta q||^2)$ in numerator and denominator, $(W[n]=O(||\delta q||))$, Then from (6.30),

$$\left.\begin{aligned} \hat{\boldsymbol{K}}[N]-\boldsymbol{K}=\boldsymbol{P}^{-1}\boldsymbol{Q} \\ \text{where, }\ \boldsymbol{P}=\boldsymbol{H}[n] \\ \text{and }\ \boldsymbol{Q}=\sum_{n=0}^{N}\boldsymbol{F}[n]\boldsymbol{W}[n+2] \end{aligned}\right\} \tag{6.32}$$

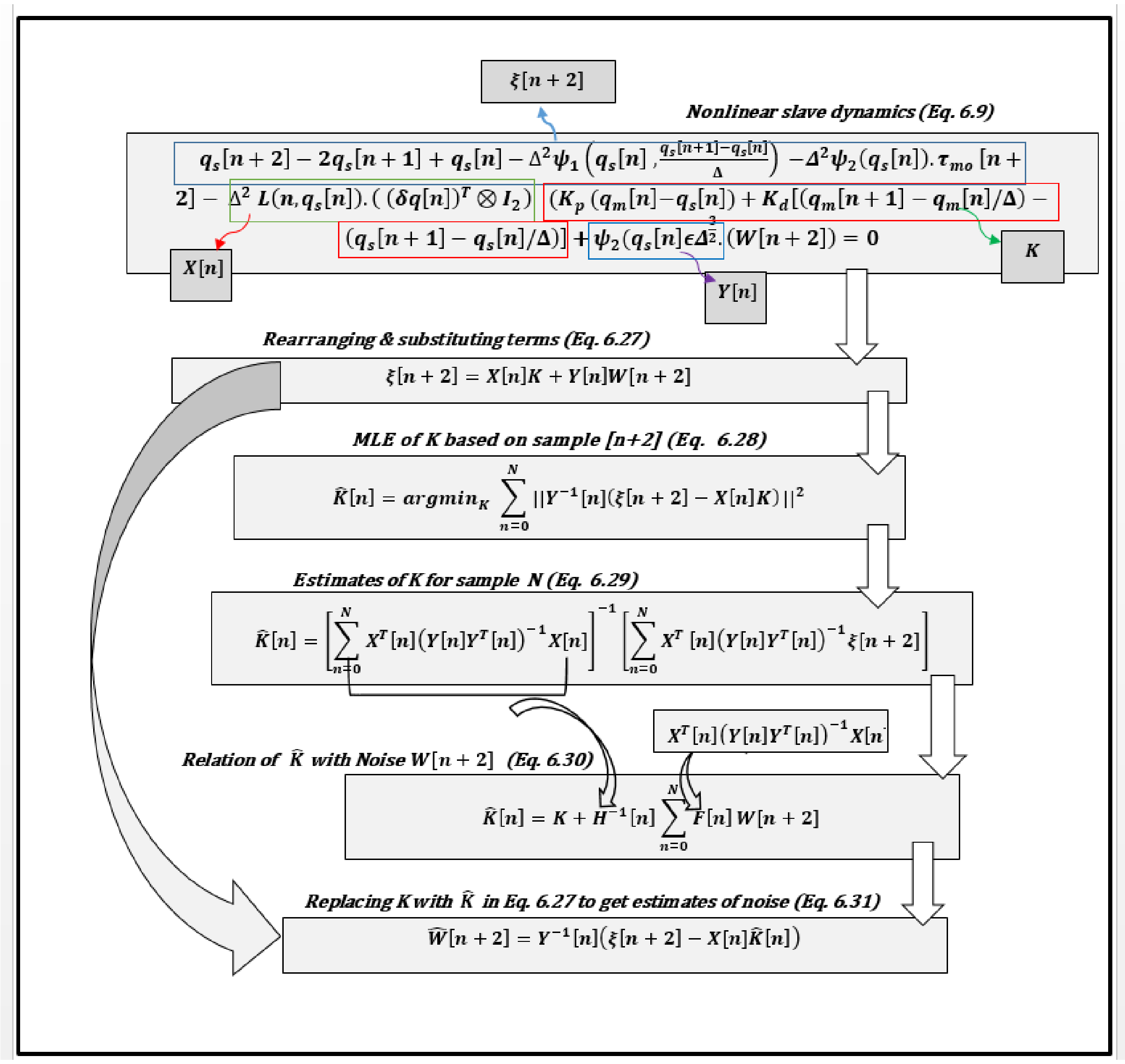

Figure 6.5: Process of Computation of Environmental Noise.

Further substituting the values of terms involved in (6.32) from (6.26) and (6.30), the aforementioned equation is written as:

$$\left.\begin{aligned} \widehat{\boldsymbol{K}}[\boldsymbol{N}] - \boldsymbol{K} =& \boldsymbol{\lambda}(\sum_{n=0}^{N}(\boldsymbol{\delta q}[\boldsymbol{n}] \otimes \boldsymbol{I_2})\boldsymbol{R}[\boldsymbol{n}]^{-1}(\boldsymbol{\delta q}[\boldsymbol{n}]^{T} \otimes \boldsymbol{I_2}))^{-1} \\ & (\sum_{n=0}^{N}(\boldsymbol{\delta q}[\boldsymbol{n}] \otimes \boldsymbol{I_2})\boldsymbol{R}[\boldsymbol{n}]^{-1}\boldsymbol{\psi_2}[\boldsymbol{n}]\boldsymbol{W}[\boldsymbol{n}+2]) \\ \text{where } & \boldsymbol{\lambda} = -\boldsymbol{\epsilon}\boldsymbol{\Delta}^{-1/2}, \\ & \boldsymbol{R}[\boldsymbol{n}] = \boldsymbol{\Psi_2}(\boldsymbol{q_m}[\boldsymbol{n}])\boldsymbol{\Psi_2}(\boldsymbol{q_m}[\boldsymbol{n}])^{T} = \boldsymbol{\Psi_2}[\boldsymbol{n}]\boldsymbol{\Psi_2}[\boldsymbol{n}]^{T} \\ & \boldsymbol{\Psi_2}[\boldsymbol{n}] = \boldsymbol{\Psi_2}(\boldsymbol{q_m}[\boldsymbol{n}]) \end{aligned}\right\} \quad (6.33)$$

From equation (6.31), the following expressions are expressed as:

$$\boldsymbol{H}[\boldsymbol{n}] \propto \sum_{0}^{N}(\boldsymbol{\delta q}[\boldsymbol{n}] \otimes \boldsymbol{I_2})\boldsymbol{R}[\boldsymbol{n}]^{-1}(\boldsymbol{\delta q}[\boldsymbol{n}]^{T} \otimes \boldsymbol{I_2}) \text{ and linearization around } \boldsymbol{q_m}[\boldsymbol{n}]; \quad (6.34)$$

$$\text{Also } \sum_{0}^{N}\boldsymbol{F}[\boldsymbol{n}]\boldsymbol{W}[\boldsymbol{n}+2] \propto \sum_{0}^{N}(\boldsymbol{\delta q}[\boldsymbol{n}] \otimes \boldsymbol{I_2})\boldsymbol{R}[\boldsymbol{n}]^{-1}\boldsymbol{\psi_2}[\boldsymbol{n}]\boldsymbol{W}[\boldsymbol{n}+2] \quad (6.35)$$

Specifically, the expression for the approximate value of $\widehat{\boldsymbol{K}}[\boldsymbol{n}]-\boldsymbol{K}$ (refer equations (6.33)-(6.34)) is evaluated as a ratio of two quadratic functions of a Gaussian process, i.e. $\widehat{\boldsymbol{K}}[\boldsymbol{n}] - \boldsymbol{K} = \boldsymbol{P}^{-1}\boldsymbol{Q}$, where, $\boldsymbol{Q} \in 8 \times 1$ is a quadratic function of $\boldsymbol{\delta q}[\boldsymbol{n}]$. We show that $\boldsymbol{Q}$ has zero mean and $\boldsymbol{P}$ has non-zero mean and this justifies the present approach that $\mathbb{E}\{\widehat{\boldsymbol{K}}[\boldsymbol{n}] - \boldsymbol{K}\}$ is small. Numerator in equation (6.33) has mean zero since $\boldsymbol{\delta q}[\boldsymbol{n}]$ is uncorrelated with $\boldsymbol{W}[\boldsymbol{n}+\boldsymbol{2}]$ and denominator has non-zero mean since $\mathbb{E}[\boldsymbol{\delta q}[\boldsymbol{n}]\boldsymbol{\delta q}[\boldsymbol{n}]^{T}] \neq \boldsymbol{0}$. Hence $\widehat{\boldsymbol{K}}[\boldsymbol{N}] - \boldsymbol{K}$ is small in probability.

6.5 Validation of proposed algorithm

This section presents the effectiveness of the proposed control scheme. Identical master and slave robot have been considered for this purpose. Before the interaction of slave robot with environment noise, PD gain parameters matrices $\boldsymbol{K_d}$ and $\boldsymbol{K_d}$ were tuned for tracking control of slave with respect to master

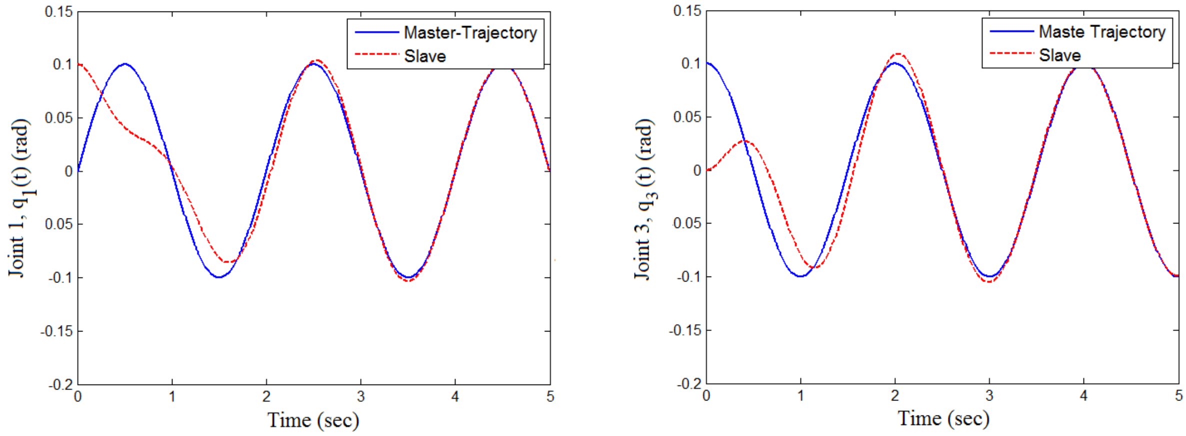

Figure 6.6: Trajectories of Joint 1 and Joint 3 of the Master-Slave System.

trajectory such that $\boldsymbol{q_s}[\boldsymbol{n}] \approx \boldsymbol{q_m}[\boldsymbol{n}]$. These parameters are given below:

$$\left.\begin{aligned} \boldsymbol{K_p} &= \begin{bmatrix} \mathbf{1.69} & \mathbf{0} \\ \mathbf{0} & \mathbf{0.6} \end{bmatrix} \\ \text{and} \quad \boldsymbol{K_d} &= \begin{bmatrix} \mathbf{0.3} & \mathbf{0} \\ \mathbf{0} & \mathbf{0.01} \end{bmatrix}. \end{aligned}\right\} \tag{6.36}$$

Then, random environmental noise with 0.01 covariance is introduced in the dynamics of the slave. The deviation $\boldsymbol{\delta q_s}[\boldsymbol{n}]$ of the slave angles due to this noise is measured and using this deviation, the estimation of $\boldsymbol{K_p}$ and $\boldsymbol{K_d}$ using MLE (refer section 6.4) is

$$\left.\begin{aligned} \widehat{\boldsymbol{K_p}} & \begin{bmatrix} \mathbf{1.71} & \mathbf{0} \\ \mathbf{0} & \mathbf{0.59} \end{bmatrix} \\ \text{and} \quad \widehat{\boldsymbol{K_d}} &= \begin{bmatrix} \mathbf{0.31} & \mathbf{0} \\ \mathbf{0} & \mathbf{0.0091} \end{bmatrix}. \end{aligned}\right\} \tag{6.37}$$

This PD controller's gain parameters are employed to reduce the tracking error between master and slave in the presence of environmental noise and tracking plots are shown for joint 1 and joint 3 of slave robot in Fig.6.5. Further, with the estimated controller gain parameter, $\widehat{\boldsymbol{K_p}}$ and $\widehat{\boldsymbol{K_d}}$, the noise trajectory of environment is computed for joint 1 and joint 3 of slave robot as shown in Fig.6.6. Error plot of this trajectory illustrates that error converges with the proposed technique. Fig.6.7 illustrates that estimated environment force

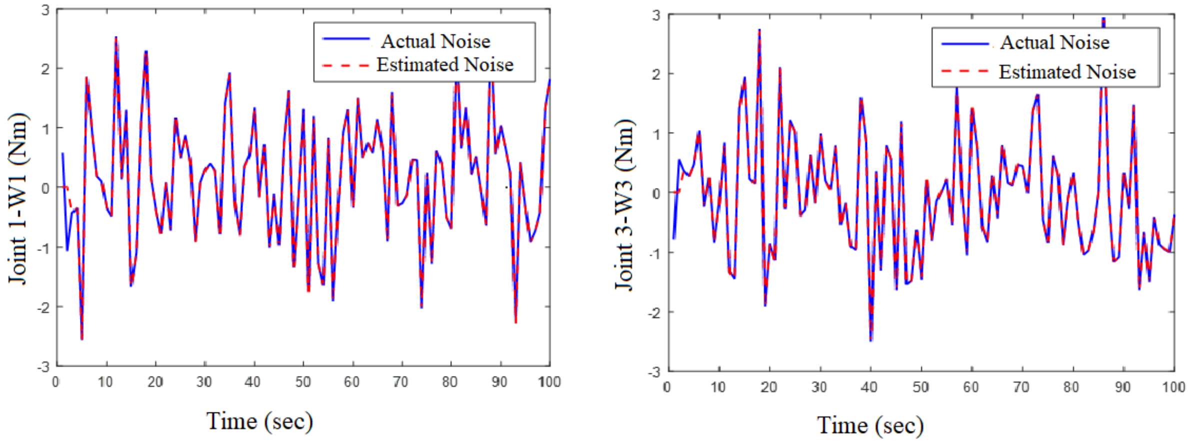

Figure 6.7: Estimation Performance of Environmental Noise of Joint 1 and Joint 3 of Slave Robot.

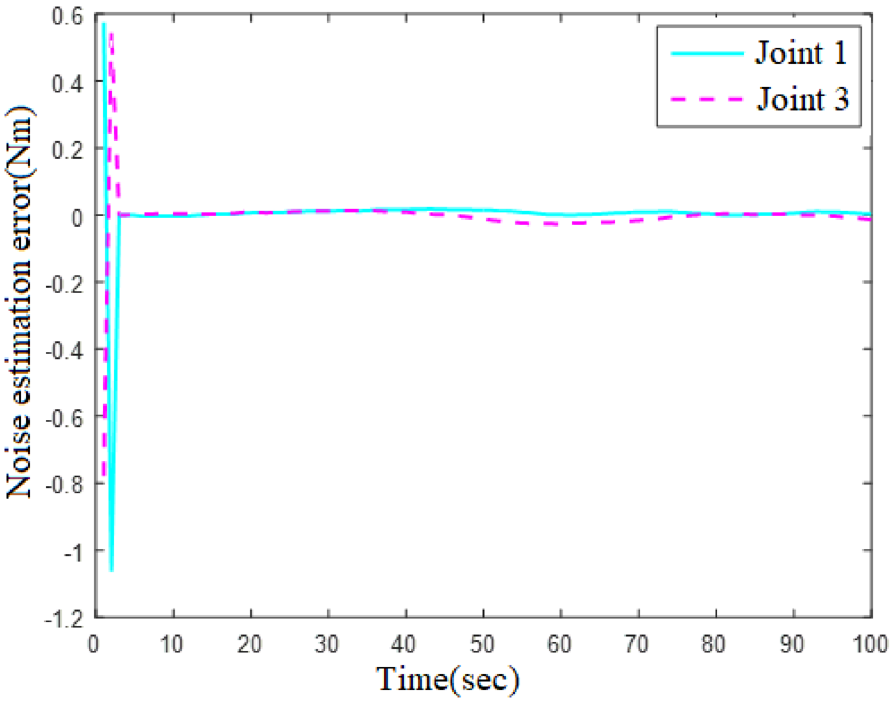

Figure 6.8: Time Histories of Estimation Error of Environmental Noise.

$(\widehat{\boldsymbol{W}}[\boldsymbol{n}])_{\boldsymbol{n=0}}^{\boldsymbol{N}}$ accurately tracks the actual environment random force, $(\boldsymbol{W}[\boldsymbol{n}])_{\boldsymbol{n=0}}^{\boldsymbol{N}}$.

6.6 Statistics of error dynamics, $\boldsymbol{\delta q}[\boldsymbol{n}]$:

In this section, the dynamics of error is represented as state model which is further used for performance analysis done in section 6.7. Define :

$$\left.\begin{aligned} \boldsymbol{\delta q_s}[\boldsymbol{n}] &= \boldsymbol{q_s}[\boldsymbol{n}] - \boldsymbol{q_m}[\boldsymbol{n}] \\ \boldsymbol{\delta \dot{q}_s}[\boldsymbol{n}] &= \boldsymbol{\dot{q}_s}[\boldsymbol{n}] - \boldsymbol{\dot{q}_m}[\boldsymbol{n}] \\ \text{State vector, } \boldsymbol{\delta q}[\boldsymbol{n}] &= \begin{bmatrix} \boldsymbol{\delta q_s}[\boldsymbol{n}] \\ \boldsymbol{\delta \dot{q}_s}[\boldsymbol{n}] \end{bmatrix} \end{aligned}\right\} \tag{6.38}$$

By considering the linearized model, we express the state equations for $\boldsymbol{\delta q}[\boldsymbol{n}]$ as a linear first-order difference equation with the white Gaussian input that readily verifies the Gaussianity of $\boldsymbol{\delta q}[\boldsymbol{n}]$. The state equations satisfied by $\boldsymbol{\delta q}[\boldsymbol{n}]$ are

$$\left.\begin{aligned} &\boldsymbol{\delta q_s}[\boldsymbol{n}+\boldsymbol{2}] - \boldsymbol{2\delta q_s}[\boldsymbol{n}+\boldsymbol{1}] + \boldsymbol{\delta q_s}[\boldsymbol{n}] \\ &\quad = \boldsymbol{\Delta^2}(\boldsymbol{\Psi_{1,1}}[\boldsymbol{n}]\boldsymbol{\delta q_s}[\boldsymbol{n}] + \boldsymbol{\Psi_{1,2}}[\boldsymbol{n}]\boldsymbol{\delta \dot{q}_s}[\boldsymbol{n}]) - \boldsymbol{\Delta^2}((\boldsymbol{\delta q_s}[\boldsymbol{n}]^{\boldsymbol{T}}, \boldsymbol{\delta \dot{q}_s}[\boldsymbol{n}]^{\boldsymbol{T}}) \otimes \boldsymbol{I_2})\boldsymbol{K} \\ &\qquad + \boldsymbol{\epsilon\Delta^{3/2}\Psi_2}[\boldsymbol{n}]\boldsymbol{W}[\boldsymbol{n}+\boldsymbol{2}] \end{aligned}\right\} \tag{6.39}$$

The difference equations are expressed as:

$$\boldsymbol{\delta q_s}[\boldsymbol{n}+\boldsymbol{1}] = \boldsymbol{\delta q_s}[\boldsymbol{n}] + \boldsymbol{\Delta\delta \dot{q}_s}[\boldsymbol{n}] \tag{6.40}$$

Following equations are used to get (6.41).

$$\left.\begin{aligned} \boldsymbol{\delta \ddot{q}_s}[\boldsymbol{n}+\boldsymbol{1}] &= \frac{\boldsymbol{\delta q_s}[\boldsymbol{n}+\boldsymbol{1}] - \boldsymbol{2q_s}[\boldsymbol{n}+\boldsymbol{1}] + \boldsymbol{\delta q_s}[\boldsymbol{n}]}{\boldsymbol{\Delta^2}} \\ \boldsymbol{\delta \ddot{q}_s}[\boldsymbol{n}+\boldsymbol{1}] &= \frac{\boldsymbol{\delta \dot{q}_s}[\boldsymbol{n}+\boldsymbol{1}] - \boldsymbol{\delta \dot{q}_s}[\boldsymbol{n}]}{\boldsymbol{\Delta}} \end{aligned}\right\}$$

$$\left.\begin{aligned} \boldsymbol{\delta \dot{q}_s}[\boldsymbol{n}+\boldsymbol{1}] &= \boldsymbol{\delta \dot{q}_s}[\boldsymbol{n}] + \boldsymbol{\Delta}(\boldsymbol{\Psi_{1,1}}[\boldsymbol{n}]\boldsymbol{\delta q_s}[\boldsymbol{n}] + \boldsymbol{\Psi_{1,2}}[\boldsymbol{n}]\boldsymbol{\delta \dot{q}_s}[\boldsymbol{n}]) \\ &\quad - \boldsymbol{\Delta}((\boldsymbol{\delta q_s}[\boldsymbol{n}]^{\boldsymbol{T}}, \boldsymbol{\delta \dot{q}_s}[\boldsymbol{n}]^{\boldsymbol{T}}) \otimes \boldsymbol{I_2})\boldsymbol{K} + \boldsymbol{\epsilon\sqrt{\Delta}\Psi_2}[\boldsymbol{n}]\boldsymbol{W}[\boldsymbol{n}+\boldsymbol{2}] \end{aligned}\right\} \tag{6.41}$$

The property, $(\eta^T \otimes I)Vec(B) = B\eta$ is used to get equation (6.41). Writing K for the 2×4 matrix formed from $K = [K_p|K_d]$, where $K_p \; and \; K_d$ are 2×2 matrices.

We thus have

$$\left.\begin{aligned}\boldsymbol{\delta\dot{q}_s[n+1]} &= \boldsymbol{\delta\dot{q}_s[n] + \Delta(\Psi_{1,1}[n]\delta q_s[n] + \Psi_{1,2}[n]\delta\dot{q}_s[n])} \\ &\quad \boldsymbol{- \Delta.K_p\delta q_s[n] - \Delta.K_d.\delta\dot{q}_s[n] + \epsilon\sqrt{\Delta}\Psi_2[n]W[n+2]}\end{aligned}\right\} \tag{6.42}$$

From equations (6.39) and (6.42), the state model is represented as:

$$\left.\begin{aligned}\begin{bmatrix}\boldsymbol{\delta q_s[n+1]} \\ \boldsymbol{\delta\dot{q}_s[n+1]}\end{bmatrix} &= \begin{bmatrix}\boldsymbol{I_2} & \boldsymbol{\Delta I_2} \\ \boldsymbol{(\delta\Psi_{1,1}[n] - \Delta K_p)} & \boldsymbol{(I + \Delta.\Psi_{1,2}[n] - \Delta K_d)}\end{bmatrix}\begin{bmatrix}\boldsymbol{\delta q_s} \\ \boldsymbol{\delta\dot{q}_s}\end{bmatrix} \\ &\quad + \begin{bmatrix}\boldsymbol{\epsilon\sqrt{\Delta}}\end{bmatrix}\begin{bmatrix}\boldsymbol{O} \\ \boldsymbol{\Psi_2[n]}\end{bmatrix}\boldsymbol{W[n+2]}\end{aligned}\right\} \tag{6.43}$$

Substituting:

$$\left.\begin{aligned}&\boldsymbol{A[n,K]} = \begin{bmatrix}\boldsymbol{I_2} & \boldsymbol{\Delta I_2} \\ \boldsymbol{(\delta\Psi_{1,1}[n] - \Delta K_p)} & \boldsymbol{(I + \Delta.\Psi_{1,2}[n] - \Delta K_d)}\end{bmatrix} \\ &\text{and } \boldsymbol{G[n]} = \boldsymbol{\epsilon\sqrt{\Delta}}\begin{bmatrix}\boldsymbol{O} \\ \boldsymbol{\Psi_2[n]}\end{bmatrix}\end{aligned}\right\} \tag{6.44}$$

Equation (6.43) can be expressed as:

$$\boldsymbol{\delta q[n+1] = A[n,k]\delta q[n] + G[n]W[n+2]} \tag{6.45}$$

Further, it is shown that

$$\left.\begin{aligned}&\text{Let } \mathbb{E}[\boldsymbol{\delta q[n]\delta q[n]^T}] = \boldsymbol{R_q[n]} \\ &\text{Then, } \boldsymbol{R_q[n+1] = A[n,k]R_q[n]A^T[n,k] + G[n]G[n]^T} \\ &\text{Also, } \mathbb{E}[\boldsymbol{\delta q[n]W[m]^T}] = \boldsymbol{0}\end{aligned}\right\} \tag{6.46}$$

$$\left.\begin{aligned}&\mathbb{E}[\boldsymbol{\delta q[n]W[m]^T}] = \boldsymbol{A[n,k]}\mathbb{E}[\boldsymbol{\delta q[n]W[m]^T}], \ \boldsymbol{n \geq m-1} \\ &\mathbb{E}[\boldsymbol{\delta q[m-1]W[m]^T}] = \mathbb{E}[\boldsymbol{\delta q[n+1]W[n+2]^T}] \\ &\mathbb{E}[\boldsymbol{\delta q[n+1]W[n+2]^T}] = \boldsymbol{A[n,k]}\mathbb{E}[\boldsymbol{\delta q[n]W[n+2]^T}] + \boldsymbol{G[n]} = \boldsymbol{G[n]}\end{aligned}\right\} \tag{6.47}$$

Note that, $\boldsymbol{\delta q}$ is a Gaussian vector sequence and its correlation is determined from the above equations.

6.7 Performance measure of estimation

The following sections examine to ensure the satisfactory performance of MLE by three ways:

(i) Unbiasness of estimation

(ii) Convergence analysis

(iii) Cramer Rao Lower Bound (CRLB) of estimation

6.7.1 Unbias estimation

The property of good unbiased estimate is analysed by showing that the mean value of a difference between the estimated and true value of the parameter is nearly zero.
In this section, an analytic justification is presented to support the unbiased estimates done in the previous section for controller gain parameters. From the equation (6.34) and (6.35) of estimation, it is noted that the proposed maximum likelihood estimator of $\boldsymbol{K}$, i.e. $\widehat{\boldsymbol{K}}$ is based on slave linearization and expressed in the form $\boldsymbol{K} + \boldsymbol{P}^{-1}\boldsymbol{Q}$ where, $\boldsymbol{Q}$ is a bilinear vector function of $\{\boldsymbol{\delta q_s}[\boldsymbol{n}]\}$ and $\{\boldsymbol{W}[\boldsymbol{n}]\}$ and $\boldsymbol{P}$ is a quadratic function $\{\boldsymbol{\delta q_s}[\boldsymbol{n}]\}$. Here, $\{\boldsymbol{\delta q_s}[\boldsymbol{n}]\}$ is the master-slave angular error. In view of the linearized dynamics, $\boldsymbol{P}$ and $\boldsymbol{Q}$ are both quadratic functions of the environmental torque noise $\boldsymbol{W}[\boldsymbol{n}]$. The mean value of $\boldsymbol{Q}$ turns out to be zero because of the system causality. The mean value of $\boldsymbol{P}$ is non-zero, and hence if approximation of $\mathbb{E}(\hat{\boldsymbol{K}} - \boldsymbol{K})$ by $(\mathbb{E}\boldsymbol{P}^{-1})(\mathbb{E}\boldsymbol{Q})$ is done, result is zero. This justifies the PD controller gain estimator of the proposed work is nearly unbiased.

6.7.2 Convergence analysis

Convergence analysis of the parameter estimates is performed by obtaining approximate expressions for the mean square parameters estimation error based on N data samples and the accuracy of environmental noise estimate is justified due to low signal to noise ratio (SNR).

In this section, it is approximating $\mathbb{E}||\widehat{\boldsymbol{K}}[\boldsymbol{n}]-\boldsymbol{K}||^{2}]$ by $\mathbb{E}||(\boldsymbol{P}^{-1})||^{2}\mathbb{E}(||\boldsymbol{Q}||^{2})$ and prove that this is small using the fact that $\boldsymbol{Q}$ is a sum of independent random variables. We then substitute the estimated value $\widehat{\boldsymbol{K}}[\boldsymbol{N}]$ of $\boldsymbol{K}$ into the nonlinear slave dynamics in place of $\boldsymbol{K}$, and solve for $\boldsymbol{W}[\boldsymbol{n}]$ in terms of $\{\boldsymbol{q}[\boldsymbol{n}]\}_{\boldsymbol{n=0}}^{\boldsymbol{N}}$ and $\hat{\boldsymbol{K}}[\boldsymbol{n}]$. The result is $\{\boldsymbol{W}[\boldsymbol{n}]\}_{\boldsymbol{n=0}}^{\boldsymbol{N}}$, an estimate of the environmental torque process. Then show that $\widehat{\boldsymbol{W}}[\boldsymbol{n}]-\boldsymbol{W}[\boldsymbol{n}]$ is a bilinear function of $\boldsymbol{\delta q_s}[\boldsymbol{n}]$ and $\{\widehat{\boldsymbol{K}}[\boldsymbol{n}]-\boldsymbol{K}\}$ and is therefore of second order of smallness i.e of $\boldsymbol{O}(||\boldsymbol{W}||^{2})$. This justifies our an accurate estimate of the environmental torque $\widehat{\boldsymbol{W}}[\boldsymbol{n}]$ from which the structure of the environment has been determined. Thus, $||\widehat{\boldsymbol{K}}-\boldsymbol{K}||^{2}=||\mathbb{E}\boldsymbol{P}^{-1}||^{2}||\mathbb{E}\boldsymbol{Q}||^{2}$ can be regarded as a "matrix ratio" of two quadratic functions of $\boldsymbol{W}[\boldsymbol{n}]$. In section 6.4, the ML parameter estimates based on the exact non-linear dynamics is presented. However, for computation of the performance of these estimates, it is required to linearize the dynamics otherwise the evaluation of the angular correlation becomes impossible. The aim is to determine the limiting mean square deviation $\lim_{\boldsymbol{n}\longmapsto\infty}\mathbb{E}\{||\boldsymbol{\delta q_s}[\boldsymbol{n}]||^{2}\}$, $\boldsymbol{\delta q_s}[\boldsymbol{n}]=\boldsymbol{q_s}[\boldsymbol{n}]-\boldsymbol{q_m}[\boldsymbol{n}]$ of the slave position which require linearization of the non-linear slave dynamics in discrete time about the master position. The linearized equation has time dependent matrix coefficients and a driving white noise term coming from the environmental torque which provides evaluation of correlation $\mathbb{E}\{\boldsymbol{\delta q_s}[\boldsymbol{n}]\boldsymbol{\delta q_s}[\boldsymbol{n}]^{\boldsymbol{T}}\}$. Aiming that the master has a limiting angular position, a linear algebraic equation for the limiting error-correlation- matrix as a function of the feedback parameters, $\boldsymbol{K_p}$ and $\boldsymbol{K_d}$ is derived.
The limiting noise to signal ratio is represented as $\dfrac{\mathbb{E}[||\boldsymbol{\delta q_s}(\infty)||^{2}]}{||\boldsymbol{q_m}(\infty)||^{2}}$.

Approximate formula for the PD-parameter error $\widehat{\boldsymbol{K}}[\boldsymbol{n}]-\boldsymbol{K}$ and the noise estimation error $\widehat{\boldsymbol{W}}[\boldsymbol{n}]-\boldsymbol{W}[\boldsymbol{n}]$ in terms of $\boldsymbol{W}[\boldsymbol{n}]$ and $\boldsymbol{\delta q}[\boldsymbol{n}]=(\boldsymbol{q_s}[\boldsymbol{n}]-\boldsymbol{q_m}[\boldsymbol{n}]),\dot{\boldsymbol{q}}_{\boldsymbol{s}}[\boldsymbol{n}]-\dot{\boldsymbol{q}}_{\boldsymbol{m}}[\boldsymbol{n}])$ is obtained. A recursive algorithm is derived for calculating the correlation $\mathbb{E}[\boldsymbol{\delta q}[\boldsymbol{n}]\boldsymbol{\delta q}[\boldsymbol{n}]^{\boldsymbol{T}}]$ and $\mathbb{E}[\boldsymbol{\delta q}[\boldsymbol{n}]\boldsymbol{W}[\boldsymbol{m}^{\boldsymbol{T}}]$ using linearized version of the dynamical model and this enables us to perform the above calculations.

From equation (6.31), the noise estimate error-energy is given by

$$\left.\begin{aligned} \widehat{\boldsymbol{W}}[\boldsymbol{n}+\mathbf{2}] - \boldsymbol{W}[\boldsymbol{n}+\mathbf{2}] = \boldsymbol{Y}[\boldsymbol{n}]^{-1}\boldsymbol{X}[\boldsymbol{n}](\boldsymbol{K} - \hat{\boldsymbol{K}}[\boldsymbol{N}]) \\ \approx \boldsymbol{\epsilon}^{-1}\boldsymbol{\Delta}^{-3/2}\boldsymbol{\Psi}_2[\boldsymbol{n}]^{-1}(-\boldsymbol{\Delta}^2)(\boldsymbol{\delta q}[\boldsymbol{n}]^T \otimes \boldsymbol{I}_2)(\boldsymbol{K} - \widehat{\boldsymbol{K}}[\boldsymbol{N}]) \\ = -\boldsymbol{\epsilon}^{-1}\sqrt{\boldsymbol{\Delta}}\boldsymbol{\Psi}_2[\boldsymbol{n}]^{-1}(\boldsymbol{\delta q}[\boldsymbol{n}]^T \otimes \boldsymbol{I}_2)(\boldsymbol{K} - \widehat{\boldsymbol{K}}[\boldsymbol{N}]) \end{aligned}\right\} \tag{6.48}$$

The approximate expression for the absolute error $|\widehat{\boldsymbol{W}}[\boldsymbol{n}] - \boldsymbol{W}[\boldsymbol{n}]|$ is obtained as a bilinear function of $\boldsymbol{\delta q}[\boldsymbol{n}]$ and $\{\widehat{\boldsymbol{K}}[\boldsymbol{n}] - \boldsymbol{K}\}$ showing that this is small in probability.

This analysis is based on substituting $\widehat{\boldsymbol{K}}$ in place of $\boldsymbol{K}$ in equation (6.31) and $\widehat{\boldsymbol{W}}[\boldsymbol{n}+\mathbf{2}]$ in place of $\boldsymbol{W}[\boldsymbol{n}]$ in the same and substituting the resulting equation from (6.27).

Since in equation (6.48), $\left(\widehat{\boldsymbol{W}}[\boldsymbol{n}+\mathbf{2}] - \boldsymbol{W}[\boldsymbol{n}+\mathbf{2}]\right)$ is proportional to the tensor product of two small quantities $\boldsymbol{\delta q}[\boldsymbol{n}]$ and $\left(\boldsymbol{K} - \widehat{\boldsymbol{K}}[\boldsymbol{N}]\right)$ so, $\left(\widehat{\boldsymbol{W}}[\boldsymbol{n}+\mathbf{2}] - \boldsymbol{W}[\boldsymbol{n}+\mathbf{2}]\right)$ is very small in probability. Thus, an environmental noise estimate is highly accurate as also demonstrated in the simulations.

Remark : The random variables $\{\boldsymbol{\delta q}[\boldsymbol{n}] \otimes \boldsymbol{W}[\boldsymbol{n}+\mathbf{2}]\}, \boldsymbol{n} = \mathbf{0}, \mathbf{1}, \mathbf{2}, \ldots\ldots$ are uncorrelated owing to the whiteness of $\boldsymbol{W}(.)$ and hence the variance of the numerator in (6.48) grows with N as O(N). Equivalently, the mean modulus of the numerator is of $O(\sqrt{N})$. On the other hand, since $\mathbb{E}(\boldsymbol{\delta q}[\boldsymbol{n}]\boldsymbol{\delta q}[\boldsymbol{n}]^T) \neq \mathbf{0}$, the mean modulus of the denominator in (6.48) grows as O(N). Hence, the mean modulus of (??) decreases with increasing N as $\frac{O(\sqrt{N})}{O(N)} = O(\frac{1}{\sqrt{(N)}})$.

6.7.3 Cramer Rao Lower Bound (CRLB) of estimation

In this section, an approximate expression is derived for the CRLB on the parameter estimation error-covariance matrix. The Cramer-Rao lower bound imposes a bound on an estimate of a parameter based on a given measurement and evaluates the performance of unbias maximum-likelihood estimate on its variance. This lower bound sets a limit to the accuracy to estimate a parameter that influences a probability density. The diagonal entries of the CRLB determine the minimum possible variance/mean square estimation error $\| \mathbb{E}(K - \widehat{K}[N]) \|^2$ of each component of K[N].

Evaluation of the CRLB for any unbiased estimator of the estimation problem under consideration requires to use the linearized model. Concrete approximations of the CRLB which give its order of magnitude are derived by assuming that the master angular position has stabilized as a constant value. In this case, the linearized slave dynamics is a linear time invariant state variable system of the form:

$$\left.\begin{aligned} \boldsymbol{\delta q}[\boldsymbol{n}+\mathbf{1}] = \boldsymbol{A}[\boldsymbol{k}]\boldsymbol{\delta q}[\boldsymbol{n}] + \boldsymbol{GW}[\boldsymbol{n}+\mathbf{2}], \\ \text{where, } \boldsymbol{\delta q} = [\boldsymbol{\delta q_s}, \boldsymbol{\delta \dot{q}_s}]^{\boldsymbol{T}} \end{aligned}\right\} \tag{6.49}$$

This is computed as a linear combination of the master-slave error angular position-velocity correlation matrix. The diagonal entries of the CRLB determine the minimum possible variance i.e. mean square estimation error $\mathbb{E}\| \boldsymbol{K} - \widehat{\boldsymbol{K}}[\boldsymbol{N}] \|^{\mathbf{2}}$ of each component of $\boldsymbol{K}[\boldsymbol{N}]$. The angular position-velocity correlation matrix, $\boldsymbol{C_q}[\boldsymbol{n}]$ approximately satisfies a linear difference equation of slave dynamics and by solving this equation recursively, Fisher information matrix and hence, the CRLB is obtained. The state variable equation (6.49) is easily solved by using the state transition matrix in discrete time and an expression for the error angular position-velocity correlation matrix $\boldsymbol{C_q}[\boldsymbol{n}] = \{\boldsymbol{\delta q}[\boldsymbol{n}].\boldsymbol{\delta q}[\boldsymbol{n}]^{\boldsymbol{T}}\}$ is immediately obtained. For stability, we assume that all the eigen values of $\boldsymbol{A}[\boldsymbol{k}]$ have magnitude smaller than unity and then, using the spectral norm, a bound on $||\boldsymbol{C_q}[\boldsymbol{n}]||$ in term of the maximum magnitude eigenvalue of $\boldsymbol{A}[\boldsymbol{k}]$ is derived. This enable us to derive the order of magnitude of the CRLB and hence of the parameter variance estimate. Further, it is shown that the CRLB $\rightarrow 0$ as N $\rightarrow \infty$ implying that efficient parameter estimates are consistent.

Consider the expression for Fisher inverse matrix (i.e. the CRLB) is obtained in the special case when the robot vibrates noisily around a fixed point. Computation of Fisher information matrix is presented as:

$$\boldsymbol{J}(\boldsymbol{K}) = -\mathbb{E}\left(\frac{\boldsymbol{\delta}^{\mathbf{2}} \log}{\boldsymbol{\delta K \delta K^T}} \boldsymbol{p}(\boldsymbol{q}(.)|\boldsymbol{K})\right) \tag{6.50a}$$

$$= \mathbb{E}\sum_{\boldsymbol{n}=\mathbf{0}}^{\boldsymbol{N}} \left(\boldsymbol{X}[\boldsymbol{n}]^{\boldsymbol{T}}(\boldsymbol{Y}[\boldsymbol{n}]\boldsymbol{Y}[\boldsymbol{n}]^{\boldsymbol{T}})^{-\mathbf{1}}\boldsymbol{X}[\boldsymbol{n}]\right) \quad \text{(Refer equation (6.27)} \tag{6.50b}$$

$$\approx \boldsymbol{\epsilon}^{-\mathbf{2}}\boldsymbol{\Delta}^{-\mathbf{3}}\boldsymbol{\Delta}^{\mathbf{4}} \sum_{\boldsymbol{n}=\mathbf{0}}^{\boldsymbol{N}} \mathbb{E}(\boldsymbol{\delta q}[\boldsymbol{n}] \otimes \boldsymbol{I_2})\boldsymbol{R}[\boldsymbol{n}]^{-\mathbf{1}}(\boldsymbol{\delta q}[\boldsymbol{n}]^{\boldsymbol{T}} \otimes \boldsymbol{I_2}) \tag{6.50c}$$

$$= \epsilon^{-2}\Delta \sum_{n=0}^{N} \mathbb{E}\left(\begin{bmatrix} \delta q[n] & 0 \\ 0^T & \delta q[n] \end{bmatrix} \begin{bmatrix} (R[n]^{-1})_{11} & (R[n]^{-1})_{12} \\ (R[n]^{-1})_{21} & (R[n]^{-1})_{22} \end{bmatrix} \begin{bmatrix} \delta q[n]^T & 0 \\ 0^T & \delta q[n]^T \end{bmatrix} \right) \tag{6.50d}$$

$$= \epsilon^{-2}\Delta \sum_{n=0}^{N} \begin{bmatrix} (R[n]^{-1})_{11}\mathbb{E}\{\delta q[n]\delta q[n]^T\} & (R[n]^{-1})_{12}\mathbb{E}\{\delta q[n]\delta q[n]^T\} \\ (R[n]^{-1})_{21}\mathbb{E}\{\delta q[n]\delta q[n]^T\} & (R[n]^{-1})_{22}\mathbb{E}\{\delta q[n]\delta q[n]^T\} \end{bmatrix} \tag{6.50e}$$

$$\left. \begin{aligned} &= \epsilon^{-2}\Delta \sum_{n=0}^{N} (R[n]^{-1} \otimes C_q[n]); \\ &\text{where, } C_q[n] = \mathbb{E}\{\delta q[n]\delta q[n]^T\} \end{aligned} \right\} \tag{6.50f}$$

The final expression for CRLB of $\mathbf{K}$ is given as:

$$J(K)^{-1} = \frac{\epsilon^2}{\Delta}\left(\sum_{n=0}^{N} R[n]^{-1} \otimes C_q[n])^{-1} \right) \tag{6.51}$$

The diagonal entries of $J(K)^{-1} \in R^{2\times 2}$ give a lower bound for the variance of the corresponding entry of $\widehat{K}[N]$.

For evaluating the CRLB, $J(K)^{-1}$, we require $C_q[n]$, the calculations of which is done as following.

Remark: If we assume that the master angle vector $q_m[n]$ has stabilised around some nominal value say q_m^*, then $\Psi_{1,1}[n]$ and $\Psi_{1,2}[n]$ are nearly constant matrix namely $\Psi_{1,1}(q_m^*, o)$ and $\Psi_{1,2}(q_m^*, o)$ and so is $\psi_2[n] = \psi_2(q_m^*)$.

Then $A[n,k] = A[k]$ is a constant matrix and so is $G[n] = G$ say.

In that case we have $\delta q[n+1] = A[k]\delta q[n] + G\omega[n+2],$ the solution to which is (assuming $\delta q[0] = 0$, $\delta q[n] = \sum_{k=0}^{n-1} A[k]^{n-k-l} GW[k+2]$)

Then, $R_q[n] = \mathbb{E}[\delta q[n]\delta q[n]^T] = \sum_{k=0}^{n-1} A[k]^{n-k-l}|GG^T(A[k]^T)^{n-k-l}|$ and this can be used to get approximate expression for the CRLB. Thus,

$$\left. \begin{aligned} G &\approx \epsilon\sqrt{\Delta} \begin{bmatrix} 0 \\ \psi_2 \end{bmatrix} \\ GG^T &= \epsilon^2\Delta \begin{bmatrix} 0 & 0 \\ 0 & \psi_2\psi_2^T \end{bmatrix} = \epsilon^2\Delta \begin{bmatrix} 0 & 0 \\ 0 & R \end{bmatrix} \end{aligned} \right\} \tag{6.52}$$

Let $\boldsymbol{A}[\boldsymbol{k}] = \sum_{\alpha=1}^{4} \boldsymbol{\lambda}_\alpha \boldsymbol{\vartheta}_\alpha \boldsymbol{\vartheta}_\alpha^T$ be the spectral representation of $\boldsymbol{A}[\boldsymbol{k}]$, then

$$\left.\begin{aligned}
\boldsymbol{R}_q[\boldsymbol{n}] &= \boldsymbol{\epsilon}^2 \boldsymbol{\Delta} \sum_{k=0}^{n-1} \sum_{\alpha,\beta=1}^{4} (\boldsymbol{\lambda}_\alpha \boldsymbol{\lambda}_\beta)^{n-k-1} \boldsymbol{\vartheta}_\alpha \boldsymbol{\vartheta}_\alpha^T \begin{bmatrix} (\boldsymbol{0} & \boldsymbol{0} \\ \boldsymbol{0} & \boldsymbol{R} \end{bmatrix} \boldsymbol{\vartheta}_\beta \boldsymbol{\vartheta}_\beta^T \\
&= \boldsymbol{\epsilon}^2 \boldsymbol{\Delta} \sum_{\alpha,\beta=1}^{4} \left(\frac{1 - (\boldsymbol{\lambda}_\alpha \boldsymbol{\lambda}_\beta)^n}{1 - \boldsymbol{\lambda}_\alpha \boldsymbol{\lambda}_\beta}\right) \boldsymbol{\vartheta}_\alpha \boldsymbol{\vartheta}_\alpha^T \begin{bmatrix} \boldsymbol{0} & \boldsymbol{0} \\ \boldsymbol{0} & \boldsymbol{R} \end{bmatrix} \boldsymbol{\vartheta}_\beta \boldsymbol{\vartheta}_\beta^T \\
&\text{As } n \to \infty, \text{it can be reduced as} \\
&= \boldsymbol{\epsilon}^2 \boldsymbol{\Delta} \sum_{\alpha,\beta=1}^{4} \left(\frac{1}{1 - \boldsymbol{\lambda}_\alpha \boldsymbol{\lambda}_\beta}\right) \boldsymbol{\vartheta}_\alpha \boldsymbol{\vartheta}_\alpha^T \begin{bmatrix} \boldsymbol{0} & \boldsymbol{0} \\ \boldsymbol{0} & \boldsymbol{R} \end{bmatrix} \boldsymbol{\vartheta}_\beta \boldsymbol{\vartheta}_\beta^T \\
&\textit{Assuming } |\boldsymbol{\lambda}_\alpha| < \boldsymbol{1} \ \forall \ \boldsymbol{\alpha} \text{ so from (6.51)} \\
&\text{CRLB} = \boldsymbol{J}^{-1} \approx \frac{\boldsymbol{1}}{\boldsymbol{\Delta}^2 \boldsymbol{N}} \boldsymbol{R}^{-1} \otimes \sum_{\alpha,\beta=1}^{4} \left(\frac{1}{1 - \boldsymbol{\lambda}_\alpha \boldsymbol{\lambda}_\beta}\right) \boldsymbol{\vartheta}_\alpha \boldsymbol{\vartheta}_\alpha^T \begin{bmatrix} \boldsymbol{0} & \boldsymbol{0} \\ \boldsymbol{0} & \boldsymbol{R} \end{bmatrix} \boldsymbol{\vartheta}_\beta \boldsymbol{\vartheta}_\beta^T
\end{aligned}\right\} \tag{6.53}$$

$$\boldsymbol{C}_q[\boldsymbol{n}] = \boldsymbol{\epsilon}^2 \boldsymbol{\Delta} \sum_{k=0}^{n-1} \boldsymbol{A}[\boldsymbol{k}]^{n-k-1} \begin{bmatrix} \boldsymbol{0} & \boldsymbol{0} \\ \boldsymbol{0} & \boldsymbol{R} \end{bmatrix} \boldsymbol{A}^T[\boldsymbol{k}]^{n-k-1} \tag{6.54}$$

$$\text{and } \mathbf{CRLB(K)} \ = \frac{\boldsymbol{1}}{\boldsymbol{\Delta}^2} [\sum_{n=0}^{N} \boldsymbol{R}^{-1} \otimes \sum_{k=0}^{n-1} (\boldsymbol{A}[\boldsymbol{k}]^{n-k-1} \begin{bmatrix} \boldsymbol{0} & \boldsymbol{0} \\ \boldsymbol{0} & \boldsymbol{R} \end{bmatrix} \boldsymbol{A}^T[\boldsymbol{k}]^{n-k-1})]^{-1} \tag{6.55}$$

In equation (6.55), for a stable linearized system, eigen values of $\boldsymbol{A}[\boldsymbol{k}]$ will all be smaller than unity in magnitude and hence the inner sum will be upper bounded by a finite positive definite matrix say **P** as $\boldsymbol{n} \to \infty$ and subsequently as $\boldsymbol{N} \to \infty$, the CRLB(K) will converge to zero as

$$\boldsymbol{CRLB}(\boldsymbol{K}) \approx \frac{\boldsymbol{1}}{\boldsymbol{N}\boldsymbol{\Delta}^2} (\boldsymbol{R}^{-1} \otimes \boldsymbol{P})^{-1} = \frac{\boldsymbol{1}}{\boldsymbol{N}\boldsymbol{\Delta}^2} (\boldsymbol{R} \otimes \boldsymbol{P}^{-1})$$

The significance of obtaining the CRLB for controller-gain parameters estimates is that, since the estimates $\widehat{\boldsymbol{K}}$ is substituted in the equation (6.33) to get an estimate of the environment noise process, these uncertainty in $\widehat{\boldsymbol{K}}$ will reflect as an error in the noise estimate, $(\widehat{\boldsymbol{W}} - \boldsymbol{W})$. Thus, the minimum variance in the noise estimate $\mathbb{E}||\widehat{\boldsymbol{W}} - \boldsymbol{W}||^2$ taken over all estimates of $\boldsymbol{K}$ will be lower bounded by a quantity proportional to the CRLB for $\boldsymbol{K}$.

6.8 Conclusion

This chapter has presented an algorithm of estimating controller gain parameters and environment force using Maximum likelihood techniques based on measurement of the slave position process over a given time range. The performance of parameter estimation has been explored through formulation of an analytical expression of convergence. The success of algorithm is exemplified by providing a low noise to signal ratio for the parameter estimates as number of samples (N) increases. Further, computation of CRLB of parameter estimation has been carried out that indicates as samples tends to infinity, its variance approaches zero which means that our parameter estimates are consistent. Also, comparison of CRLB with variance of MLE supports that estimates are asymptotically efficient. The expression for the parameter and noise estimation errors show via intuitive arguments that these are small in probability and decrease with increasing data length. The simulation results show the effectiveness of the estimation and encourages the contribution of the present work to recast the approach of conventional control in tracking of master-slave robotics system.

Chapter 7

Conclusions and Further Scope of Work

7.1 Introduction

The research work present in this thesis is based on the objectives mentioned in chapter 1. The respective chapter 3, 4, 5 and 6 meet the defined objectives, explain the research work carried out and present the contributions. The summary of main contributions and further scope of work related to the objectives are presented in the following sections.

7.2 Contributions of work

The contributions of this work are summarized into two parts:
(i) Major contribution (ii) Minor contribution
Under major contributions following innovations are presented:

- Formation of joint error dynamics of estimation error and tracking error using $It\hat{o}'$s formulae which provides a feasible on-line implementation of control action based on the instantaneous error to the nonlinear and uncertain system.

- Validated by real-time experiments of the proposed control solution based on instantaneous observer output. The performance of the proposed control scheme and its robustness are explored in multiple operating scenarios.

- Developed sensitivity model to examine the robustness of the controller and observer to check the effects of fluctuation in error-energies of state tracking and state observer due to parametric uncertainties and PD controller fluctuations.

- Design of controller for tracking in the presence of noise in the closed loop dynamics of a robot by using maximum likelihood estimation of a robot from a sample of noisy position measurements. The present control algorithm is used when a robot interacts with the fluctuating environment, particularly, in the case where online information is not available.

- Computation of sample trajectory of random environment noise from the estimation of controller parameters, without the need of any force sensor or disturbance observer.

Under minor contributions following work has been carried out:

- Developed It$\hat{o}$'s stochastic framework in which joint dynamics of state evolution and observer is described using a vector stochastic differential equation (SDE).

- Formulation of an optimal control law while designing of a state observer and tracker which accommodates the gain matrix quadrature energy constraint and guarantees bounded errors.

- Designed a state-observer-based control algorithm in which EKF is used to observe the state vector. The proposed algorithm is applicable to all kinds of state-observer, not limited to EKF and eliminates the need for a velocity sensor.

- Evaluation of the estimation performance by conducting different analytical tests.

7.3 Conclusions

The research work has focused on investigating the trajectory control problems of an n-link robot in the presence of uncertainty. The uncertainty in the system dynamics has been introduced due to the presence of process noise, measurement noise, and the interaction of a robot with the random-structured environment. The research has proposed control solutions in different situations. A dynamical state-observer and tracker which work in real-time have been designed successfully to mitigate the effects of process noise and measurement noise from the system. Further, the present approach has been validated by implementing a sequence of PD-controller recursively subject to energy constraints on a real device. The main thrust of the present technique is to emphasize that tracking performance is satisfactory while keeping all the variables in the system under control which indicates robust behaviour.

Thus, the work has contributed to the development of a unique control scheme with features of both robust and on-line control.

The work has also accomplished the objective to track a system dynamically in the presence of environmental noise. In this scenario, estimation of controller gain parameters has been computed using maximum likelihood estimation. In this context, it is worth mentioning that it is assumed that the state observer and tracker have already been designed and the challenge is to cope with the effects of environmental uncertainty.

The work has two manifold approaches: In the first one, the work is focused on improving the tracking capabilities of a robot by accounting for the unstructured uncertainty usually encountered in a real industrial application. Additionally, one of the main objectives is to surpass theoretical developments to validate the proposed control strategies through real-time experiments. The design of the proposed state observer based control is to achieve tracking control with the features of robustness and adaptation. The work has presented both theoretical developments and application-based validation, related to a nonlinear dynamical system with noise.

The attempt is made to devise an optimal PD controller which not only tackles the problem of nonlinearity and uncertainty but also maintains its original simple structure. The present study has exploited the mathematical formulae and tools to develop new ideas for applying in the control of stochastic, nonlinear, time-varying, constraint optimal problem.

Another approach is to focus on developing an efficient estimation for the computation of controller gain parameters to determine the stochastic environment force, based on a batch of noisy observations. This is done in the situation when a robot is interacting with a randomly structured environment. Moreover, the performance of estimation is to be verified analytically and through simulations carried out on a master-slave robotic system.

It would be interesting to make a comparison between these two situations and corresponding approaches. Whereas in the first approach, the controller is designed by minimizing the instantaneous square of error energy, the second deals with the design of the controller using MLE from the handful of observations of joint positions. The two problems are distinct, but there is a specific relationship between them. If we have to design a controller adaptively at the slave end of the robotic system, apply the first approach directly. Further, if we have to determine the parameter at the master end (teleoperation), we have to use the method of maximum likelihood estimation.

In the present study, through the development of theoretical concepts, the applications of online and off-line estimation have been implementing on real problems successfully.

7.4 Suggestions for further work

The process and technology is a dynamic and innovative thought phenomenon. Presently, the systems are designed to incorporate intelligence which can account for data uncertainty in the modeling and control. Thus, the present work opens up the following areas for the future:

- In this research, we have assumed that process noise and measurement noise is not related to each other. So, in stochastic sense, $cov.(\nu^T \omega^T) = 0$. The general state equation and measurement dynamics for an observer used is in

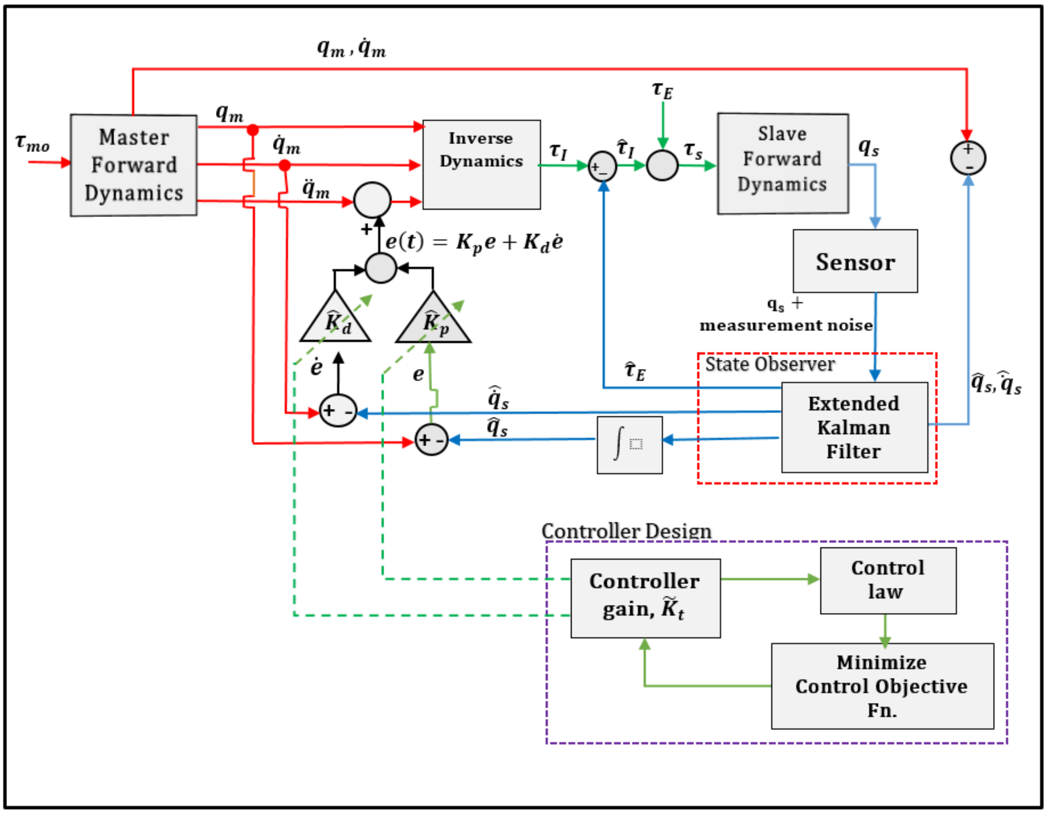

Figure 7.1: Suggested Disturbance-observer for Master-slave System.

the present work is

$$\left.\begin{aligned} dX_t &= f(x_t, t)dt + g(X_t, t)dB(t) \\ dZ_t &= h(x_t, t)dt + dV(t) \end{aligned}\right\}$$

It would be a different approach to work in filtering theory with a correlated process and measurement noise being applied to the robotic system.

- In the present study, EKF has been employed as a state observer. However, the approach of state observer based control is not only limited to this observer but can be applied to any type of observer. EKF can be employed with the assumption of Gaussian nature of noise with zero mean and covariance one. However, when there is no knowledge of pdf of noise, the design and implementation of other options of an observer is an open area of research.

- The controller is designed by linearizing the dynamics and applying it to the robot system to study the performance of state-observer-based control. The approach used is the linear optimal control method unified with estimation by an observer. Nonlinear control techniques, viz. sliding mode, intelligent control in combination with observer can be developed in future.

- The problems of parameter uncertainty, time delay, disturbance, loss of information have not been considered while designing the controllers for the master-slave robotic system. The work considering the mentioned problems can be done for the purpose of robust controller design.

- The study carried out in Chapter 6 assumed that optimal tracker and the optimal controller has already been designed and it led to a situation when the robot started encountering random structured environment. In such a situation, controller gain parameters have been estimated by using a block processing approach, MLE. The further extension of work may be carried out by treating environment force as a disturbance. This disturbance can now be estimated utilizing appropriate design of DOB by assuming disturbance ($\widehat{\boldsymbol{\tau}}_{\boldsymbol{E}}$) as one of the states. The difference of actual and computed disturbance may be assumed as WGN. Further, state estimation in a noisy environment may be done by EKF, as shown in Fig. 7.1. Thereafter, trajectory tracking can be achieved by the optimal design of the controller considering estimated states as has been found in Chapter 3. The validation of the suggested control scheme through experimentation is a proposal for future research.

BIOGRAPHY

I, Neelu Nagpal, an Assistant Professor in Guru Govind Indraprastha University have been working since last 13 years in Electrical and Electronics Engineering Department of Maharaja Agrasen Institute of Technology, Delhi. I completed my Master's in 2007 from Delhi University in Control and Instrumentation specialization with distinction. Prior to that, I graduated in Electrical Engineering with first division from Delhi College of Engineering in the year 1999. Besides having 19 years of experience in teaching, I have 5 years of industrial experience and lot more educational contributions to my name. I have 11 publications in different journals, conferences, and proceedings.

Publications

The work conducted in this thesis has resulted in the following major publications::

- Neelu Nagpal, Vijyant Agarwal, Bharat Bhushan, "Real-Time State Observer Based Controller for Stochastic Robotic Manipulator", IEEE Transactions on Industrial Applications, Vol. 54, No. 2, pp. 1806-1822, March/April 2018.
- Neelu Nagpal, Bharat Bhushan, Vijyant Agarwal, "Estimation of stochastic environment force for master-slave robotic system", Sadhana-Academy Proceedings in Engineering Science-Springer, Vol. 42, No. 6, pp. 889-899, June 2017.
- Neelu Nagpal, Hardik Nagpal, Bharat Bhushan, Vijyant Agarwal, "Tracking Control of 4 DOF Robotic Arm Using Krill Herd Optimized Fuzzy Logic Controller, The International Conference on Signals, Machines and Automation held at NSIT, Delhi, India, 23-25 February, 2018 and published in Applications of Artificial Intelligence Techniques in Engineering-Advances in Intelligent Systems and Computing, Vol. 697, Springer book series, Singapore, pp. 629-643, April 2019, DOI: 10.1007/978-981-13-1822-1-59.
- Neelu Nagpal, Bharat Bhushan, Vijyant Agarwal, "Intelligent Control of 4-DOF Robotic Arm, IEEE International Conference on Power Electronics, Intelligent Control and Energy Systems held at DTU, Delhi, India, 4-6 July 2016, DOI:10.1109/ICPEICES.2016.785335.

Bibliography

[1] B. Siciliano, O. Khatib, Springer Handbook of Robotics, Springer, Heidelberg, ISBN:978-3-540-23957-4, 2008.

[2] D.S. Naidu, Optimal Control Systems, CRC Press, Ist Edition, ISBN: 978-0849308925, 2002.

[3] J.C. Hsu and A. U. Meyer, Modern Control Principles and Applications, McGraw Hill, New York, NY, ISBN-13: 978-0070306356, 1968.

[4] A. Mohammed, B. Schmidt, L. Wanga and L. Gao, Minimizing Energy Consumption for Robot Arm Movement, International Conference on Digital Enterprise Technology, Procedia CIRP, Germany, Vol. 25, pp. 400-405, DOI: 10.1016/j.procir.2014.10.055, 2014.

[5] C. Treesatayapun, Balancing Control Energy and Tracking Error for Fuzzy Rule Emulated Adaptive Controller, Applied Intelligence, Springer, DOI:10.1007/s10489-013-0493-x, 2013.

[6] H.K. Khalil, Nonlinear Systems, 3rd edition, Prentice Hall, Upper Saddle River, New Jersey, ISBN: 978-0130673893, 2001.

[7] A. Isidori, Nonlinear Control Systems: Communications and Control Engineering, 3rd edition, Springer, ISBN: 978-354-13, 1995.

[8] J.J.E. Slotine and W. Li, Applied Nonlinear Control, 1st Edition, Prentice-Hall, New Jersey, ISBN:978-0130408907, 1991.

[9] H. Nijmeijer and A.J. V. Schaft, Nonlinear Dynamic Control Systems, Springer-Verlag, New York, ISBN: 978-1-4757-2101-0, 1990.

[10] F. Lin, Robust Control Design: An Optimal Control Approach, 1st edition, John Wiley and Sons Ltd, England, ISBN:978-0-470-03191-9, 2007.

[11] J.S. Chen and Y.H. Chen, Robust Control of Nonlinear Uncertain Systems: A Feedback Linearization Approach, IEEE Conference on Decision and Control, Brighton, UK, DOI:10.1109/cdc.1991.261805, 1991.

[12] J. Peng, J. Wang, and Y. Wang, Neural Network Based Robust Hybrid Control for Robotic System: An H-∞ Approach, Nonlinear Dynamics, Vol. 65, No. 4, pp. 421-431, 2010.

[13] E. Atam, L. Mathelin, and L. Cordier, A Hybrid Approach for Control of a Class of Input-affine Nonlinear Systems, International Journal of Innovative Computing, Information and Control, Vol. 10, No. 3 pp. 1207-1228, 2014.

[14] A.I.S. Shankar Sastry, Adaptive Control of Linearizable Systems, IEEE Transaction on Automatic Control, Vol. 34, No. 11, pp. 1123-1131, 1989.

[15] Abdallah, T. Chaouki, D. Dawson, P. Dorato and M. Jamshidi, Survey of Robust Control for Rigid Robots, Control Systems Magazine, Vol. 11, No. 2, pp. 24-30, 1991.

[16] H. G. Sage, M. F. D. Mathelin and E. Ostertag, Robust Control of Robot Manipulators: A survey, International Journal of Control, Vol. 72, No. 16, 1498-1522, 1999.

[17] C. Canudas de Wit, B. Siciliano and G. Bastin, Theory of Robot Control, Springer-Verlag, London, ISBN-13:978-1-4471-1503-8, 1st Edition, 1997.

[18] R. Kelly, PD Control with Desired Gravity Compensation of Robotic Manipulators-A Review, The International Journal of Robotics Research, Vol. 16, No. 5, pp. 660-672, 1997.

[19] V. Santibanez and R. Kelly, PD control with Feedforward Compensation for Robot Manipulators: Analysis and experimentation, Robotica, Vol. 19, No. 1, pp. 11-19, 2001.

[20] M. O. Efe, An Augmented PID control Scheme for Robust Control, IEEE International Workshop on Recent Advances in Sliding Modes, Istanbul, Turkey, 2015, DOI:10.1109/RASM.2015.7154582.

[21] Y.X. Zhang, S. Cong, W.W. Shang, Z.X. Li, and S.L. Jiang, Modeling, Identification and Control of A Redundant Planar 2-dof Parallel Manipulator, International Journal of Control Automation and Systems, Vol. 5, No. 5, pp. 559-569, 2007.

[22] Y. D. Song, A.T. Alouani, and J.N. Anderson, Robust Path Tracking Control of Industrial Robots: An H_∞ Approach, Conference on Control Applications, pp. 25-30, Dayton, USA, DOI: 10.1109/CCA.1992.269904, 1992.

[23] L. Xie, E. de Souza Carlos, Robust H_∞ Control for Linear Systems with Norm-bounded Time-varying Uncertainty, IEEE Transactions on Automatic Control, Vol. 37, No. 8, pp. 1188-1191, 1992.

[24] T. Hatanaka, N. Chopra and M.W. Spong, Passivity-based Control of Robots: Historical Perspective and Contemporary Issues, IEEE Conference on Decision and Control, Osaka, Japan, DOI:10.1109/cdc.2015.7402575, 2015.

[25] J.P.O. Oliver, O.A. Domnguez-Ramirez and E. S. E. Quezada, Trajectory Tracking Control for Robotics Manipulators Based on Passivity, Electronics, Robotics and Automotive Mechanics Conference, Morelos, Mexico, DOI:10.1109/cerma.2008.105, 2008.

[26] A. Ferreira de Loza, E. Punta, L. Fridman, G. Bartolini and S. Delprat, Nested Backward Compensation of Unmatched Perturbations via HOSM observation, Journal of the Franklin Institute, Vol. 351, No. 5, pp. 2397-2410, 2014.

[27] A. Estrada, L. Fridman and R. Iriarte, Combined Backstepping and HOSM Control Design for a Class of Nonlinear MIMO Systems, International Journal of Robust and Nonlinear Control, Vol. 27, No. 4, pp. 566-581, 2016.

[28] Y. Tang, M. Tomizuka, G. Guerrero and G. M. Mayor, Decentralized Robust Control of Mechanical Systems, IEEE Transactions on Automatic Control, Vol. 45, No.4, pp. 771-775, 2000.

[29] J. Baek, J. Maolin, and H. Soohee, A New Adaptive Sliding-Mode Control Scheme for Application to Robot Manipulators, IEEE Transactions on Industrial Electronics, Vol. 63, No. 6, pp. 3628-3637, 2016.

[30] S. Islam and P. X. Liu, Robust sliding mode control for robot manipulators, IEEE Trans. Industrial Electronics, Vol. 58, No. 6, pp. 2444-2453, 2011.

[31] Zhang, B., Yang, X., Zhao, D., Spurgeon, S. K., and Yan, X., Sliding Mode Control for Nonlinear Manipulator Systems, IFAC-PapersOnLine, Vol. 50, NO. 1, pp. 5127-5132, 2017.

[32] W.L. Stout and M.E. Sawan, Application of H-∞ Theory to Robot Manipulator Control, in Proc. of IEEE Int. Conf. Control Appl., pp. 148-153, Dayton, Ohio, 1992.

[33] Z. Song, J. Yi, D. Zhao, and X. Li, A Computed Torque Controller for Uncertain Robotic Manipulator Systems: Fuzzy Approach, Fuzzy Sets and Systems, Vol. 154, No. 2, pp. 208-226, 2005.

[34] Y.X. Su, D. Sun and B.Y. Duan, Design of An Enhanced Non-linear PID Controller, Mechatronics, Vol. 15, No. 8, pp. 1005-1024, 2005.

[35] V. Agarwal, Trajectory Planning of Redundant Manipulator using Fuzzy Clustering Method, International Journal of Advanced Manufacturing Technology, Vol. 61, No. 528, pp. 727-744, 2012.

[36] H.D. Patino, R. Carelli and B. R. Kuchen, Neural Networks for Advanced Control of Robot Manipulators, IEEE Transactions on Neural Networks, Vol.13, no.2, pp. 343-354, 2002.

[37] C. Park, Robust Stable Fuzzy Control via Fuzzy Modeling and Feedback Linearization with its Applications to Controlling Uncertain Single-Link Flexible Joint Manipulators, Journal of Intelligent and Robotic Systems 39, pp-131-147, 2004.

[38] P. Kheirkhahan, Robust Anti-Windup Control Design for PID Controllers, Theory and Experimental Verification, Journal of Modern Processes in Manufacturing and Production, Vol. 6, No. 3, 2017.

[39] Z. Qu and J. Dorsey, Robust Tracking control of Robots by a Linear Feedback law, IEEE Transactions on Automatic Control, Vol. 36, No. 9, pp. 1081-1084, 1991.

[40] Y. Chen, Replacing a PID Controller by a Lag-Lead Compensator for a Robot-A Frequency Response Approach, IEEE Transactions on Robotics and Automation, Vol. 5, No.2, pp. 174-182, 1989.

[41] J. Han, From PID to Active Disturbance Rejection Control, IEEE Transactions on Industrial Electronics, Vol. 56, No. 3, pp. 900-906, 2009.

[42] R. Marino and P. Tomei, Robust Stabilization of Feedback Linearizable Time-Varying Uncertain Nonlinear Systems, Automatica 29, pp. 181-189, 1993.

[43] H. Tan, S. Shu, F. Lin, An Optimal Control Approach to Robust Tracking of Linear Systems, International Journal of Control, Vol. 82, pp. 525, 2009.

[44] H. Pan and M. Xin, Nonlinear Robust and Optimal Control of Robot Manipulators, Nonlinear Dynamics, Vol. 76, pp. 237, 2014.

[45] O. U. Rehman, B. Fidan and I. R. Petersen, Robust Control System Design for an Uncertain Nonlinear System using Minmax LQG Design Method, Asian Journal of Control, Vol. 16, No. 4, pp. 1029-1041, 2014.

[46] R. Sharma and A. Tewari, Optimal Nonlinear Tracking of Spacecraft Attitude Maneuvers, IEEE Transactions on Control Systems Technology, Vol. 12, No. 5, 2004.

[47] M. Sassano, and A. Astolfi, Dynamic solution of the HJB equation and the Optimal Control of Nonlinear Systems, IEEE Conference on Decision and Control, DOI:10.1109/cdc.2010.5716990, 2010.

[48] S. Zhang and Y. Ning, Parametric Approach to Trajectory Tracking Control of Robot Manipulators, Journal of Applied Mathematics, Vol. 2013, Article ID 958597, 6 pages, http://dx.doi.org/10.1155/2013/958597, 2013.

[49] L. Zhang, L. Liu, Z. Wang and Y. Xia, Continuous Finite-time Control for Uncertain Robot Manipulators with Integral Sliding Mode, IET Control Theory and Applications, Vol. 12, No. 11, pp. 1621-1627, 2018.

[50] B. Xian, D.M. Dawson, M.S. de Queiroz, and J. Chen, A Continuous Asymptotic Tracking Control Strategy for Uncertain Multi-Input Nonlinear Systems, Proceedings of the IEEE International Symposium on Intelligent Control, Houston Texas, 2003.

[51] R. Ortega and M.W. Spong, Adaptive Motion Control of Rigid Robots: A Tutorial, Automatica, Vol. 25, No. 6, pp. 877-888, 1989.

[52] H. Arimi and K. B. McAuley, A Maximum-likelihood Method for Estimating Parameters, Stochastic Disturbance Intensities and Measurement Noise Variances in Nonlinear Dynamic Models with Process Disturbances, Computers and Chemical Engineering, Vol. 67, pp. 178-198, 2014.

[53] M. Rajotte, Stochastic Differential Equations and Numerical Application, Virginia Commonwealth University, Thesis and Dissertations, 2014.

[54] A. Papoulis, Probability, Random Variables, and Stochastic Processes, McGraw-Hill Book Co., 3rd edition, ISBN 0-07-048477-5, 1991.

[55] R. Singla, V. Agarwal, and H. Parthasarathy, Statistical Analysis of Tracking and Parametric Estimation Errors in a 2-link Robot based on Lyapunov function, Nonlinear Dynamics, Vol. 82, No. 1, pp. 217-238, 2015.

[56] P. B. L. S. Rao, Non-parametric Inference for a Class of Stochastic Partial Differential Equations Based on discrete Observations, Indian Journal of Statistics, Vol. 64, pp. 1-15, 2002.

[57] I. Karatzas and S. E. Shreve, Brownian Motion and Stochastic Calculus, 2nd Edition, Springer-Verlag, New York, ISBN: 978-1-4612-0949-2, 1991.

[58] B. Chen and W. Zhang, Stochastic H_2 / H_∞ Control With State-Dependent Noise, IEEE Transactions on Automatic Control, Vol. 49, No. 1, pp. 45-57, 2004.

[59] A. Bagchi, Optimal Control of Stochastic Systems, Series in Systems and Control Engineering. Prentice-Hall, London, UK, ISBN-13:978-0136386100, 1993.

[60] A.H. Jazwinski, Stochastic Processes and Filtering Theory, ist Edition, New York: Academic Press, ISBN:0-12-381550-9, 1970.

[61] B. Oksendal, Stochastic Differential Equations: An Introduction with Applications, 6th Edition, Springer, New York, ISBN:3-387-53335-4, 2003.

[62] H. Liu, Y. Huang, and W. Wu, Improved Adaptive Output Feedback Controller for Flexible-joint Robot Manipulators, IEEE International Conference on Information and Automation, Ningbo, China, DOI: 10.1109/ICInfA.2016.7832083, 2016.

[63] Z. Chen, Bayesian Filtering: From Kalman Filters to Particle Filters and Beyond Statistics, Vol. 182, No. 1, pp. 1-69, 2003.

[64] M.K. Steven, Fundamentals of Statistical Signal Processing: Estimation Theory, 1st Edition, Vol. 1, Prentice-Hall Inc., ISBN: 0-13-042268, 1993.

[65] J.M. Ali, N.H. Hoang, M.A. Hussain, D. Dochainc.m Review and Classification of Recent observers Applied in Chemical Process Systems, Computers and Chemical Engineering, Vol. 76, pp. 27-41, 2015.

[66] S. J. Julier, J. Uhlmann, and H. Durrant-Whyte, A New Method for the Nonlinear Transformation of Means and Covariances in Filters and Estimators, IEEE Transactions on Automatic Control, Vol. 45, No. 3, pp. 477-482, 2000.

[67] T. Wigren, Recursive Prediction Error Identification and Scaling of Non-linear State Space Models Using a Restricted Black box Parameterization, Automatica, Vol. 42, No.1, pp. 159-168, 2006.

[68] C.V. Rao, J.B. Rawlings and J.H. Lee, Constrained Linear State Estimation-Moving Horizon Approach, Automatica, Vol. 37, No. 10, pp. 1619-1628, 2001.

[69] A. Doucet and A.M. Johansen, Handbook of Nonlinear Filtering, Chapter: A tutorial on particle filtering and smoothing: Fifteen years later, Vol. 12, pp. 656-704, 2009.

[70] M.F. Hassan, M.T. Alrifai1, H.M. Soliman, and M.A Kour ah, Observer Based Controller for Constrained Uncertain Stochastic Nonlinear Discrete-Time Systems, International Journal of Robust Nonlinear Control, Vol. 26, No. 10, pp. 2090-2115, 2016.

[71] Y.H. Kim, F.L. Lewis, Neural Network Output Feedback Control of Robot Manipulators, IEEE Transactions on Robotics and Automation, Vol. 150, No. 2, pp. 301-309, 1999.

[72] J. Davila, L. man and A. Levant, Second-Order Sliding-Mode Observer for Mechanical Systems, IEEE Transactions on Automatic Control, Vol. 50, No. 11, pp. 1785-1789, 2005.

[73] V. Chawda, O. Celik and K.M. O'Malley, Evaluation of Velocity Estimation Methods Based on Their Effect on Haptic Device Performance, IEEE/ASME Transactions on Mechatronics, Vol. 23, No. 2, pp. 604-613, 2018.

[74] J. Koshkouei and A.S.I. Zinober, Sliding mode Controller-observer Design for Multivariable Linear Systems with Unmatched Uncertainty, Kybernetika, Vol. 36, No. 1, pp. 95-115, 2000.

[75] A.G. Parlos, S.K. Menon and A.F. Atiya, An Adaptive State Filtering Algorithm for Systems With Partially Known Dynamics, Journal of Dynamic Systems, Measurement, and Control, Vol. 124, pp. 364-373, 2002.

[76] W. Chen, J. Yang, L. Guo and S. Li, Disturbance-observer Based control-An overview, IEEE Transactions on Industrial Electronics, Vol. 63, No. 2, pp. 1083-95, 2016.

[77] A. Eidehall, T. B. Schon and F. Gustafsson, The Marginalized Particle Filter for Automotive Tracking Applications, IEEE Proceedings, Intelligent Vehicles Symposium, pp. 370 - 375, DOI: 10.1109/IVS.2005.1505131, Las Vegas, USA, 2005.

[78] M. Soroush, State and Parameter Estimations and Their Applications in Process Control, Computers and Chemical Engineering, Vol. 23, No. 2, pp. 229-245, 1998.

[79] E. A. Misawa and J. K. Hedrick, Nonlinear Observers, A State of the Art A survey, Transactions of ASME, Vol. 111, pp. 344-352, 1989.

[80] S. M. Kay, Fundamentals of Statistical Signal Processing, Volume 2, Detection Theory, Prentice Hall, ISBN: 0-13-345711-7, 1998.

[81] H. Karimi and B. K. McAuley, A Maximum-likelihood Method for Estimating Parameters, Stochastic Disturbance Intensities and Measurement Noise Variances in Nonlinear Dynamic models with Process Disturbances, Computers and Chemical Engineering, Vol. 67, pp. 178-198, 2014.

[82] L. E, Lehmann, Theory of Point Estimation. Probability and Mathematical Statistics, John Wiley and Sons Ltd., ISBN: 0-471-05849-1, 1983.

[83] D.V. Raman, J. Anderson and A. Papachristodoulou, A new approach for estimating the robustness of parameter estimates to measurement noise, American Control Conference, Boston, MA, USA, DOI:10.1109/acc.2016.7525183, 2016.

[84] H. L. Van Trees, K. L. Bell and Z. Tian, Detection, estimation and modulation theory, part I: detection, estimation and filtering theory, 2nd edition, Wiley, London, ISBN: 978-0-470-54296-5, 2013.

[85] R. C. Rao, Linear statistical inference and its applications, 2nd edition, London: Wiley, ISBN: 978-0-471-21875-3, 2001.

[86] M. M Olsen, J. Swevers, W. Verdonck, Maximum Likelihood Identification of a Dynamic Robot Model: Implementation Issues, The International Journal of Robotics Research Vol. 21, No. 2, pp. 89-96, 2002.

[87] A. Farina, A. D. Lallo, L. Timmoneri, T. Volpi, B. Ristic, CRLB and ML for a parametric estimate: New Results, Elsevier, Signal Processing, Vol. 86, pp. 804-813, 2005.

[88] P. Doerschuk, Cramer-Rao Bounds for Discrete-time Nonlinear Filtering Problems, IEEE Transactions on Automatic Control Vol. 40, No. 8, pp.1465-1469, 2002.

[89] H.L.V. Trees, K.L. Bell, Z.Tian, Detection Estimation and Modulation Theory, 2nd Edition, Part -I, Wiley, ISBN: 978-0-470-54296-5, 2013.

[90] M.M. Olsen and H.G. Petersen, A New Method for Estimating Parameters of a Dynamic Robot Model, IEEE Transaction on Robotics and Automation Vol. 17, No. 1, pp. 95-100, 2001.

[91] A.S. Sergeev, R.K. Agapova, The Use of the Expectation Maximization (EM) Algorithm for Maximum Likelihood Estimation of Gametic Frequencies of Multilocus Polymorphic Codominant Systems Based on Sampled Population Data, Russian Journal of Genetics, Vol. 38, No. 3, pp. 321-331, 2002.

[92] L.E. Peterson, Maximum Likelihood Logistic Regression Using Metaheuristics, International Conference on Machine Learning and Applications, DOI 10.1109/ICMLA.2009.140, 2009.

[93] T. Pierre, Joint Estimation of Model and Observation Error Covariance Matrices in Data Assimilation: a Review in Data Assimilation: a Review, arXiv, accepted for submission to Monthly Weather Review, pdf, 2018.

[94] I.J. Myung, Tutorial on maximum likelihood estimation, Journal of Mathematical Psychology, Vol. 47, No. 1, pp. 90-100, 2003.

[95] J.M. Mendel, Lessons in digital estimation theory, Prentice Hall, Signal Processing Series, ISBN:10:0135308097, 1987.

[96] A. Moschitta and P. Carbone, Noise Parameter Estimation from Quantized Data, IEEE Transactions on Instrumentation and Measurement, Vol. 56, No. 3, pp. 736-742, 2007.

[97] E. Saatci and A. Akan, Inverse Modeling of Respiratory System During Noninvasive Ventilation by Maximum Likelihood Estimation, EURASIP Journal on Advances in Signal Processing, DOI:10.1155/2010/237562, 2010.

[98] J. Rehor and V. Havlena, Maximum Likelihood Estimation of LTI Continuous-Time Grey-box Models, The International Federation of Automatic Control Cape Town, South Africa, August 24-29, 2014.

[99] A. Wiesel, Y.C. Eldar and A. Beck, Maximum Likelihood Estimation in Linear Models with a Gaussian Model Matrix, IEEE Signal Processing Letters, Vol. 13, No. 5, 2006.

[100] L. Chan, F. Naghdy, and D. Stirling, Extended Active Observer for Force Estimation and Disturbance Rejection of Robotic Manipulators, Robotics and Autonomous Systems, Vol. 61, No. 12, pp. 1277-1287, 2013.

[101] M.N. Kamarudin, S.M. Rozali and A. R. Husain, Observer-Based Output Feedback Control with Linear Quadratic Performance, Procedia Engineering Vol. 53, pp. 233-240, 2013.

[102] P.J. Nicklasson, Passivity-Based Control of Electric Machines, PhD thesis 96-17-W, Department of Engineering Cybernetics, Norwegian University of Science and Technology, Trondheim, Norway, 1996.

[103] A. Valera, M. Daz-Rodrguez, M. Valles, E. Oliver, V. Mata, and A. Page, Controller-observer Design and Dynamic Parameter Identification For Model-based Control of an Electromechanical Lower-limb rehabilitation system, International Journal of Control, Vol. 90, No. 4, pp. 702-714, Mar. 2017.

[104] A.N. Atassi, H.K. Khalil, A Separation Principle for the Stabilization of A Class of Nonlinear Systems, IEEE Transactions on Automatic Control, Vol. 44, No. 9, pp. 1672-1687, 1999.

[105] A. Rodriguez-Mata, R. Lopez, A. Martinez-Vasquez, S. Salazar, A. Osorio, R. Lozano, Robust control with disturbance observer for UAV translational tracking, Workshop on Research, Education and Development of Unmanned Aerial Systems, Mexico, DOI: 10.1109/RED-UAS.2015.7441035, 2015.

[106] Z. Wang and K.J. Burnham, Robust Filtering for a Class of Stochastic Uncertain Nonlinear Time-Delay Systems via Exponential State Estimation, IEEE Transactions on Signal Processing, Vol. 49, No. 4, pp. 794-804, 2001.

[107] C. A. Lightcap and S. A.Banks, An Extended Kalman Filter for Real-time Estimation and Control of A Rigid-link Flexible-joint Manipulator, IEEE Transactions on Control System and Technology, Vol. 18, No. 1, pp. 91-103, 2010.

[108] W. He, Y. Chen, and Z. Yin, Adaptive Neural Network Control of An Uncertain Robot with Full-state Constraints, IEEE Transactions on Cybernetics, Vol. 46, No. 3, pp. 620-629, 2016.

[109] J. Cortes-Romero, G.A. Ramos, H. Coral-Enriquez, Generalized Proportional-Integral Control for Periodic Signals Under Active Disturbance Rejection Approach, ISA Transactions, Vol. 53, pp. 1901-1909, 2014.

[110] T.T. Tran, S.S. Ge, and W. He, Adaptive Control for An Uncertain Robotic Manipulator with Input Saturation, Control Theory Technology, Vol. 14, No. 2, pp. 113-121, 2016.

[111] Z. Qu, Robust Control of Nonlinear Uncertain Systems, 1st edition, John Wiley and Sons, Inc. New York, NY, USA, ISBN:0471115894, 1998.

[112] M.R. Soltanpour, J. Khalilpour and M. Soltani, Robust Nonlinear Control of Robot Manipulator with Uncertainties in kinematics, Dynamics and Actuator models, International Journal of Innovative Computing and Control, Vol. 8, No. 8, pp. 5487-5498, 2012.

[113] V. Parra-Vega, S. Arimoto, Yun-Hui Liu, G. Hirzinger and P. Akella, Dynamic sliding PID control for Tracking of Robot Manipulators: Theory and experiments, IEEE Transactions on Robotics and Automation, Vol. 19, No. 6, pp. 967-976, 2003.

[114] Y. Zuo, Y. Wang, X. Liu, S. X.Yang, L. Huang, X. Wu and Z.Wang, Neural network robust H-∞ Tracking Control Strategy for Robot Manipulators, Applied Mathematical Modelling, Vol. 34, No. 7, pp. 1823-1838, 2010.

[115] R. Sharma and M. Gopal, A Hybrid Markov Game Controller for Nonlinear systems, International Journal of Computer and Cognition, Vol. 5, No. 1, pp. 1-7, 2007.

[116] V. Agarwal and H. Parthasarathy, Disturbance Estimator as a State Observer with Extended Kalman Filter for Robotic Manipulator, Nonlinear Dynamics, Vol. 85, No. 4, pp. 2809-2825, 2016.

[117] A. Mohammadi, M. Tavakoli, H. J. Marquez and F. Hashemzadeh, Nonlinear disturbance Observer Design for Robotic Manipulators, Control Engineering Practice, Vol. 21, No. 3, pp. 253-267, 2013.

[118] W. Chen, J. Yang, L. Guo and S. Li, Disturbance-observer-based Control: An Overview, IEEE Transactions on Industrial Electronics, Vol. 63, no. 2, pp. 1083 -1095, 2016.

[119] G. Lei and C. Songyin, Anti-disturbance Control Theory for Systems with Multiple Disturbances: A survey, ISA Transactions, Vol. 53, No. 4, pp. 846-849, 2014.

[120] H. Wang, B. Chen, and C. Lin, Adaptive Neural Tracking Control for A Class of Stochastic Nonlinear Systems, International Journal of Robust and Nonlinear Control, Vol. 53, No. 7, pp. 1695-1701, 2012.

[121] Y. Niu, D. W. C. Ho, and X. Wang, Robust H-∞ Control for Nonlinear Stochastic Systems: A Sliding-Mode Approach, IEEE Transactions on Automatic Control, Vol. 53, No. 7, pp. 1695-1701, 2008.

[122] R. Sharma, V.Kumar, P. Gaur, and A. P. Mittal, An Adaptive PID Like Controller using Mix Locally Recurrent Neural Network for Robotic Manipulator with Variable Payload, ISA Transactions, Vol. 62, pp. 258-267, 2016.

[123] W. He, Y. Dong and C. Sun, Adaptive Neural Impedance Control of a Robotic Manipulator with Input Saturation, IEEE Transactions on Systems, Man, and Cybernetics, Vol. 46, No. 3, pp. 334-344, 2016.

[124] W. He and Y. Dong, Adaptive Fuzzy Neural Network Control for a Constrained robot using Impedance Learning, IEEE Transactions on Neural Networks and Learning Systems, Vol. 29, No. 4, pp. 1174-1186, 2017.

[125] C. Chen, C. Wen, Z. Liu, K. Xie, Y. Zhang and C. L. P. Chen, Adaptive consensus of nonlinear Multi-agent Systems with Non-identical Partially Unknown Control Directions and Bounded Modelling Errors, IEEE Transactions on Automatic Control, Vol. 62, No. 9, pp. 4654-4659, 2017.

[126] C. Chen, Z. Liu, K. Xie, Y. Liu, Y. Zhang, and C.L.P. Chen, Adaptive Fuzzy Asymptotic Control of MIMO Systems with Unknown Input Coefficients via a Robust Nussbaum Gain-based Approach, IEEE Transactions on Fuzzy Systems, Vol. 25, No. 5, pp. 1252-1263, 2017.

[127] C. Chen, Z. Liu, K. Xie, Y. Liu, Y. Zhang, and C.L.P. Chen, Adaptive asymptotic Control of Multivariable Systems Based on a one-parameter estimation approach, Automatica, Vol. 83, No. C, pp. 124-132, 2017.

[128] S. S. Saab and P. Ghanem, A Multivariable Stochastic Tracking Controller for Robot Manipulators without Joint Velocities, IEEE Transactions on Automatic Control, Vol. 63, No. 8, pp. 2481-2495, 2018.

[129] B. Ponton, S. Schaal, and L. Righetti, The Role of Measurement Uncertainty in Optimal Control for Contact Interactions, Submitted in Systems and Control, arXiv:1605.04344 [cs.SY].

[130] H. Kobayashi, H. Kobayashi, S. Katsura, K. Ohnishi, An analysis of parameter Variations of Disturbance Observer for Motion Control, IEEE Transactions on Industrial Electronics, Vol. 54, No. 6, pp. 3413-3421, 2007.

[131] Emre and O. Kouhei, Stability and Robustness of Disturbance-Observer-Based MotionControl Systems, IEEE Transactions on Industrial Electronics, Vol. 62, No. 1, pp. 414-422, 2015.

[132] M. Cui, Z. Wu and X. J. Xie, Stochastic Modeling and Tracking Control for a Two-link Planner Rigid Robot Manipulator, International Journal of

Innovative Computing, Information and Control ICIC International, Vol. 9, No. 4, ISSN: 1349-4198, 2013.

[133] P. F. Hokayem and M. W. Spong, Bilateral teleoperation: A Historical survey, Automatica, Vol. 42, No. 12, pp. 2035-2057, 2006.

[134] S. Islam,P. X. Liu and E. Saddik, Nonlinear control for teleoperation systems with time-varying delay, Nonlinear Dyn, Vol. 76, No. 2, pp. 931-954, 2013.

[135] S. Sirouspour and A. Shahdi, Model Predictive Control for Transparent Teleoperation Under Communication Time Delay, IEEE Transactions on Robotics, Vol. 22, No.6, pp. 1131-1145, 2006.

[136] I. G. Polushina, A. Tayebib and H. J. Marquez, Control Schemes for Stable Teleoperation with Communication Delay based on IOS Small Gain Theorem, Automatica, Vol. 42, pp. 905-915, 2006.

[137] T. Namerikawa, S. Ito and H. Kawada, Robust Control of Master-slave Robot System Considering Environment Uncertainties, Proc. SPIE 60520F-1, 2005.

[138] H. Shao, K. Nonami, T. Wojtara, R. Yuasa, S. Amano and D. Waterman, Neuro-fuzzy Position Control of Demining Tele-operation System based on RNN Modeling, Robotics and Computer-Integrated Manufacturing, Vol. 22, No. 1, pp. 25-32, 2006.

[139] Z. Li and C.Y. Su, Neural-adaptive control of Single Master Multiple-Slaves Teleoperation for Coordinated Multiple Mobile Manipulators with Time-varying Communication Delays and Input Uncertainties, IEEE Transactions on Neural Network Learning System, Vol. 24, No. 9, pp. 1400-1413, 2013.

[140] P. N. Watcharin, Adaptive Four-channel Neuro-fuzzy Control of a Master-Slave Robot, International Journal of Advanced Robotic System, Vol. 10, DOI:10.5772/55591, 2013.

[141] B. Y. Kim and H. S. Ahn, A Design of Bilateral Teleoperation Systems Using Composite Adaptive Controller, Control Engineering Practice, Vol. 21, pp. 1641-1652, 2013.

[142] C. Passenberg, A. Peer and M. Russ, A Survey of Environment, Operator, and Task Adapted controllers for Teleoperation Systems, Mechatronics, Vol. 20, pp. 787-801, 2010.

[143] N. Hogan, Impedance control: An Approach to Manipulation: Part II-Implementation, Journal of Dynamic System Measurement and Control, Vol. 107, No. 1, pp. 8-16, 1985.

[144] M. T. Mason, Compliance and Force Control for Computer Controlled Manipulators, IEEE Transactions on System, Man and Cybernetics, Vol. 11, No. 6, pp. 418-432, 1981.

[145] C. Yang, G. Peng, Y. Li, R. Cui, L. Cheng, and Z. Li, Neural Networks Enhanced Adaptive Admittance Control of Optimized Robot-Environment Interaction, IEEE Transactions on Cybernetics, DOI: 10.1109/TCYB.2018.2828654, 2018.

[146] M. Cohen and T. Flash, Learning impedance parameters for robot control using an associative search network, IEEE Transactions on Robotics and Automation, Vol. 7, No. 3, pp. 382-390, 1991.

[147] C. W. S. Cho, Nonlinear random vibration, analytical techniques and applications, 2nd edition, Boca Raton, FL: CRC Press, ISBN: 9781138076624 - CAT K34225, 2000.

[148] D. Erickson, M. Weber and I. Sharf, Contact Stiffness and Damping Estimation for Robotic Systems, International Journal of Robotics Research, Vol. 22, No.1, pp. 41-57, 2003.

[149] C. C. Hua and P. X. Liu, Convergence Analysis of Teleoperation systems with Unsymmetric Time-varying Delays, IEEE Transactions on Circuits and Systems II, Vol. 56, No. 3, pp. 240-244, 2009.

[150] L. J. Love and W. J. Book, Force Reflecting Teleoperation with Adaptive Impedance Control, IEEE Transactions on System, Man and Cybernetics, Vol. 34, No.1, pp. 159-165, 2004.

[151] T. Yamamoto, Bernhardt, A. Peer, M. Buss and A. M. Okamura, Techniques for Environment Parameter Estimation During Telemanipulation, IEEE/RAS-EMBS International Conference on Biomedical Robotics and Biomechatronics, USA, DOI: 10.1109/BIOROB.2008.4762830, 2008.

[152] M. Cui, X. Xie, and Z. Wu, Dynamics Modeling and Tracking Control of Robot Manipulators in Random Vibration Environment, IEEE Transactions on Automatic Control, Vol. 58, No. 6, pp. 1540-1545, 2013.

[153] Q. Liao, D. Sun and H. Ren, Novel Force Estimation-based Bilateral Teleoperation applying Type-2 Fuzzy logic and Moving Horizon Estimation, rXiv:1805.06634 [cs.RO], 2018.

[154] M. A. Zagrobelny, and J, B. Rawlings, Identifying the Uncertainty Structure Using Maximum Likelihood Estimation, American Control Conference, USA, DOI: 978-1-4799-8684-2, 2015.

[155] H. Son, Estimation of Environmental Force for the Haptic Interface of Robotic Surgery, The International Journal of Medical Robotics and Computer Assisted Surgery International Journal of Medical Robotics and Computer Assist Surgery, Vol. 6, 221-230, 2010.

[156] M. Sharifi1, H.A. Talebi and M. Shafiee, Adaptive Estimation of Robot Environmental Force Interacting with Soft Tissues, RSI International Conference on Robotics and Mechatronics, Tehran, Iran, DOI: 10.1109/ICRoM.2015.7367813, October 7-9, 2015.

[157] P. Eykhoff, System identification: parameter and state estimation, London: Wiley-Interscience, ISBN: 0-471-24980-7, 1974.

[158] X. Ling, Parameter Estimation and Controller Design for Dynamic Systems from the Step Responses Based on the Newton Iteration. Nonlinear Dynamics. Vol. 79, pp. 2155-2163, 2015.

[159] C. S. Liu and H. Peng, Disturbance Observer Based Tracking control, ASME Transactions on Dynamic Systems, Measurement, and Control, Vol. 122, No. 2, pp. 332-335, 2000.

[160] J. Tsinia, Stabilization of affine in control nonlinear systems, Nonlinear Analysis, Theory, Methods Appl., Vol. 12, pp. 1283-1296, 1998.

[161] E. Sontag, A Lyapunov-Like Characterization of Asymptotic Controllability,? SIAM Journal on Control and Optimization, Vol. 21, No. 3, pp. 462-471, 1983.

[162] P. Florchinger, Lyapunov-Like Techniques for Stochastic Stability, SIAM Journal on Control and Optimization, Vol. 33, No. 4, pp. 1151-1169, 1995.

[163] U. Vaidya and P. G. Mehta, Lyapunov Measure for Almost Everywhere Stability, IEEE Transactions on Automatic Control, Vol. 53, No. 1, pp. 307-323, 2008.

[164] S.H. Zak, On the Stabilization and Observation of Nonlinear Uncertain Dynamic Systems, IEEE Transactions on Automatic Control, Vol. 35, No. 5, pp. 604-607, 1990.

[165] Alexander, Uncertain Models and Robust Control, 1st Edition, Springer-Verlag Wien, DOI:10.1007/978-3-7091-6711-3, 1991.

[166] W.W. Shang, S. Cong, Robust Nonlinear Control of a Parallel Manipulator with Redundant Actuation, Robotics and Computer-Integrated Manufacturing, Vol. 30, No. 6, pp. 597-604, 2014.

[167] M. M. Fateh, Proper Uncertainty Bound Parameter to Robust Control of Electrical Manipulators using Nominal Model, Nonlinear Dynamics, Vol. 61, pp. 655-666, 2010.

[168] A.P. Sage and C.C. White III, Optimum Systems Control, 2nd Edition, Prentice-Hall, Englewood Cliffs, ISBN:0136382967, 1977.

[169] L. Jetto and V. Orsini, An Eigenvalue Perturbation Result for Stability Bound with Respect to Biased Structured Perturbations, Mediterranean Conference on Control and Automation, DOI:10.1109/med.2006.328832, 2006.

[170] R. M. Murray, S. S. Sastry, L. Zexiang. A Mathematical Introduction to Robotic Manipulation, 1st edition, CRC Press Inc., USA, 1994.

[171] I.N. Doyea, M. Zasadzinski, M. Darouacha, N. Radhyb, A. Bouaziz, Exponential stabilization of a class of nonlinear systems: A generalized Gronwall - Bellman lemma approach, Nonlinear Analysis, Vol. 74, pp. 7333-7341, 2011.

[172] G. Leitmann, Guaranteed Asymptotic Stability for Some Linear Systems With Bounded Uncertainties, Journal of Dynamic Systems, Measurement, and Control, Vol. 101, No. 3, pp. 212-216, DOI:10.1115/1.3426427, 1979.

[173] Y. Wang and C. Chien, An Observer-Based Adaptive Iterative Learning Control Using Filtered-FNN Design for Robotic Systems, Advances in Mechanical Engineering, Volume 2014, Article ID: 471418, 14 pages, DOI: 10.1155/2014/471418, 2015.

[174] A. Trofino and T. J. M.Dezuo, LMI Stability Conditions for Uncertain Rational Nonlinear Systems, International Journal of Robust and Nonlinear Control, Vol. 24, No. 18, 3124-3169, 2013.

[175] E. R. Rohr, L. F. A. Pereira, D. F. Coutinho, Robustness Analysis of Nonlinear Systems Subject to state Feedback Linearization, Revista Controle and Automaao Sociedade Brasileira de Automatica, Vol. 20, No. 4, pp. 482-489, 2009.

[176] M. Corless, Robust Stability Analysis and Controller Design with Quadratic Lyapunov functions, Variable Structure and Lyapunov Control, Lecture Notes in Control and Information Sciences, Vol. 193, Springer, Berlin, Heidelberg, ISBN:978-3-540-39325-2, 1994.

[177] J. Wu, H. R. Karimi, and P. Shi, Observer-Based Stabilization of Stochastic Systems with Limited Communication, Hindawi Publishing Corporation Mathematical Problems in Engineering, DOI:10.1155/2012/781542, 2012.

[178] A.J. Silva, O. A. D. Ramirez, V. P. Vega, and J. P. O. Oliver, Phantom Omni haptic device: Kinematic and manipulability, IEEE Conference on Electronics, Robotics and Automotive Mechanics Conference, pp. 193-198, DOI:10.1109/CERMA.2009.55, 2009.

[179] J. Apkarian, P. Karam, D. Crymble, A. Abdossalami and R. Sara, Instructor Workbook-Omni Bundle Robotics Experiment, Canada, http://www.quanser.com.